REPUBLIC OF IRAQ

MINISTRY OF HIGHER EDUCATION AND SCIENTIFIC RESEARCH

AL-FURAT AL-AWSAT TECHNICAL UNIVERSITY

ENGINEERING TECHNICAL COLLEGE NAJAF

AN EXPERIMENTAL STUDY THE PERFORMANCE OF SINGLE - SLOPE SOLAR STILL UTILIZING PARABOLIC TROUGH COLLECTOR WITH FRESNEL LENSES

AKEEL SALMAN AHMOED

BAH. DAGREE
IN MECHANICAL ENGINEERING TECHNIQUES OF POWER

2023

AN EXPERIMENTAL STUDY THE PERFORMANCE OF SINGLE - SLOPE SOLAR STILL UTILIZING PARABOLIC TROUGH COLLECTOR WITH FRESNEL LENSES

A THESIS

SUBMITTED TO THE DEPARTMENT OF MECHANICAL ENGINEERING TECHNIQUES OF POWER

IN PARTIAL FULFILLMENT OF THE REQUIREMENTS FOR

MASTER OF THERMAL TECHNOLOGIES DEGREE IN MECHANICAL ENGINEERING TECHNIQUES OF POWER (M.TECH.)

BY

AKEEL SALMAN AHMOED

Supervised by

Prof. Dr. Ahmed Hashim

2023

بِسْمِ اللَّهِ الرَّحْمَٰنِ الرَّحِيمِ

﴿هُوَ الَّذِي خَلَقَ لَكُمْ مَا فِي الْأَرْضِ جَمِيعًا ثُمَّ اسْتَوَىٰ إِلَى

السَّمَاءِ فَسَوَّاهُنَّ سَبْعَ سَمَاوَاتٍ وَهُوَ بِكُلِّ شَيْءٍ عَلِيمٌ﴾

صدق الله العلي العظيم

سورة البقرة اية ﴿٢٩﴾

DECLARATION

I hereby declare that the work in this thesis is my own and has not been submitted to other organizations or for acquiring any other degree.

Signature:

Name: Akeel Salman Ahmoed

Date: / / 2023

ACKNOWLEDGMENT

Praise be to God for all His blessings, and thanks be to God for His success in completing this work. I extend my sincere thanks and appreciation to my supervisor, **Prof. Dr. Ahmed Hashem Youssef**, for his continuous support and guidance in the completion of this work.

And I express my special thanks to the head of the Department of Mechanical Power Technologies Engineering and the professors working at the Technical College / Najaf for their help. My sincere thanks and gratitude go to every member of my family, especially my dear father and patient mother, and all my brothers for their support and standing with me all the way.

Akeel Salman Ahmoed

2023

SUPERVISORS CERTIFICATION

We certify that the thesis entitled " **An experimental study the performance of single - slope solar still utilizing parabolic trough collector with fresnel lenses** " submitted by Akeel Salman Ahmoed has been prepared under our supervision at the Department of Mechanical Engineering Techniques of Power, College of Technical Engineering-Najaf, AL-Furat Al-Awsat Technical University, as partial fulfillment of the requirements for the degree of Master of Techniques in Thermal Engineering.

Signature:

Name prof. Dr. Ahmed Hashem Youssef

(Supervisor)

Date: / / 2023

In view of the available recommendation, we forward this thesis for debate by the examining committee.

Signature:

Name: Asst. prof. Dr. Adel A. Eidan

Head mechanical Eng. Tech of power Dept.

COMMITTEE CERTIFICATION

We certify that we have read the thesis entitled, " **An experimental study the performance of single - slope solar still utilizing parabolic trough collector with fresnel lenses** " submitted by Akeel Salman Ahmoed and, as examining committee, examined the student's thesis in its contents. And that, in our opinion, it is adequate as a thesis for the degree of Master of Techniques in Thermal Engineering.

Signature:

Name: prof. Dr. Ahmed Hashem Youssef

(Supervisor)

Date: / / 2023

Signature: Signature:

Name: Name:

Member Member

Date: / / 2023 Date: / / 2023

Signature:

Name:

(Chairman)

Date: / / 2022

Approval of the Engineering Technical College- Najaf

Signature:

Name: Asst. Prof. Dr. Hassanain Ghani Hameed

Dean of Engineering Technical College- Najaf

Date: / / 2023

LINGUISTIC CERTIFICATION

This is to certify that this thesis entitled "**An experimental study the performance of single - slope solar still utilizing parabolic trough collector with fresnel lenses**" was reviewed linguistically. Its language was amended to meet the style of the English language.

Signature:

Name:

Date:

ABSTRACT

Solar energy is considered one of the most important sources of alternative energy in the world, as it is available and has low costs, especially in areas with abundant solar radiation, such as our country, Iraq. It is also clean energy that leaves no environmental impact when used. They are used in many applications, such as solar panels used to generate electrical energy or by taking advantage of their heat content, such as those used for desalination, water heating, and cooking. Solar distillers are among the most widespread applications to solve the scarcity of fresh water. The main objective of this study is to improve the performance of stationary solar systems through the use of solar concentrators. In this study, a single-slope solar still unit and another unit with the same dimensions and specifications connected to a parabolic trough collector (without lenses, with lenses over parabolic trough collector, and with lenses on both sides of the parabolic trough collector) were tested.The work was carried out experimentally under the climatic conditions of the city of Diwaniyah in Iraq (31.99°N latitude, 44. 93°E longitude) in April, May and June of 2023.

An experimental model was built on which practical experiments were conducted, with the possibility of changing the location of the Fresnel lenses to focus the solar radiation on the tube inside or outside the PTC, and there's a possibility of rotating the system towards the solar radiation.The experiments were carried out within values of water discharge (0.38, 0.5, and 0.78) L/min.

The results showed the temperature gradually increases to reach its highest value at noon, where the highest value of solar radiation, then begins to gradually decrease. The maximum water basin temperature of solar still coupled to the parabolic trough collector with Fresnel lenses outside parabolic trough was 76.8 °C at 1:00 p.m with volume flow rate 0.5 L/min in May, while maximum water basin temperature (71.7, 74.2, and 75.5) °C at 1:00 p.m for conventional, solar still with parabolic trough, solar still coupled to the parabolic trough collector with Fresnel lenses over parabolic trough respectively. Using a solar distillation

unit with a parabolic trough with fresnel lenses on both sides of the PTC contributed significantly to improve productivity. The freshwater production in May was 7.7 L/m^2d, the thermal efficiency was 19.32%, and the rate of improvement in productivity was 44.1% compared to conventional. While the yield of conventional solar still, and solar still associated with a parabolic basin collector, solar energy associated with a parabolic trogh collector, and Fresnel lenses over the solar concentrator were (5.3, 6.7, and 7.5) L/m^2 d and the daily thermal efficiency was (46.9%, 18.1%, and 20.3 %) respectively. The production improvement rate was about (28.2%, and 43.3) for solar still associated with a parabolic trough collector, and solar still associated with a parabolic trough collector with Fresnel lenses over parabolic trough collector, respectively, compared to conventional.

Table of contents

List of tables

List of figures

NOMENCLATURE

Symbol	Definition	Unit
A_{F}	Aperture area of a Fresnel lens	m^2
A_{foc}	Aperture area of focus on absorber tube	m^2
A_{p}	Aperture area of a parabolic trough	m^2
A_{s}	Area surface of solar radiation incident	m^2
$C\mathrm{R}_p$	The concentration ratio of a parabolic trough	
$\mathrm{D}_{\mathrm{abs}}$	Diameter of the absorbent tube	m
D_F	Diameter of a Fresnel lens	m
D_{knot}	knot diameter	m
f_F	Focal length for Fresnel lens	m
f_p	Focal length for parabolic trough	m
h_{fg}	The latent heat of the vaporization of water	J/kg
I_{S}	The incident solar radiation intensity	W/m^2
L_{abs}	The length of the absorbent tube	m
L_{knot}	The length of the knot tube	m
L	Length	m
M_{ev}	The amount of daily productivity of fresh water	kg/s
P_C	Productivity Classic	L/m^2
P_{Enh}	Productivity enhancement ratio	
P_{M}	Modified water productivity	L/m^2
Q_s	The amount of energy received by the aperture area	W
Q_u	The amount of useful energy	W
T_W	Temperature basin water	°C
W	Width	m

η_{th}	Energy thermal efficiency	-
Greek Symbols		
η	efficiency	
α	depends on the prism angle	
	Subscripts	
abs	Absorber	
amb	Ambient air	
b	basin	
d	Daily	
F	Fresnel lens	
g	Glass	
n	refractive index	
p	parabolic trough	
R	Lens radius	
w	Water	
Abbreviations		
Symbols	**Description**	
CSP	Concentrators solar power	
CSS	Conventional Solar still	
DS	Double slope	
PTC	Parabolic trough collectors	
SSSS	Single-slope solar still	
TDS	Total dissolved solids	
VFR	Volume flow rate	

Chapter One

Introduction

CHAPTER ONE

Introduction

1.1 General introduction

Water is an essential element for life. Although water covers 71% of the total surface area of the Earth, 98% of it is salty water unfit for human use [1]. The problem of scarcity of fresh water is one of the biggest problems facing societies today [2]. Most countries in the world use desalination systems powered by electric or thermal energy, which consume a lot of energy, in which production costs increase by about 50% compared to systems powered by renewable energy, in addition to the environmental pollution it causes [3][4]. Humanity resorted to alternative energy sources to solve the problem of water scarcity with long-term and sustainable capabilities [5]. Solar energy is one of the alternative solutions with great potential in many parts of the world. The greatest benefit of solar energy compared to other energy sources is that it is pure and can be generated without any pollution to the atmosphere [6]. Nowadays, one of the enormous challenges is how to reduce the demand for fossil fuels, using renewable energy is the best option and has been the subject of research around the world. Recently, considerable efforts have been made to find alternative energy sources and improve their efficiency to reduce problems resulting from the use of fossil fuels and the focus on renewable energy use [7]

1.2 Solar energy

The sun is an important source of unlimited energy on this planet. The concept of solar energy is the use of solar radiation or thermal energy obtained from solar radiation. The distribution of solar radiation falling on the Earth's surface varies according to latitude and longitude, as some countries receive abundant solar radiation, including Iraq at a location of 32.1°N / 44.19°E. Iraq annually receives between 1968-2244 kWh / m^2 of direct radiation, as shown in Figure (1.1)[8][9].

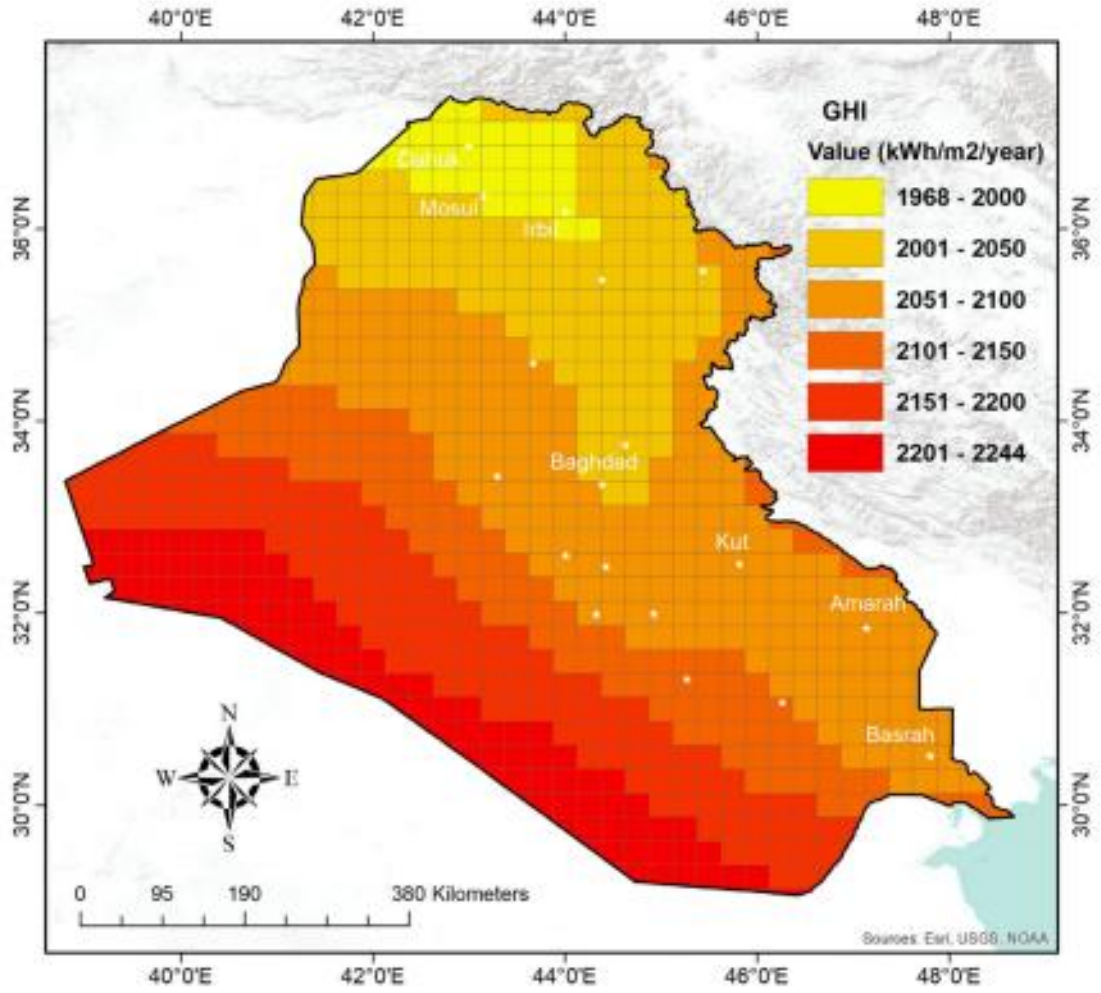

Figure (1.1): Map of horizontal solar radiation in Iraq[9].

Using sunlight and converting it into thermal energy requires solar concentrators.

1.3 Solar radiation concentration.

These are techniques that focus solar radiation falling on their surfaces through reflection or refraction. They are mostly coated with a layer of nickel, aluminum sheets, or mirrors. Reflects the sunlight falling on the mirror's surface or lens towards the center of the surface of the receiver with a smaller area. It often requires a tracer to get as much heat as possible. Solar energy is collected and converted into electrical or thermal energy used in many fields, such as freshwater production, electricity generation, heating, industry, sterilization, etc.[10]. Depending on the nature of the concentration, there are two types of concentrating solar collector reflectors.

1.3.1 Linear solar energy concentrating

The area of concentrated solar radiation in this type of solar reflector is a linear shape whose length is equal to the length of the focusing element. The system operates at an average temperature (150 - 400°C), and its efficiency ranges from 50 to 60%. It can divide into two types as follows [11]:

a) **Parabolic trough collector (PTC):** It consists of a highly reflective U-shaped surface with a high thermal conductivity absorption tube placed along its focal line. The absorbent tube is often painted black to increase its heat absorption. This type of solar collector needs one-axisb system to track the sun, as shown in Figure (1.2) [12].

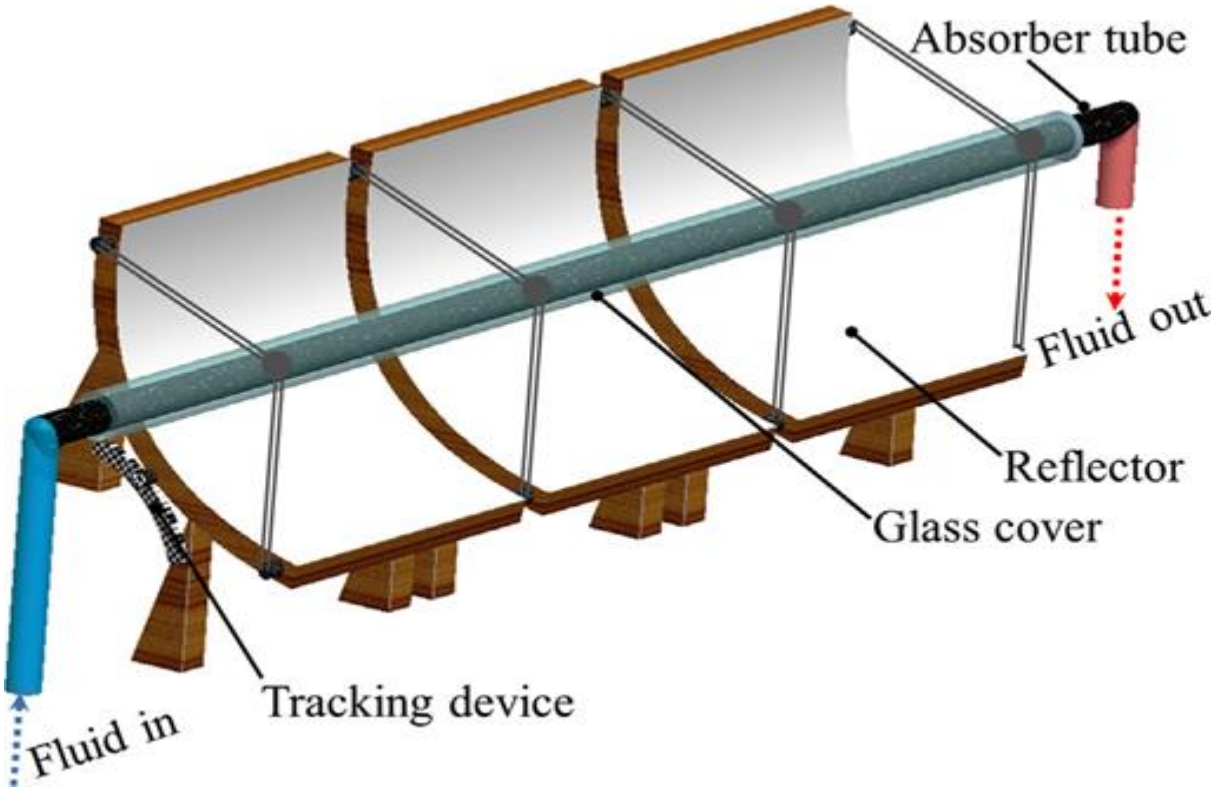

Figure (1.2): Solar reflector concentrator (PTC) [12].

b) **Linear Fresnel reflector (LFR):** It's a modified version of a parabolic trough, a linear Fresnel reflector that divides the trough into long, flat, or slightly curved rows to focus the solar beam. The parabolic shape of a mirrored basin focuses on flowing in a way that resembles a small basin. A straight-line receiver, mounted downward, takes this large influx of solar spectrum that is

widely spread in the working environment to be converted into another form of energy, as shown in Fig (1.3) [13].

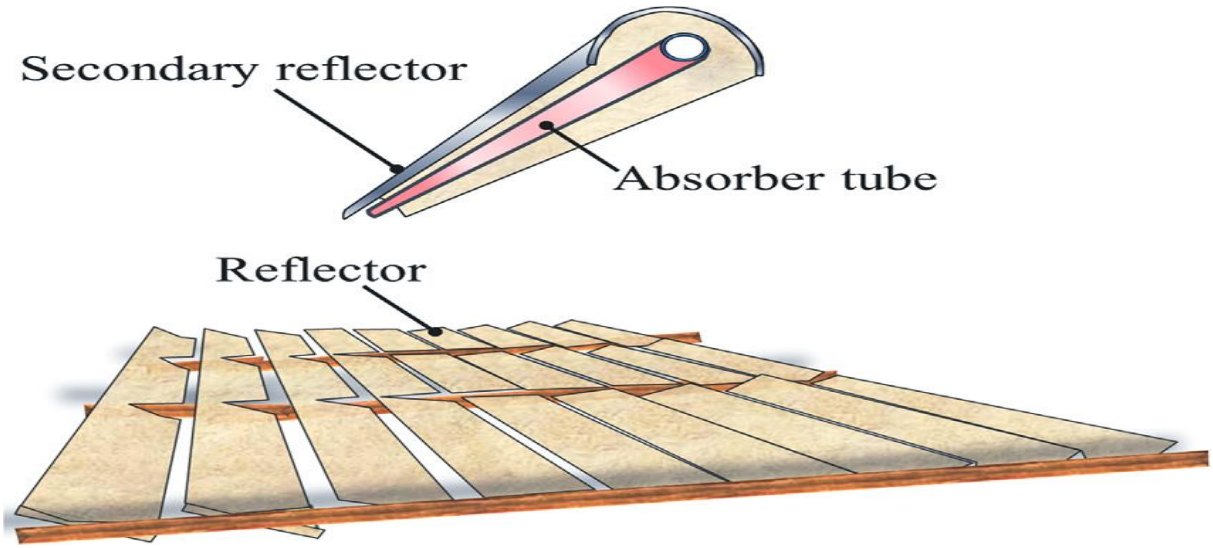

Figure (1.3): Solar reflector concentrator linear **[12].**

1.3.2 Point solar energy concentrating

a) **A parabolic dish collector (PDC)** is a technology that produces high sunlight concentrations, reaching between 100°C and 500 °C. Cylindrical, spherical, conical, and screw pipettes are used with these assemblies. The receivers are usually insulated chambers to reduce heat losses by convection. This focusing technology works effectively with the dual-axis tracking system, as shown in Figure (1.4) [14].

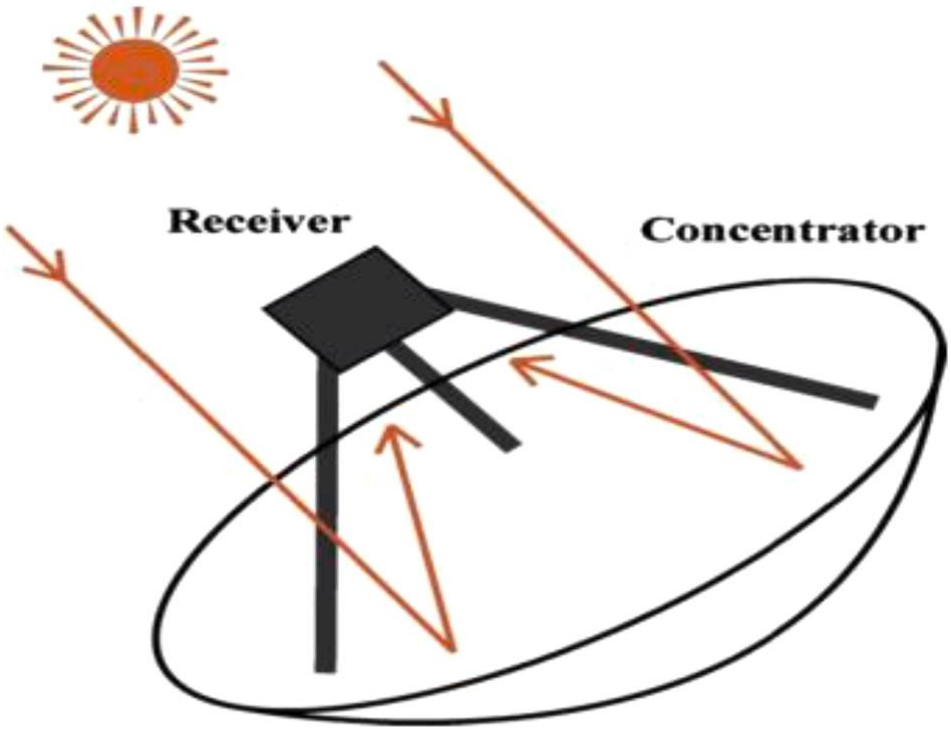

Figure (1.4): Schematic of a parabolic dish reflector [15].

b) Solar concentrator Fresnel

There are two types of solar collector lenses: flat and convex Fresnel lenses, as in Figure (1.5). The sun's rays falling on the lens's surface are refracted perpendicular to the axis. The point at which the sun's rays meet is called the focus (focal point), which is at a distance from the lens called the focal length. Point-focus Fresnel lenses (PFFL) have a series of grooves that bend sunlight into a common focal point along one length that is highly focused. The French mathematician and physicist Augustin-Jean Fresnel in 1822 invented it. Initially, PFFL lenses were made of glass, which was heavy and expensive. Nowadays, most Fresnel lenses are made of polymethyl methacrylate (PMMA), a lighter and cheaper material that is optically equivalent to glass. This lens is widely used in solar engineering due to its many benefits [16].

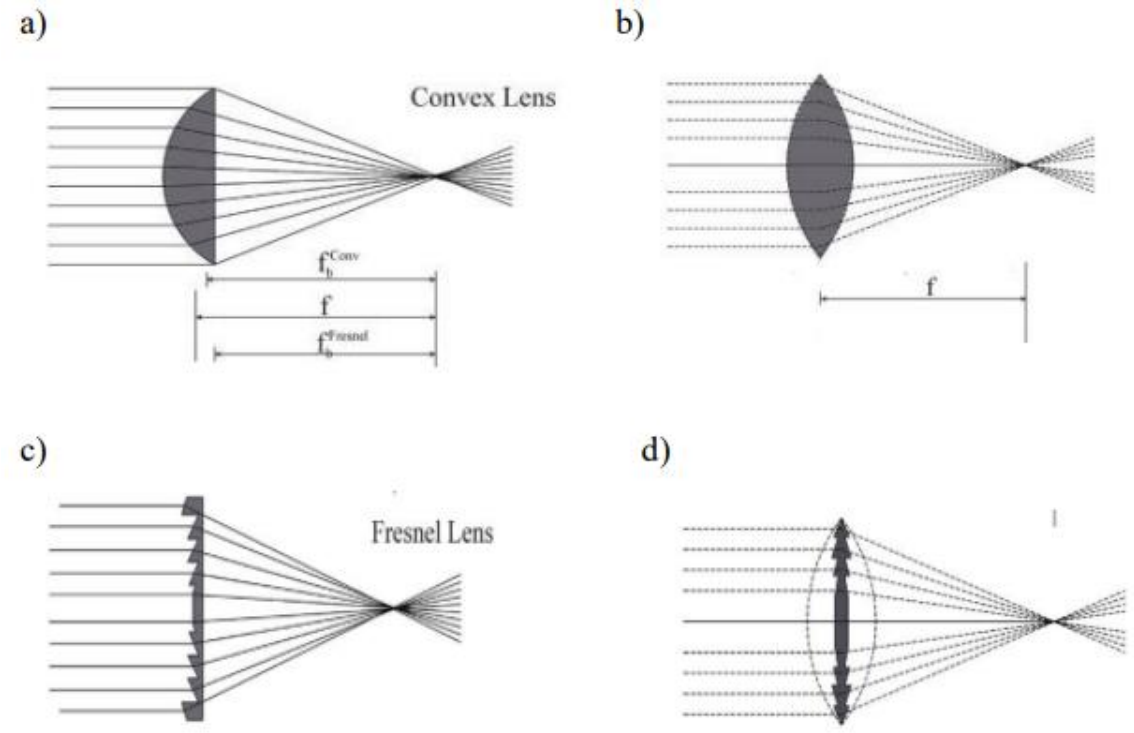

Figure (1.5): a) A convex lens on one side. b) Double-sided convex lens. c) Flat lens with one groove point. d) Flat lens with two sides of grooves [17].

The concept behind Fresnel lenses is that sunlight is refracted at the surface of the lens and reduce the size of the bulk material by forming the grooves in the form of a prism, and turning it into a flat plate increases the absorption of solar radiation and reduces the losses and the total weight of the lens as well, as shown in the figure (1.6)[18].

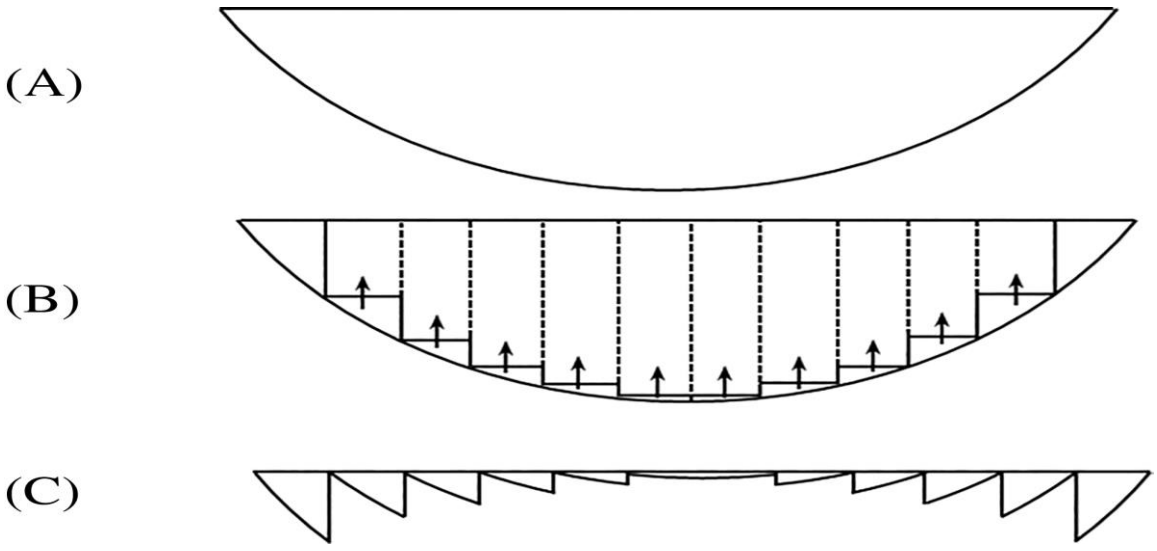

Figure (1.6): (A) Convex lens. (B) Cutting grooves for convex lenses. (C) Fresnel lens [18].

There are two types of concentrating Fresnel lenses:

1. **Spot Fresnel lenses:** They have a circule of grooves that bend sunlight into a common focal point along one length, which is highly focused and short focal length, as in Fig (1.7- a)[19].
2. **Linear Fresnel lens:** They are series of linear grooves that act as a refractive surface and bends parallel sunlight into a common focal line. The sunlight is collected and distributed over one dimension, so the focal ratio of the lens is small compared to the lens of the sport as in Fig (1.7- b) [20].

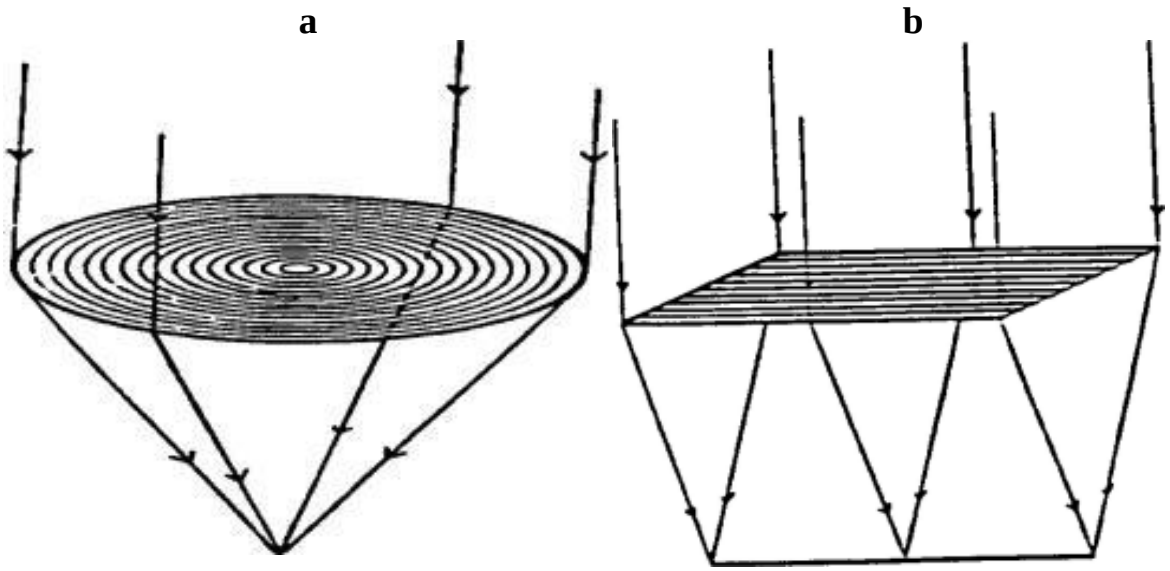

Figure (1.7): a) Schematic point focus Fresnel lenses. b) Schematic linear Fresnel lens [21].

1.4 Solar desalination types

Solar desalination systems are divided into two parts: direct, which uses solar energy to produce distillate directly, and indirect, which uses two sub-systems, one to collect solar energy and the other to desalinate water[22]. Direct solar energy is also divided into passive and active solar energy. Passive solar energy is the collection and storage of solar heat at the same time, while the active solar system collects solar radiation and converts it into thermal or electrical energy using electrical or mechanical devices (such as fans, pumps, etc.). Active solar energy is subdivided into Active solar thermal energy technology and photovoltaic technology; solar thermal energy is applied in domestic and

commercial uses such as drying, heating, cooling, and cooking [23]. There are many factors that affect the yield of solar distilation system such as the concentration of solar radiation, wind speed, working environment temperature, temperatures difference between water and glass, absorption plate area, inlet water temperature into still, glass inclination angle, and salt water depth in basin [24].

1.4.1 Passive solar distillation

There are many types of passive solar distillers, of which we mention two main types:

1.4.1.1 Single basin with single slope (SS)

It is used to filter salty or brackish water. A traditional distillation has a hermetic basin and a highly absorbent surface coated with a usually black material. The basin water heats up and evaporates as the basin absorbs the sun's energy. Water vapor condenses on the inner surface of the cover glass. The condensed water that flows into the basin is collected in the form of distilled water and placed in a storage vessel, as shown in Figure (1.8) [25].

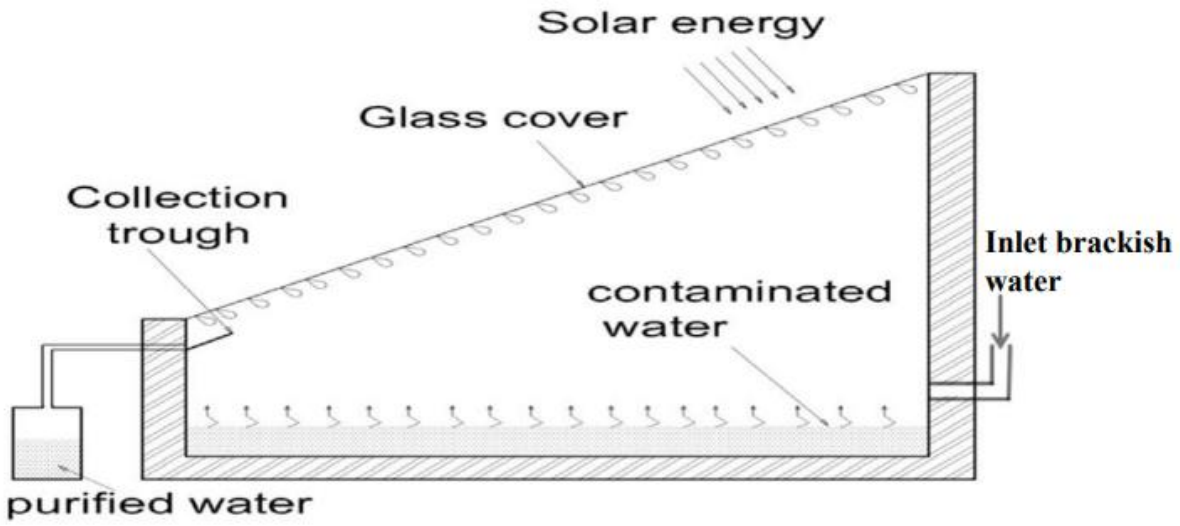

Figure (1.8): Schematic single-slope solar still [25].

1.4.1.2. Single basin with double slope (DS)

It has a basin in the middle and two sides covered with 3 mm thick slanted glass. Concerning the inclination angles of the condensation hood, the smallest (10°), the medium (30°), and the largest (45°), and the height of the sides is 15 cm. Solar radiation can heat the water thanks to the clear glass. The evaporated water condenses under the cover glass before it flows out of the distiller, where it will be collected as shown in Figure (1.9) [26].

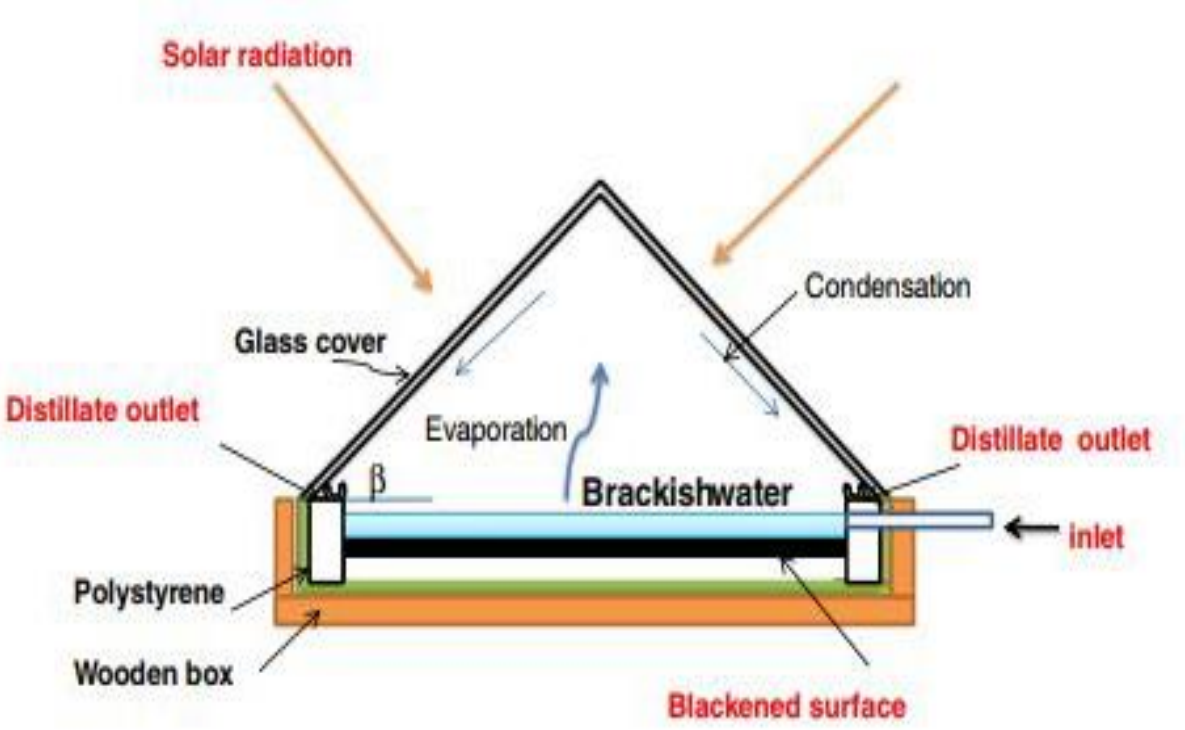

Figure (1.9): Diagram of double-slope solar still (symmetrical) [26].

1.4.2 Active solar distillation

Various techniques are used to improve freshwater productivity due to lower passive distillate production [27]. The water brackish temperature is raised in active distillation using several external sources such as reflective mirrors, Fresnel lenses, solar energy concentrators, evacuated tubes, etc. as in Figure (1.10) [28].

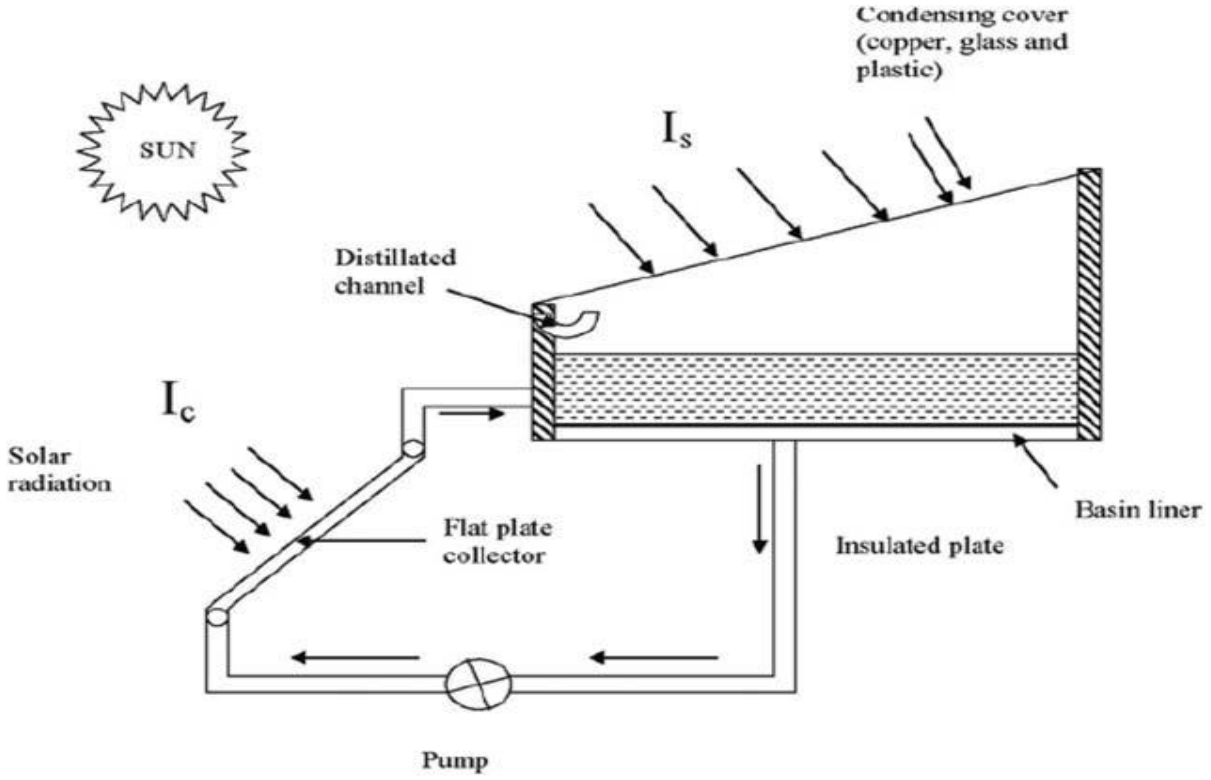

Figure (1.10): View of active solar still with flat collactor [27].

1.5 Solar still disadvantages

1. In most cases, the temperature of the water in the solar still does not reach the boiling point, which does not contribute to killing germs and bacteria.
2. Tilted glass cover due to reduced efficiency.
3. Low productivity of freshwater in conventional solar still.

1.6 Contribution of study

The problem of polluted water requires action to increase the availability of clean water, as it threatens life in general and the individual's health in particular. Most previous researchers have focused on minimizing this problem and improving freshwater productivity. The primary objective of this study is to investigate and develop a fixed solar system design using a parabolic trough collector that positively affects the cumulative yield to increase the yield. In addition, raster Fresnel lenses are used to increase the concentration of sunlight on the receiving tube in the parabola basin, thus increasing the heat of the liquid transported by the pump between the solar collector and the heat exchanger inside the solar distiller.

1.7 Aims of the study

1. Experimental study the performamce of SSS, SSS with PTC, SSS with PTC with Fresnel lenses inside, SSS with PTC with Fresnel lenses outside PTC at actual weather condation of iraqi climate.
2. Studying the effect solar radiation, wind speed, and volume flow rate (VFR) (0.38, 0.5, 0.76) L/min on productive of freshwater.
3. Comparing the results of experimental with previous studies

1.8 Outline of the thesis

The present thesis is divided into five chapters and fife appendices as follows:

1. Chapter one includes an introduction to solar energy and its use, as well as types of solar energy concentrators and the types of solar stills.

2. Chapter two includes an evaluation of previous literature on the use of parabolic troughs and Fresnel lenses for freshwater production.

3. Chapter three describes the practical part of the experiment, such as the materials used, construction and measuring devices. It also includes equations for construction, energy efficiency, productivity improvement ratio.

4. Chapter four presents a discussion of the results of the current study.

5. Chapter five highlights the conclusions obtained in the current study and future recommendations.

Chapter Two

Review of Previous Literature

CHAPTER TWO

Review of Previous Literature

Introduction

In this chapter, the experimental results reached by previous researchers in the field of fresh water production using solar stills will be reviewed and summarized. There are many different methods and techniques for obtaining pure water suitable for human use, but in this chapter the focus is on solar stills integrated with Fresnel lenses or with a parabolic trough.

2.1 Previous studies

2.1.1 Single-slope solar still

Z. A. Faisal et al. (2021) [29] testing a traditional solar still with an area of 0.39 m^2, another still with the same specifications, and a heating basin theoretically and experimentally. The performance of the traditional and modified solar still was also tested, where the glass is cooled by a water spray pump for periods of time (5, 10, 20, and 30 seconds for every 30 minutes). The fresh water productivity for the traditional solar still was 1820 ml per day, and 2410 ml for the equipped solar still. With a glass cooling system for a spraying duration of 10 seconds every 30 minutes (10 seconds / 30 minutes).

2.1.2 Solar still with Fresnel lenses

D. Nagasundaram and K. Karuppasamy. (2016) [30] showed that seawater desalination using a single-slope solar distillation basin with an area of 0.062 m^2 with a Fresnel lens achieves an increase in distillate by 33%. In March Fresh water production for 8 hours by using the lens was 7.5 L/m^2 d. **Rajesh V R et al.** (2016) [31] investigated the performance of a single-slope solar distillation machine with area (0.175 m^2) with a Fresnel lens centered on a preheating tank, as shown in Figure (2.1). The maximum yield of the solar still 15.42 L/m^2 day

with a production efficiency of 55.97% with 33 liters of brackish water in the preheating basin.

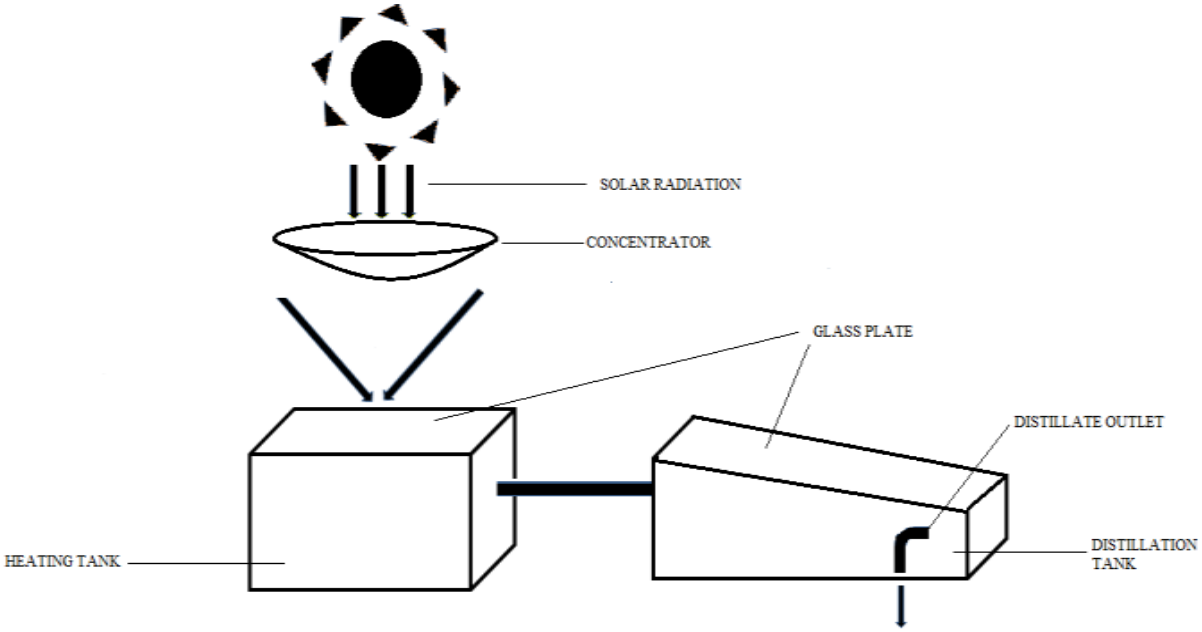

Figure (2.1): Scheme of solar distillers with heating tank and Fresnel lens [31]**.**

Aed Ibrahim toward et al. (2017) [32] used the addition of a Fresnel lens mounted on a two-axis tracker to a traditional single-slope solar distillation unit, as seen in Figure (2.2). In the summer, the production of pure water without using the lens was 4.7 L/m^2 per day, and with the presence of the lens 7.14 L/m^2 per day. The enhancement of production was about 51.9% compared to traditional.

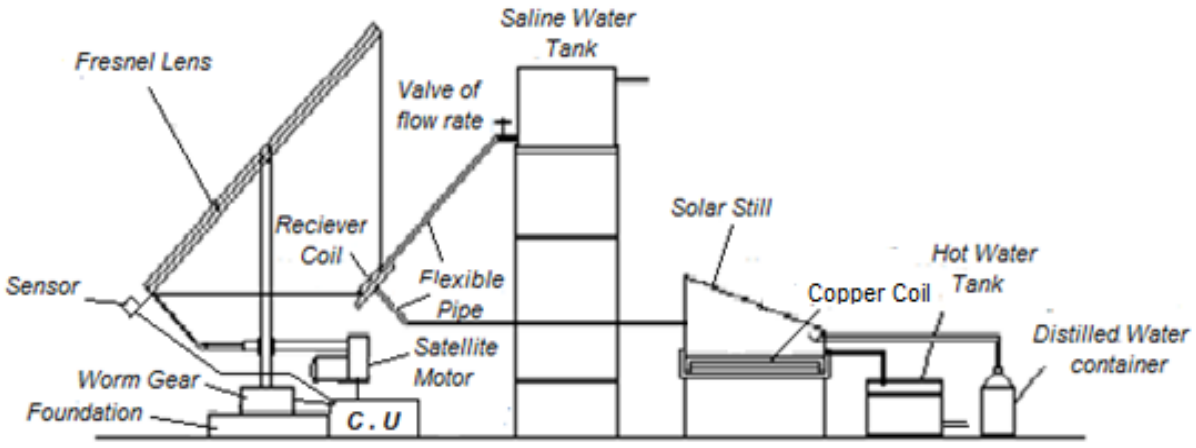

Figure (2.2): An illustration of a solar still with a Fresnel lens [32]**.**

Ravishankar Sathyamurthy and Elsayed El-Agouz (2018)[33], conducted an experimental study by adding a glass cover containing fifteen convex lenses with a diameter of 90 mm (with a total area of 0.095 m^2) to a solar still with an area of 1 m^2. The results showed that the convex lenses work to increase degrees of Heat and thus enhance productivity under the actual conditions of Egypt's climate, where the percentage of improvement in production reached 26.64% compared to the traditional distillery. **Lei Mu et al.** (2019)[34], investigated in the improvement of the performance of a solar still with area 0.2 m^2 by using a Fresnel lens with area 0.75 m^2. A Fresnel lens focuses the sun's rays onto a focal point inside a solar still. Fresh water production was 8.32 L/m^2 per day for the solar still with lens and 1.625 L/m^2 per day without the lens. The results showed an improvement in daily productivity compared with conventional, reaching 467% and a thermal efficiency of 18.4% for the solar still with lens.

Ana Johnson et al. (2019) [35] used a point-focus Fresnel lens (0.275 m^2) coupled with single-slope solar still (0.2 m^2) to improve throughput. Experiments were carried out at depths of 2 cm and 10 cm. With a Fresnel lens, the maximum yield of pure water at a depth of 2 cm was 10.573 L/m^2, and without a Fresnel lens it was 2.755 L/m^2 at the same depth. With an increase in productivity of 281% compared to traditional productivity. **Rakesh Borase et al.** (2019) [36] examined the performance of a single-slope solar distiller (0.36 m^2) containing a heat exchanger. The distillation apparatus's water temperature is improved by a focused Fresnel lens coupled with a biaxial tracking device, which focuses sunlight onto a copper tube moving parallel to the lens, as shown in Figure (2.3). The production of fresh water during 10 working hours was 14.78 liters with a volume of 15 liters of water in the basin.

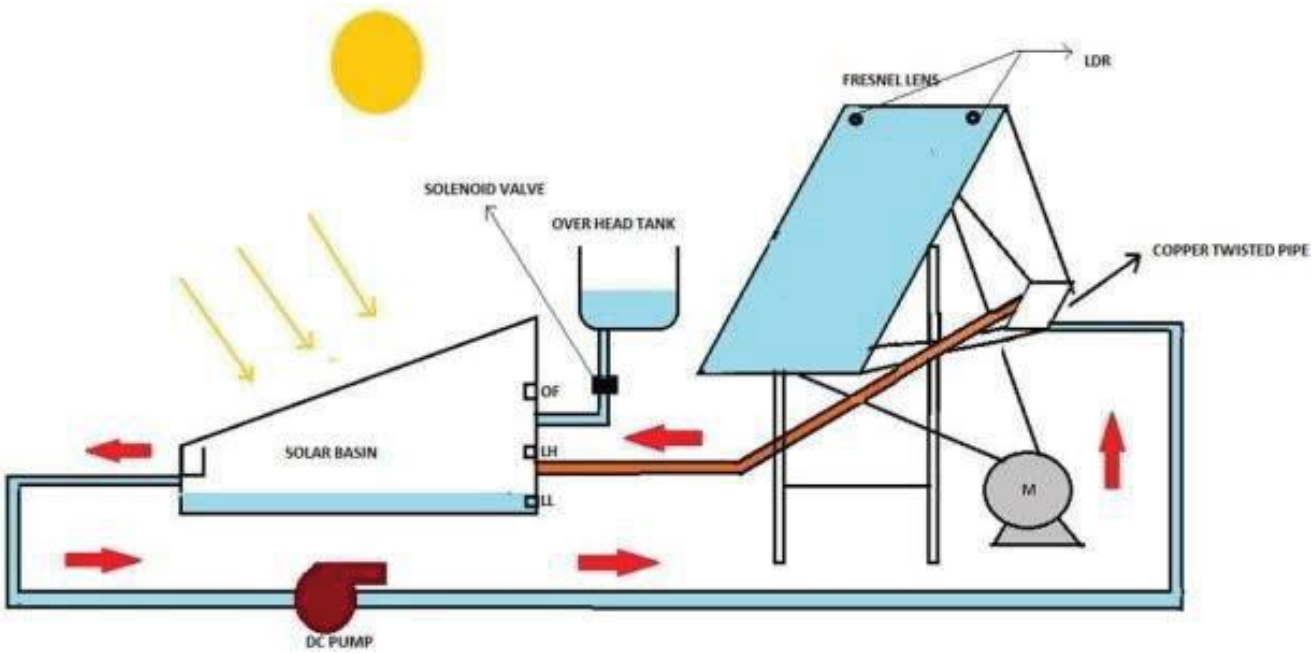

Figure (2.3): Diagram of single–slope with Fresnel lens [36]

M. Muraleedharan et al. (2019) [37] used a comparison of the performance of the solar distillation system, which consists of (a single-slope distiller with an area of 1 square meter, a concentrating Fresnel lens, a receiving tube inside an evacuated glass tube, and a toroidal heat exchanger) with a conventional solar system (CSS) as in Figure (2.4). Water and nanofluids (Al2O3) were used as the heat transfer fluid. Tested under climatic and solar conditions prevailing in Trichy, India. The daily production of the system with water as the heat transfer fluid was 7.404 L/m^2 versus 3.48 L/m^2 for CSS. The system showed a productivity improvement of 112.6% compared to a conventional system and a thermal efficiency of 42%.

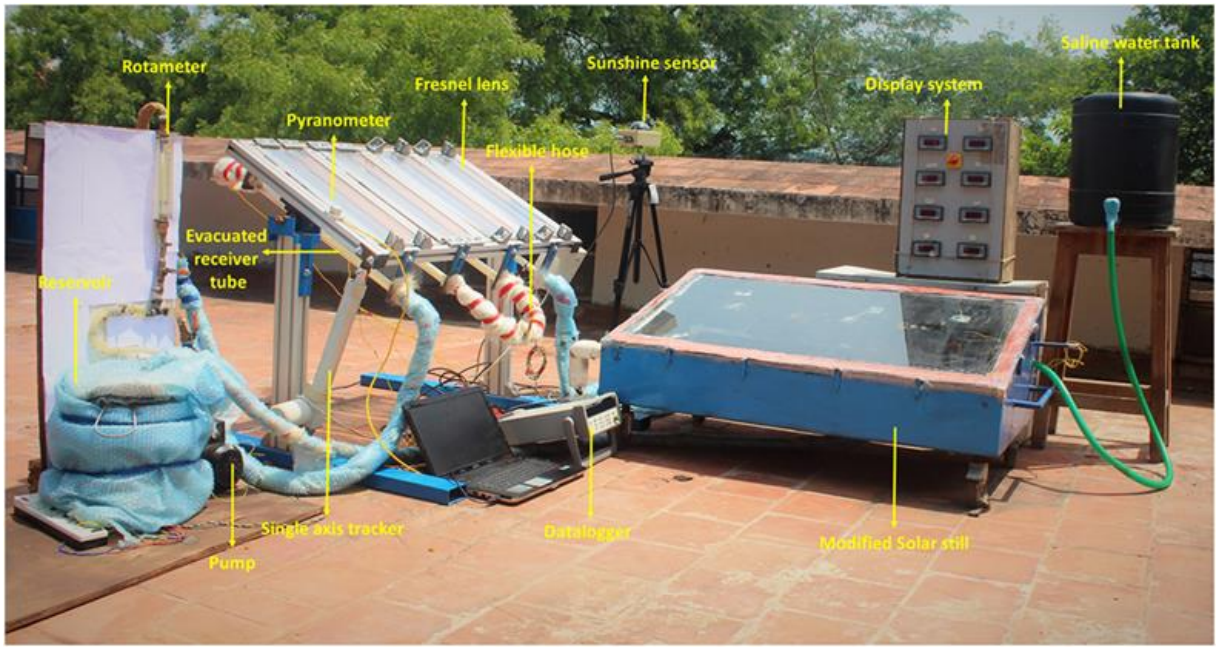

Figure (2.4): Pictures of a modified solar distillation system (MSDS) [37]**.**

Mohammed H.R. AlKtranee et al. (2020) [38] showed that Fresnel lenses improved solar energy productivity under the climatic conditions of Iraq. Three lenses were used with a total area of 0.0081 m^2 with a solar still of 0.2 m^2. In July, the freshwater production for solar energy with Fresnel lenses and conventional energy was 7.87 L/m^2 d and 4.94 L/m^2 d, respectively. It also improved the production by 58.6% compared to traditional methods. Thermal efficiency is 26% for CSS integrated with lenses.

Parimal S. Bhambare et al. (2021) [39] tested the performance of a solar distiller with an aperture area of 0.42 m^2 with a Fresnel lens with an aperture area of 1.06 m^2 experimentally as in Figure (2.5). The experiment was conducted in May. The results showed the maximum freshwater productivity was 1.3 L/m^2d, with an improvement rate of 32.19 % and a thermal efficiency of 43.9%.

Figure (2.5): Photograph of a solar still with a Fresnel lens [39].

2.1.3 Solar still with PTC

Dattatraya G. Subhedar et al. (2020) [40] studied the performance of a parabolic basin integrated with single slope solar still ($1m^2$). Use water and nanomaterials (Al2O3) with a concentration of 0.05% and 0.1% as the heat transfer fluid. With water as the heat transfer fluid and a depth of 25 mm, the maximum freshwater production was 1.5 L/m^2 and the system productivity was improved by 36% compared to the conventional one. **Hossein Amiri et al.** (2021) [41] used a parabolic trough under hybrid solar still (0.6 m long, 0.25 m wide, and 0.075 m high), as in Figure (2.6). In summer, a stationary solar system produces 0.96 liters of fresh water per day, 55% more than it has in winter. The solar collector with tracking systems made 1.266 L per day in the summer.

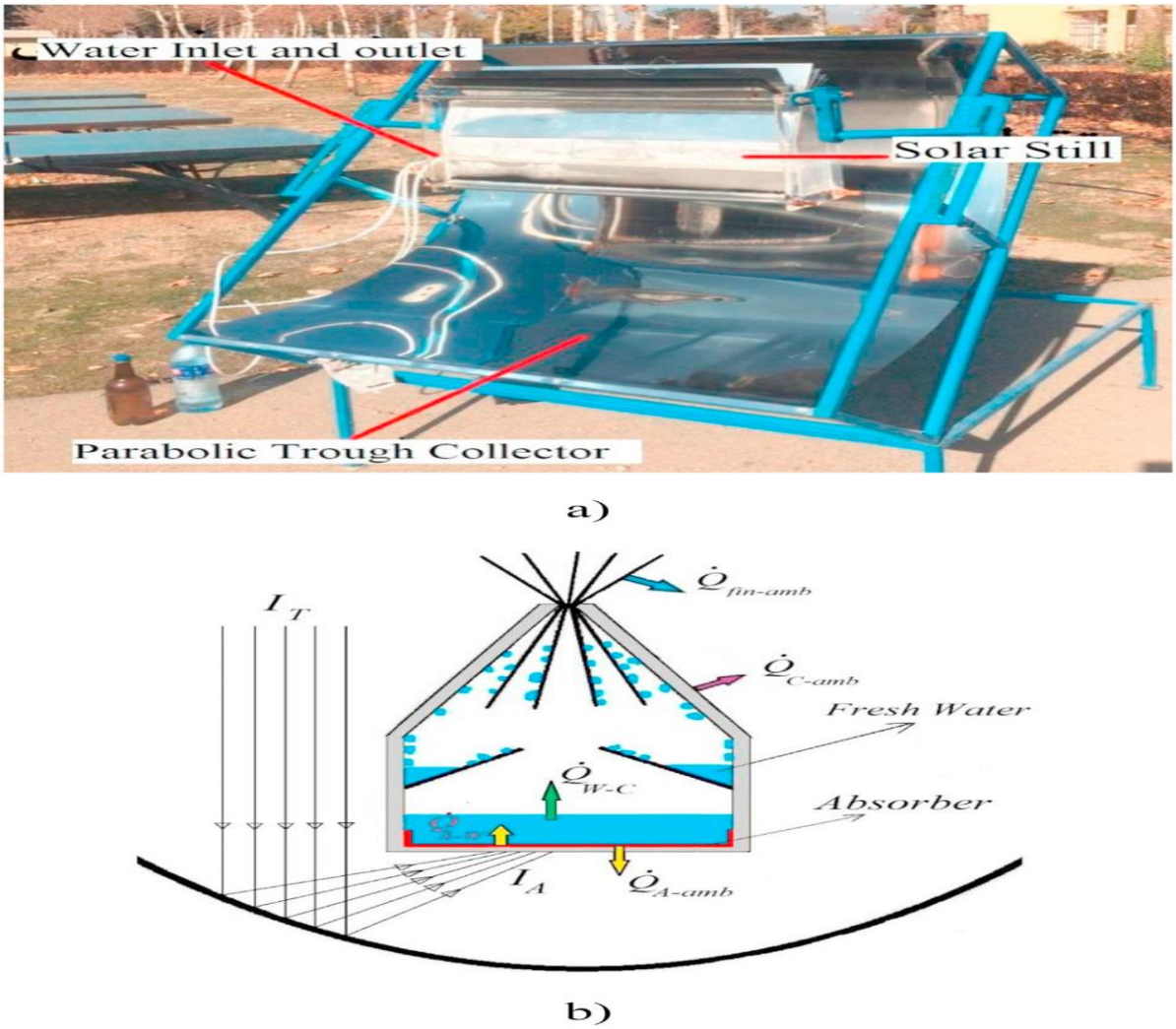

Figure (2.6): a) a picture of the new solar still, b a schematic drawing of the new stellar still, and a flowchart of heat transfer [41]**.**

Randha Bellatreche et al. (2021) [42] compared the performance of a single-slope solar still (1 m2) integrated with aparabolic trough collector with and without sand inside the solar still basin. The combined solar system produced an aquarium equivalent of 5.1 L/m^2 d of fresh water, a 50% improvement compared to the sand less solar still produced 3.4 L/m^2 d.

Amrit Kumar Thakur et al. (2021) [43] tested the performance of a single-slope solar distillation basin of 0.5 m^2 containing granular activated carbon by use a parabolic trough collector with an area of 4.2 m^2. The system with a layer of activated carbon showed increased evaporation rates. The production of fresh

water was 4.36 L/m^2 per day for the conventional design and 8.08 L/m^2 per day for the system with an activated carbon layer. The production efficiency of the modified design was 85.2% compared to the traditional solar still.

Hamdy Hassan et al. (2020) [44] studied the performance of a single-slope solar distillation basin with an area of 1.5 m^2 for six cases are conventional, a single-slope solar still containing a steel grid, single- slope solar still with a sand layer inside, a single-slope solar still integrated with a parabolic solar concentrator with area 3m^2, a single-slope solar still containing a steel grid integrated with a parabolic concentrator as in Figure (2.7), single - slope solar still with sand layer combined with a parabolic concentrator. The maximum fresh water production in May is 3.96, 4.32, 4.67, 7.74, 8.15, and 8.77 L/m^2 for six cases, respectively. The percentage of productivity enhancement is 70.4% and the thermal efficiency is 23% for solar still integrated with a parabolic trough.

Figure (2.7): Photo of the solar distiller (CSS) integrated with PTC[44]**.**

Anil Kumar et al. (2020) [45] used a single-slope 1m^2 solar collector with a 1.513 m^2 parabolic trough collector as shown in Figure (2.8). Test the system with three saltwater levels (0.15 m, 0.10 m, and 0.05 m). The hot water flows from the receiving tube to the solar distiller basin, as it is less dense than the water inside. Freshwater production was (3.2 L/m^2, 3.645 L/m^2, and 4.1 L/m^2) for each level,

respectively. The thermal energy efficiency was 16% at a water level in basin of 0.15 m.

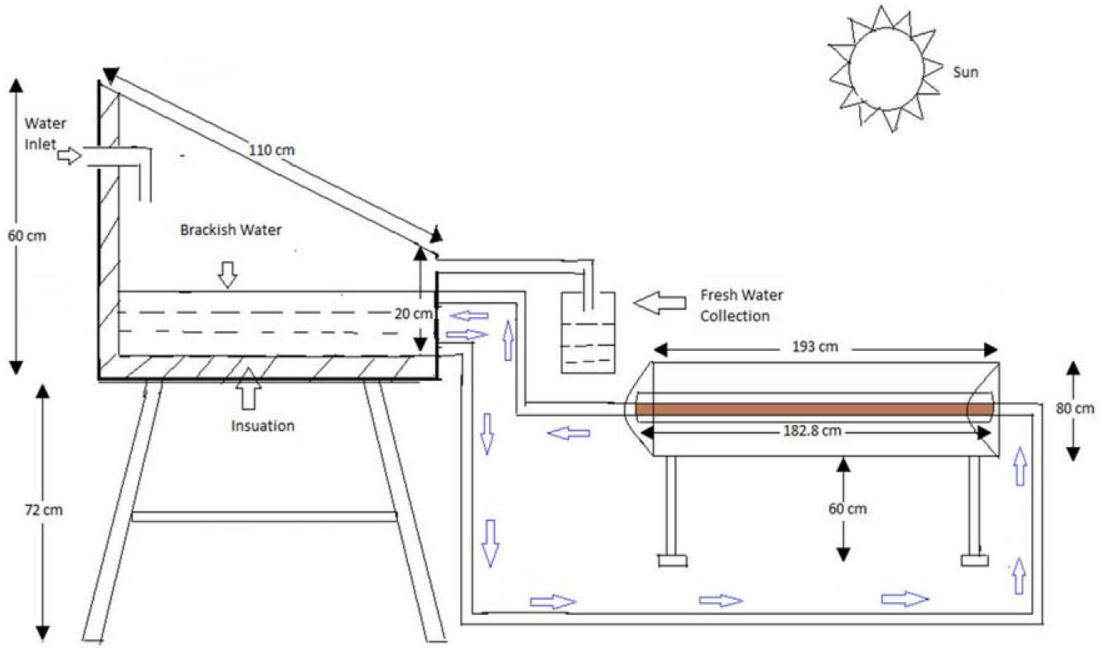

Figure (2.8): Scheme of preheater with solar distiller (CSS) [45].

Jamel Madiouli et al. (2020) [46] used an empirical comparison of three solar systems with a constant area of 1 m^2 (conventional still, single-slope solar still coupled with a parabolic trough collector, single-slope solar still contains balls glass coupled with a parabolic trough collector). Use a heat exchanger made of steel and oil as heat transfer fluid. It showed freshwater production and thermal efficiency in December (0.95 L/m^2, 2.19 L/m^2, and 2.4 L/m^2) and (13.5%, 13.65%, and 14.96%) for the three systems, respectively. The energy productivity improvement associated with a parabolic tub without glass balls is 130% compared to a conventional still.

Tamer Nabil and Mohamed M. K. Dawood. (2021)[47] studied the performance of a single-slope solar distiller 1m^2 coupled with a parabolic trough of 2.52 m^2 theoretically and experimentally. A vacuum glass tube was used for the receiving tube and three heat transfer fluids (water, oil, 3% CuO/mineral oil). A finned heat exchanger with oil and nanomaterials was used. In August the pure water yield showed 2.955, 3.475, 4.29, and 5.04 L/m^2 per day for the conventional

and the system with heat transfer fluids, respectively, at depth of 1 cm of salty water inside solar still as seen in fig (2.9). The productivity improvement rate was about 17.6% at use water as heat transfer fluid.

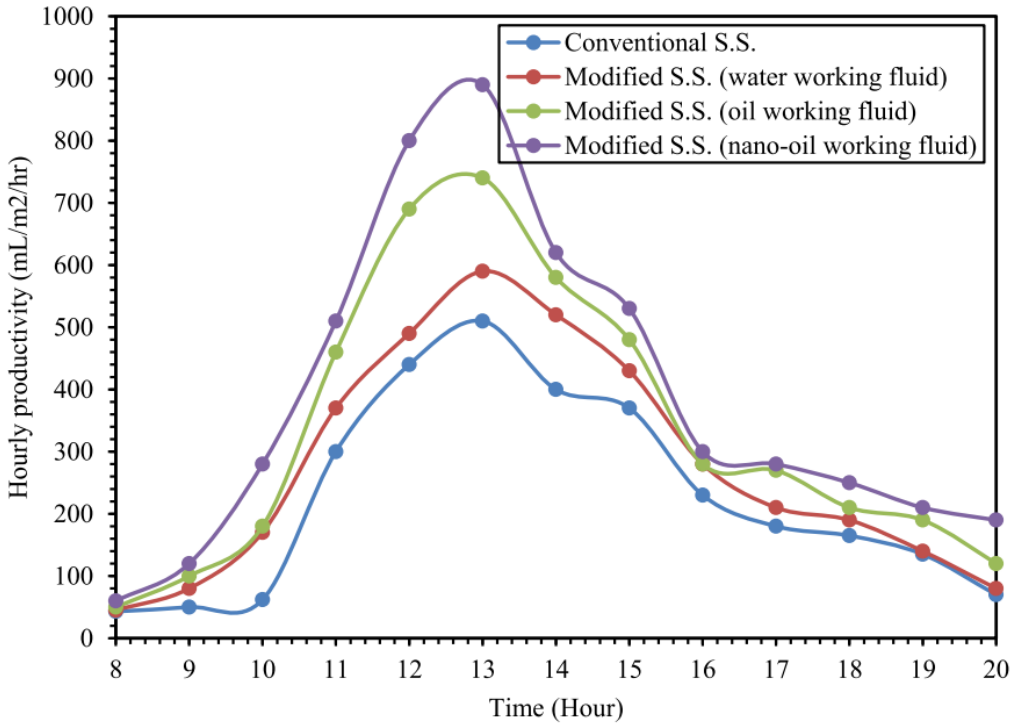

Figure (2.9): Freshwater yield scheme of (CSS, CSS + PTC + water, CSS + PTC+ oil, and CSS + PTC+ 3% CuO /mineral oil) [47].

Hamdy Hassan (2019) [48] studied the effectiveness of stationary solar collectors (single-slope (SS) and double-slope (DS)) with and without PTC on freshwater production. They showed a 6% increase in DS solar energy production compared to SS solar energy as in Figure (2.10). In August the collector (SS+ PTC) produced 8.2 L/m^2 of fresh water and 4.03 L/m^2 of conventional water. The improvement in production was 103.4% compared to the conventional water and the thermal efficiency was at 22.2%.

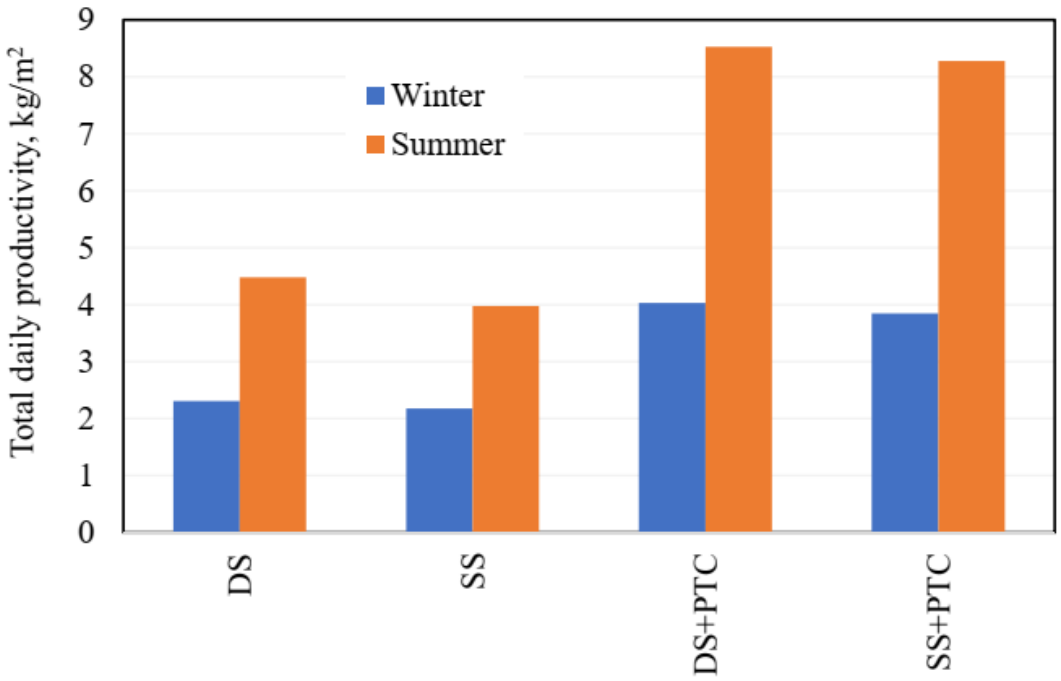

Figure (2.10): Scheme the freshwater yield of (SS, DS, SS+PTC, and DS+PTC) [48]**.**

Muhammad Amin et al. (2021) [49] studied the performance of tubular solar energy consisting of a solar concentrator (parabolic trough) with an area of 5.1 m2 and a receiving tube made of aluminum containing a heat exchanger made of copper. The system produced 5.32 liters in 6 hours with an efficiency of 44.59%. **Hamdy Hassan et al**. (2018) [50] experimentally studied the relationship of the feed water medium with the efficiency of solar dual-slope stills combined with a solar concentrator (PTC) with a tracker. Media (salt water, salt water with steel wire mesh, and sand moistened with salt water) were used as in Figure (2.11). Daily pure water production during summer from a solar still with sand with the parabolic trough, solar still with wire mesh coupled with the parabolic trough, solar still with the parabolic trough, solar still with sand, and conventional stil, is 12.47, 11.31, 10.93, 5.28, and 4.51 L/m^2, respectively. The production improvement of the solar distiller with a parabolic yrough and saltwater medium only was about 142.5% and the thermal efficiency reached 30.1%.

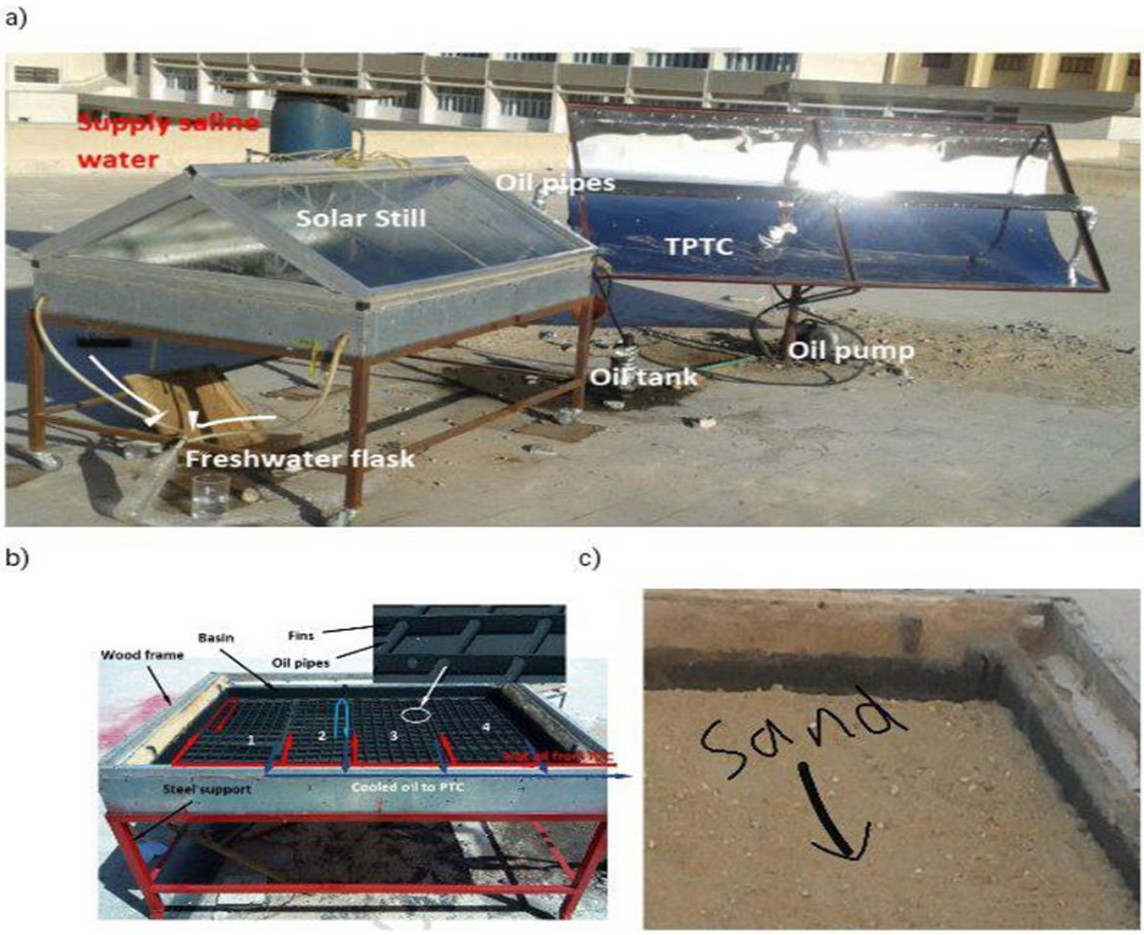

Figure (2.11): (a) The experimental setup. (b) A picture of a solar still with an oil warmth exchanger. (c) The basin's mediums (sand) [50]**.**

Mohamed Fathy et al. (2018) [51] studied the experimental performance of a double-slope with area (1.5 m^2) solar still coupled to a parabolic trough collector. A finned heat exchanger with oil as the heat transfer fluid is used. Fresh water production for a depth of 0.2 m was (2.31, 4.51) L/m^2 for the double-slope distiller, and (4.03, 8.53) L/m^2 for the system coupled with parabolic trough collector, and (5.11, 10.93) L/m^2 for the system coupled with parabolic trough collector with the tracer in winter and summer, respectively. Show systm thermel efficiency of 36.87% for conventional solar and 23.26% and production improvement ratio of 110.9% for solar still with PTC, respectively at a depth of 2 cm.

Hawraa Fadel et al. (2022) [52] examined the performance of a single-slope solar still with an area of 0. 154 m^2 and another with the same dimensions and

specifications combined with a parabolic basin with an area of 1.12 m^2. The practical tests were conducted under the actual conditions of the city of Najaf in Iraq. Water and nano fliud were used as work fluid. The freshwater productivity showed 4.16 L/m^2d, 6.8 L/m^2d in May for CSS and SSSS with PTC when using water as working fluid respectively.

2.2 Summary of literature studies

Table (2-1): A summary of previous studies in terms of productivity and thermal efficiency, experiment type and geographical location.

Author(s), Year, and Reference	Geographical location	Type of study	Solar still area (m^2)	Lens or PTC area (m^2)	Productivity (L/m^2d)	Thermel efficiency (%)
Z. A. Faisal et al. (2021) [29]	Iraq - Najaf	theoretical and experimental	0.39		4.66	
Lei Mu et al. (2019) [34]	32.28 °N, 106.75 °E	experimental	0.2	0.75	8.32	18.4%
Amrit Kumar Thakur et al. (2021) [43]	13.0821°N, 80.2702°E	experimental	0.5	4.2	8.08	8.55%
Anil Kumar et al. (2020) [45]	23,16 °N, 77,36 °E	experimental	1	1.513	4.1 (for level 0.15 m)	16.6%
Jamel Madiouli et al. (2020) [46]	18.2465 °N, 42.517°E	experimental	1		2.19	13.6%
Hamdy Hassan (2019) [48]	26.33°N, 31.41°E	experimental	1.5	3	8.2	22.2%
Mohamed Fathy et al. (2018) [51]	26.33°N, 31.41°E	experimental	1.5	3	8.5 use DS and oil as work fluid	23.26%
Hawraa Fadel et al.(2022) [52]	32.1° N, 44. 19 °E	theoretical and experimental	0. 154 m^2	1.12	6.8 L/m^2d	
Present study	31.99°N, 44. 93°E	experimental	0.23	1.12	7.7	19.23%

2.3 Scope of the present study

Most of the rural and remote areas in Iraq, especially the center and the south, suffer from desertification and drought due to the scarcity of fresh water and the difficulty of access to it, with high turbidity in the water of deep wells. These problems can be solved by using solar distillation devices at a low cost, through which sufficient drinking water is produced for a family of three to four people.The presnt work will focus on:

1- Manfacturing single -slope solar still using parabolic trough concentrator with heat exchanger unit.
2- Testing the effect of Fresnel lenses on freshwater production.
3- Investigation effect of the water flow discharge, solar radiation, wind speed, on basin water tempratuer, and freshwater production.

Chapter Three
Experimental Works

CHAPTER THREE

Experimental Works

3.1 Introduction

The main objectives of the experimental work is to investigate the effects of some ambient factors on the evaporation process, in addition to the effects of some parameters, including (Fresnel lenses and parabolic trough collectors). This chapter includes a description of the experimental apparatus with all its parts and how the experimental measuring instruments were used in the present work.

3.2 Experimental setup

The solar system has been installed in the city of Diwaniyah, Iraq at 31.99°N latitude, and 44. 93°E longitude. function of the experimental system is to produce fresh water, which consists several main units that were built from low-cost materials and are available in the local markets. They are single-slope solar still, parabolic trough collactor, Fresnel lenses, and in addition the heat exchanger unit, as shown in Figures (3.1-a, 3.1-b).

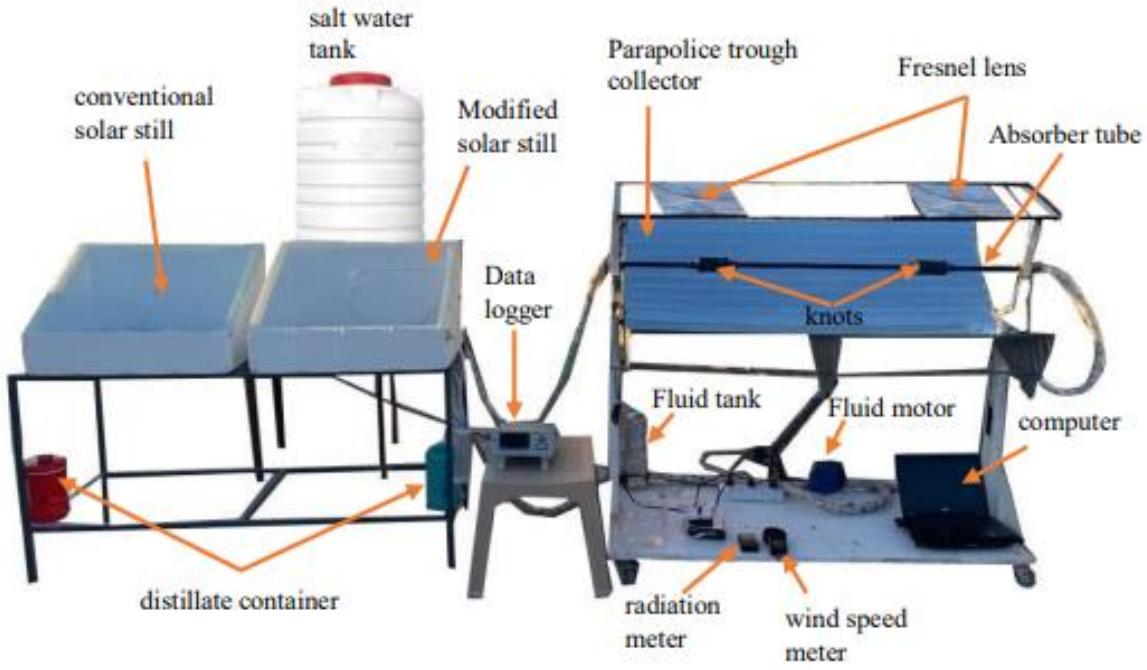

a)

b)

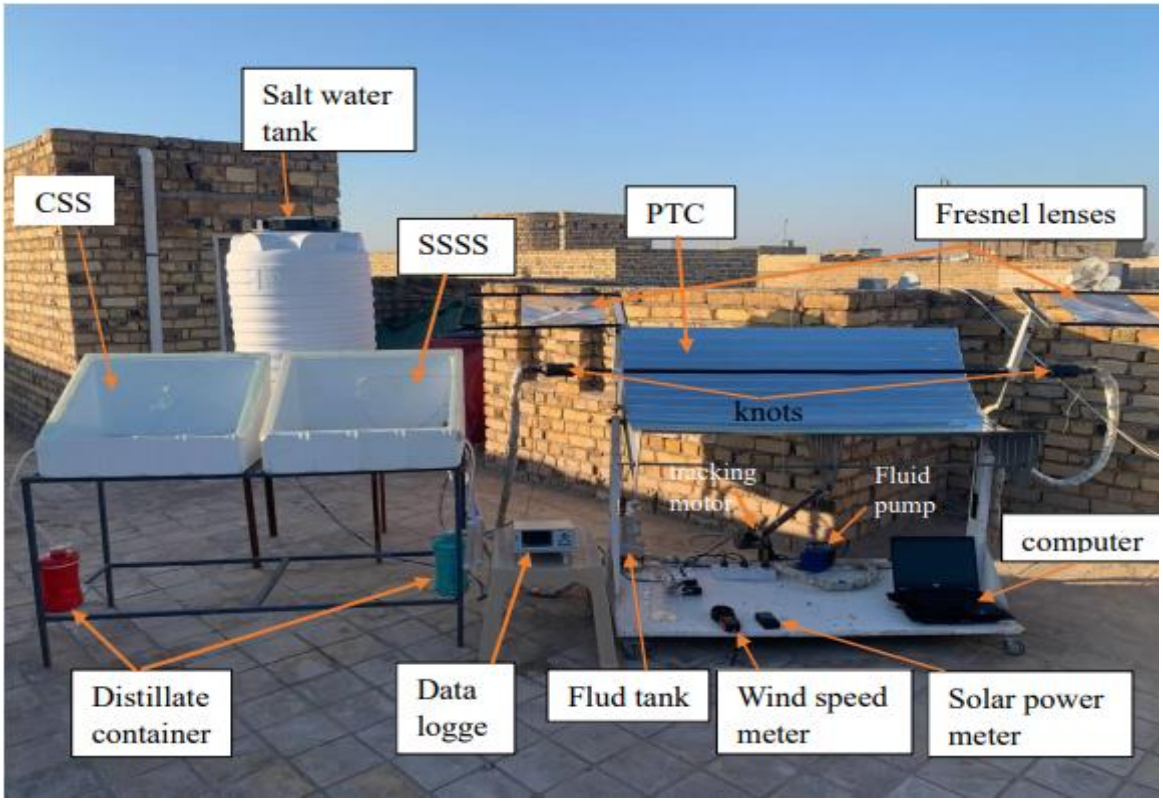

Figure. (3.1): a) Photograph of parts the experiment when using lenses inside the parabolic trough. b) Photograph of parts the experiment when using lenses outside the parabolic trough

Figure 3.2 shows a schematic representation of the solar desalination system used in this thesis.

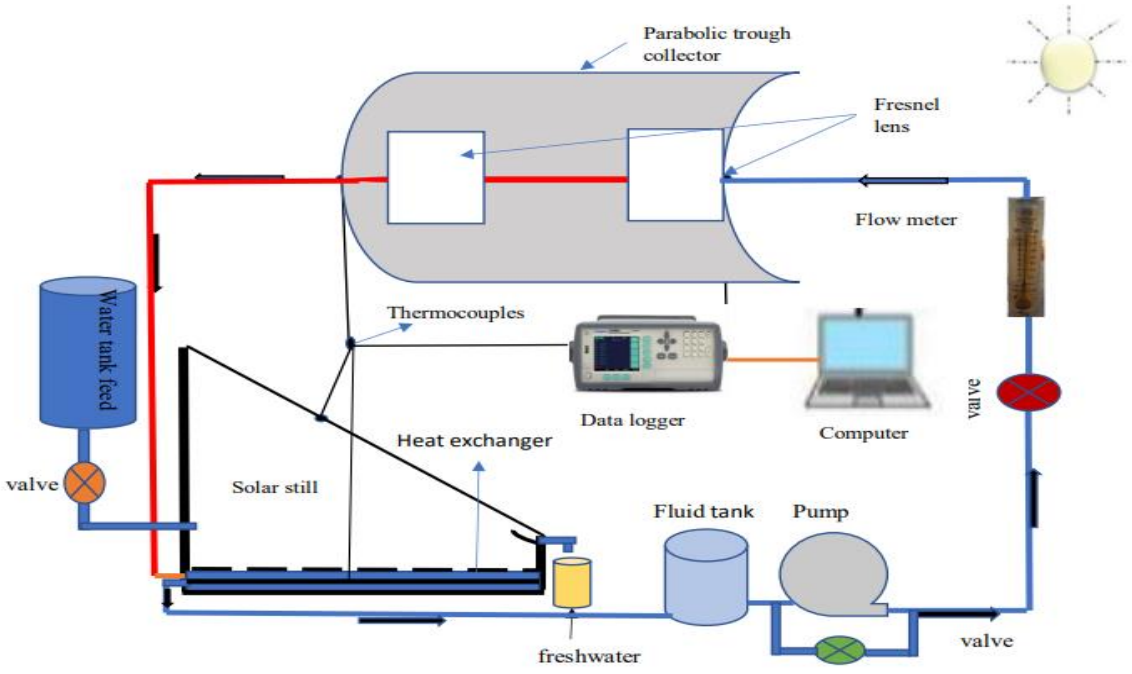

Figure (3.2): Schematic diagram of the device with all its components.

3.2.1 Solar still traditional unit

3.2.1.1 Solar still basin

The solar basin used from polystyrene with area (0.231 m^2) and has dimensions of 69 cm in length, 46 cm in width, 41.25 cm in back height, 14 cm in front height, and 4 cm in thickness, as shown in Figure (3.3). The slope was created by cutting it at an angle of 32 degrees using a CNC machine to maintain clean ends. Polystyrene is characterized by adapting to changes in temperature and pressure and extreme resistance to moisture. Polystyrene is also a good thermal insulator and has practically no leakage.

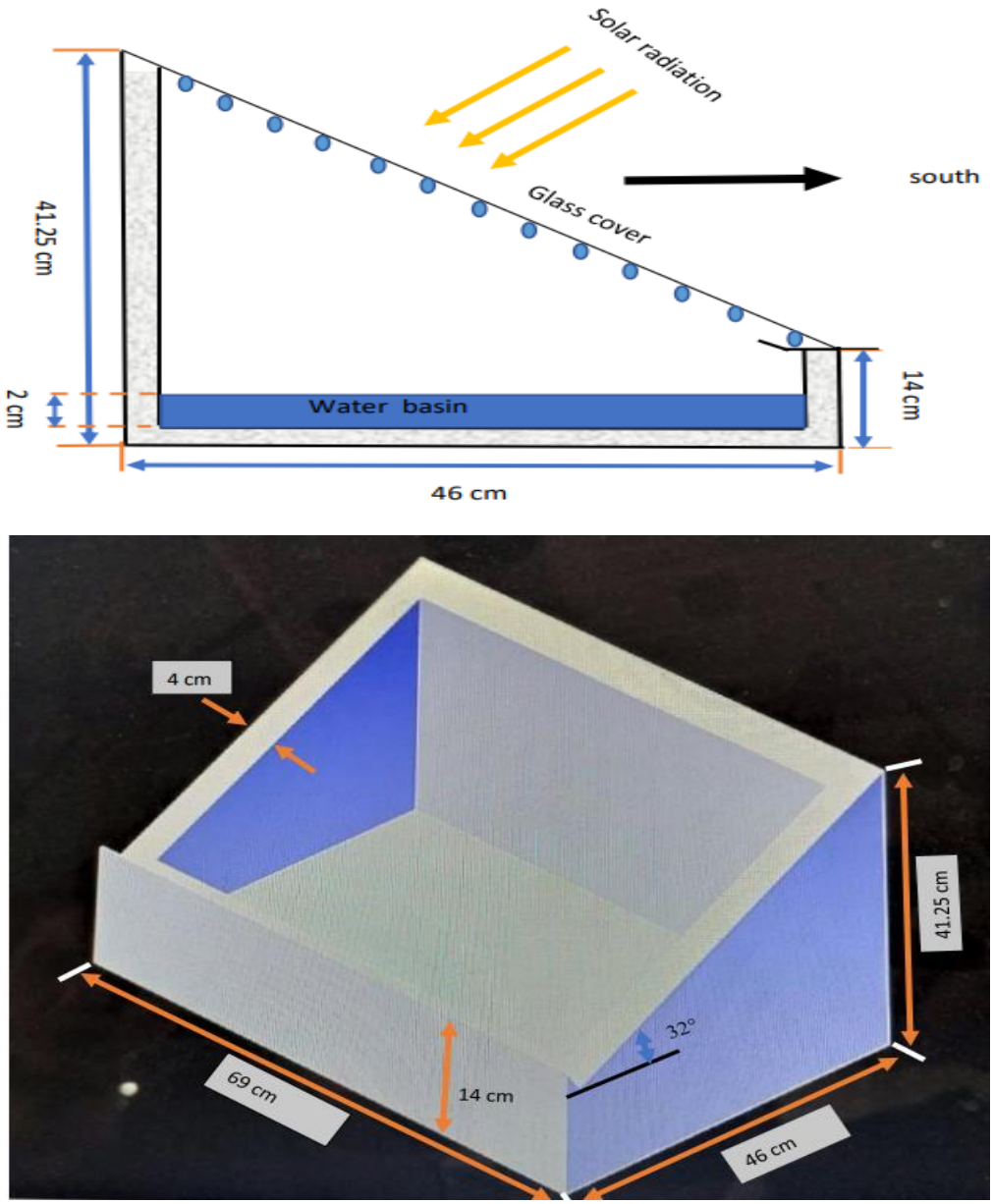

Figure. (3.3): Images and a schematic of a single-slope solar still.

3.2.1.2 Single-slope glass cover

A transparent glass cover was used for the solar distillation basin, with a thickness of 4 mm and an angle of 32 degrees, to transmit most of the incoming solar energy. To prevent steam from leaking out from the solar distillation tank, the transparent cover is securely attached to the basin using adhesive.

3.2.1.3 Distillate collection channel

To collect the condensed distilled water from the basin, the end of the cover glass is placed flush with the inside of the front wall. An opening was made in the front wall (distillation channel) to ensure the outflow of distilled water, with a length of (69) cm, a width of 3 mm, and (1.5 cm) height on one end and (0) cm on the other end, as shown in Figure (3.4).

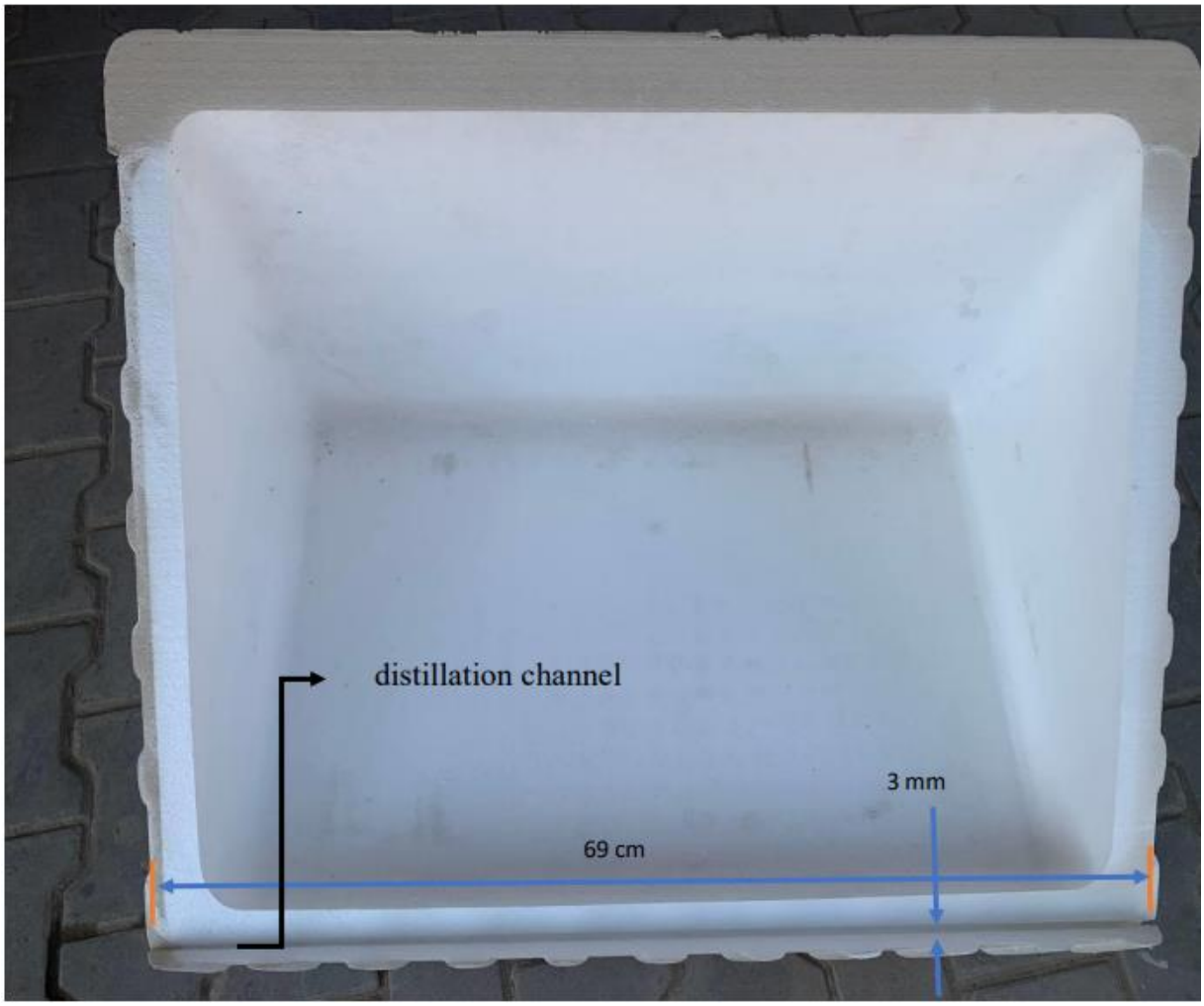

Figure. (3.4): Distillation channel.

3.2.2 Salt water feeding mechanism

A small feeding trough with the same water level was used inside the solar distiller connected with the solar distillation trough directly using a pipe. The small trough is fed from the salt water tank using a mechanical buoy to control the water level inside the two basins (the small trough and the solar distiller trough) i.e. at a depth of 2 cm for the solar distillation basin as shown in the figure (3.5).

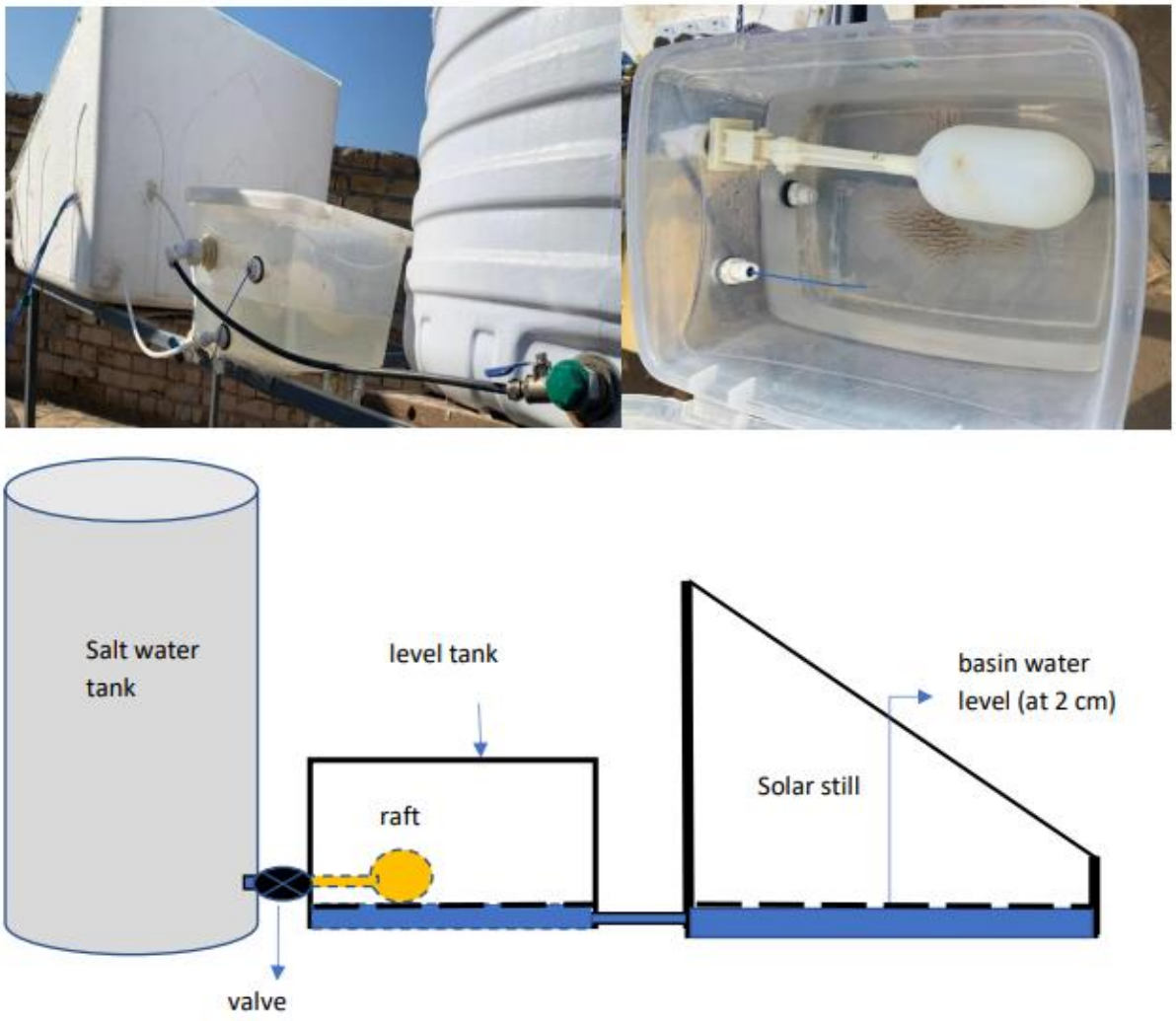

Figure. (3.5): Images and a schematic of a salt water feeding mechanism.

3.2.3 Concentration unit

3.2.3.1 Parabolic trough collector

3.2.3.1.1 The design structure of the parabolic trough collector

The external structure of the parabolic trough with a length of 140 cm and a width of 80 cm was made of iron. The arc of the parabolic trough was determined by CNC machining, and the angle of the parabola edge was 90 degrees. The focal distance from the middle of the parabolic collector arc was also determined to find out the reflected radiation on the receiving tube, as shown in Figure (3.6).

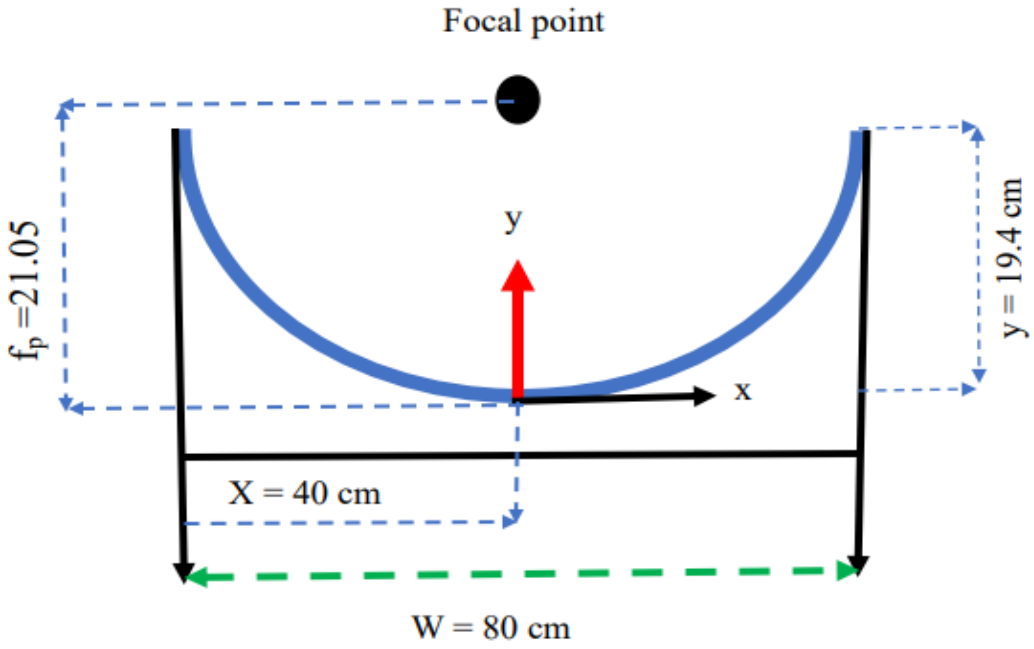

Figure (3.6): Parabolic trough dimensions.

Table (3-1): Specifications of the parabolic trough used.

parameter	value	unit
Aperture area	1.12	m^2
Focal length	21.05	cm
width	80	cm
length	140	cm
Type of PTC	Concave	
Type of mirror	glass reflective	
Absorptivity	0.9	
Concentration ratio	9.91	
Inner receiver diameter	18	mm

Outer receiver diameter	19	mm
Ram angle	90	degree

3.2.3.1.2 The reflector surface

Mirrors placed on the frame of a parabolic trough that acts as a reflector have high reflectivity. Each single mirror piece measures 5 cm wide and 140 cm long. They are paved to create a parabolic basin collector surface as in Figure (3.7).

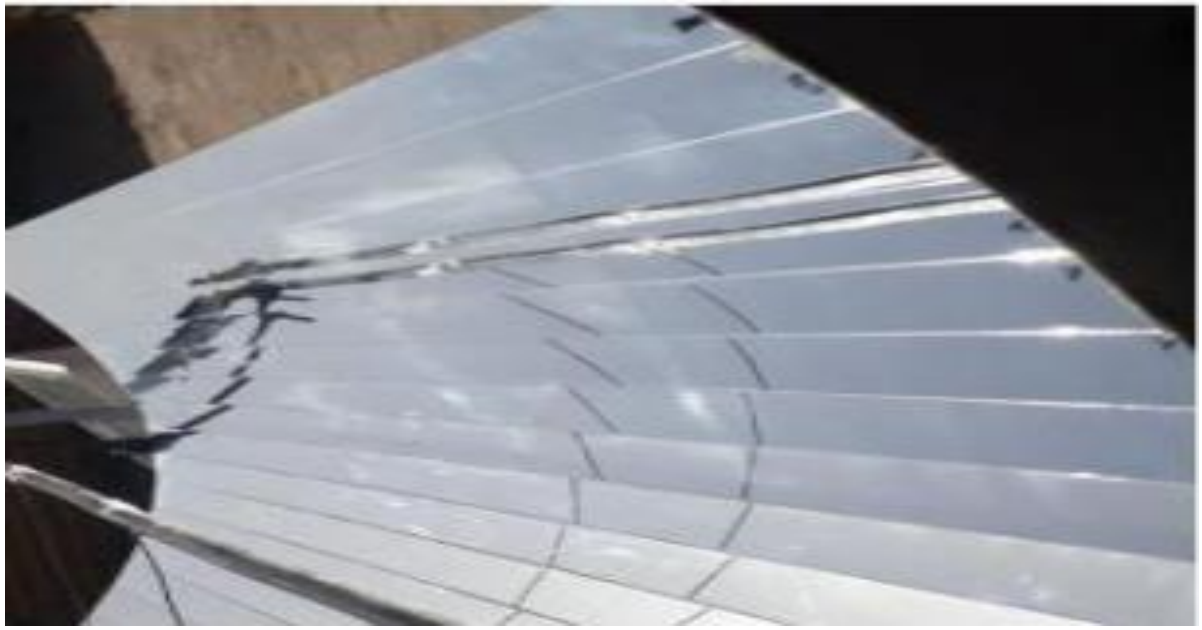

Figure (3.7): Reflector

3.2.3.1.3 Receiver tube

Two receiving tubes are designed with an inner diameter of (18) mm and an outer diameter of (19) mm. A receiver tube of length (158) cm was used with the lenses above the parabola and a length of (215) cm with the lenses on both sides of the basin of the parabola. Each of them contains two cylindrical knots with a length of (10) cm, a diameter of (52) mm, and a thickness of (1) mm. They have been painted black as in Figure (3.8).

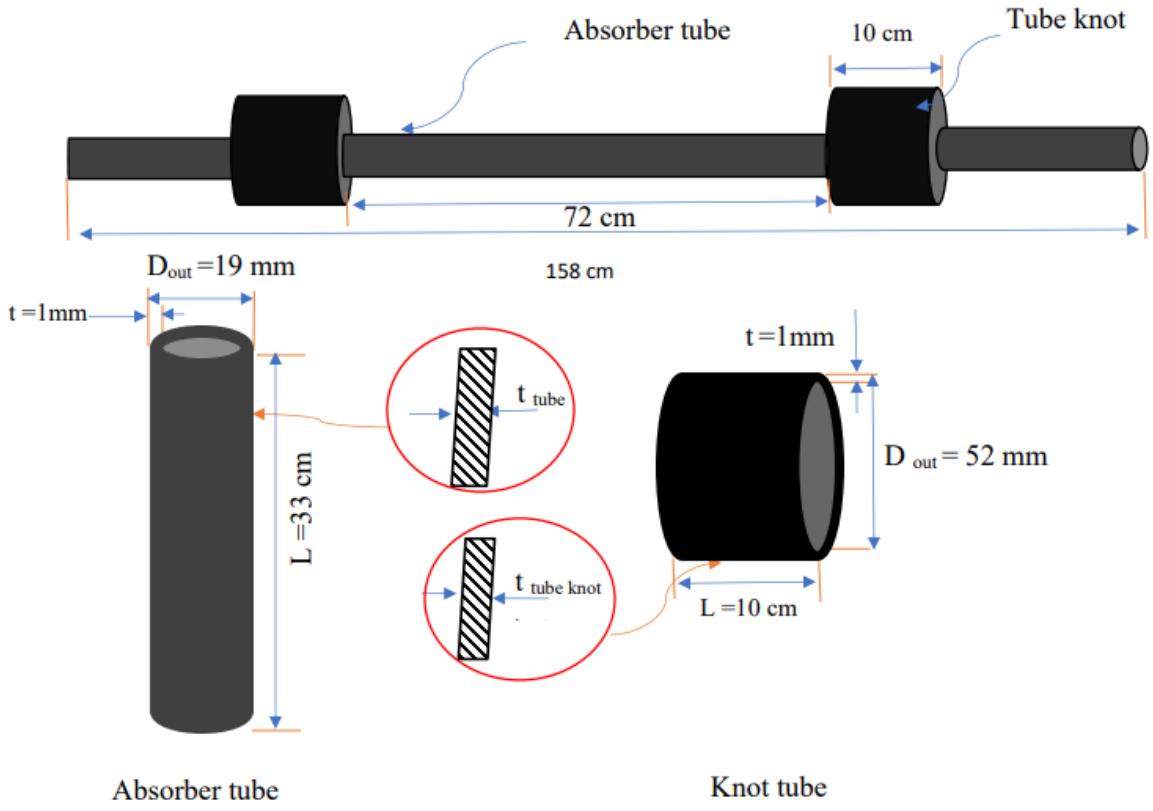

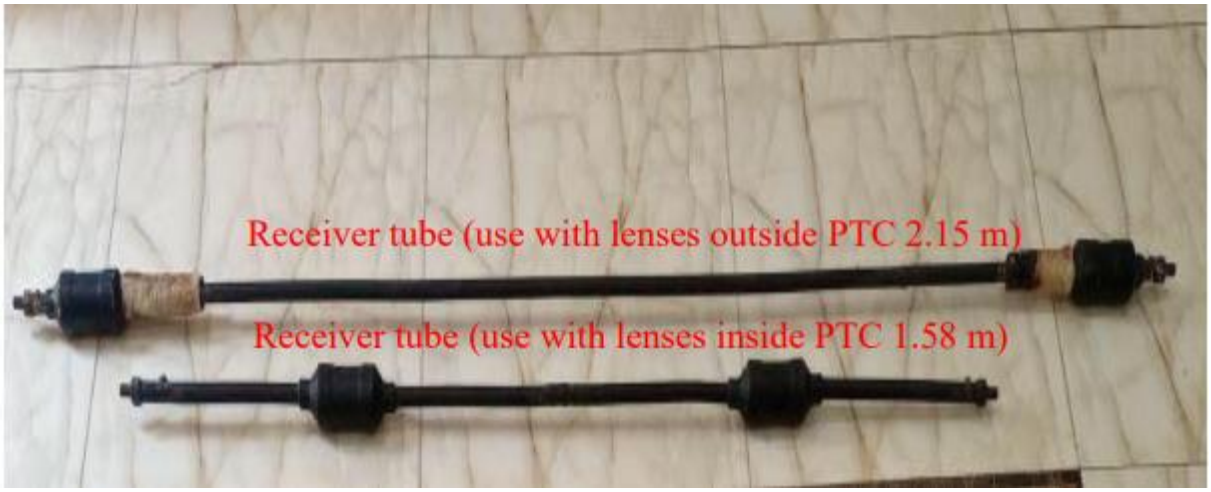

Figure. (3.8): Schematic drawing and photo of the receiving tube.

3.2.3.1.4 Parabolic trough tracking system

Sunlight was manually tracked using an 18-inch motor with an arm length of 50 cm in the closed position and 100 cm in the open position as in Figure (3.9). The tracking motor operates at a voltage of 220 volts, and the maximum weight that the tracking motor can work with is 300 kg. The tracking motor base is installed in the iron frame of the parabolic trough, and the movable arm of the tracking motor is connected to the frame of the reflecting mirrors trough.

Figure. (3.9): Motor of parabolic trough tracking.

3.2.3.2 Fresnel lens

The Fresnel lenses used in the tester are of the square spot type. The length of its side is 30 cm, which is equal to the diameter of its largest prism, and its axial distance is 30 cm as in Figure (3.10).

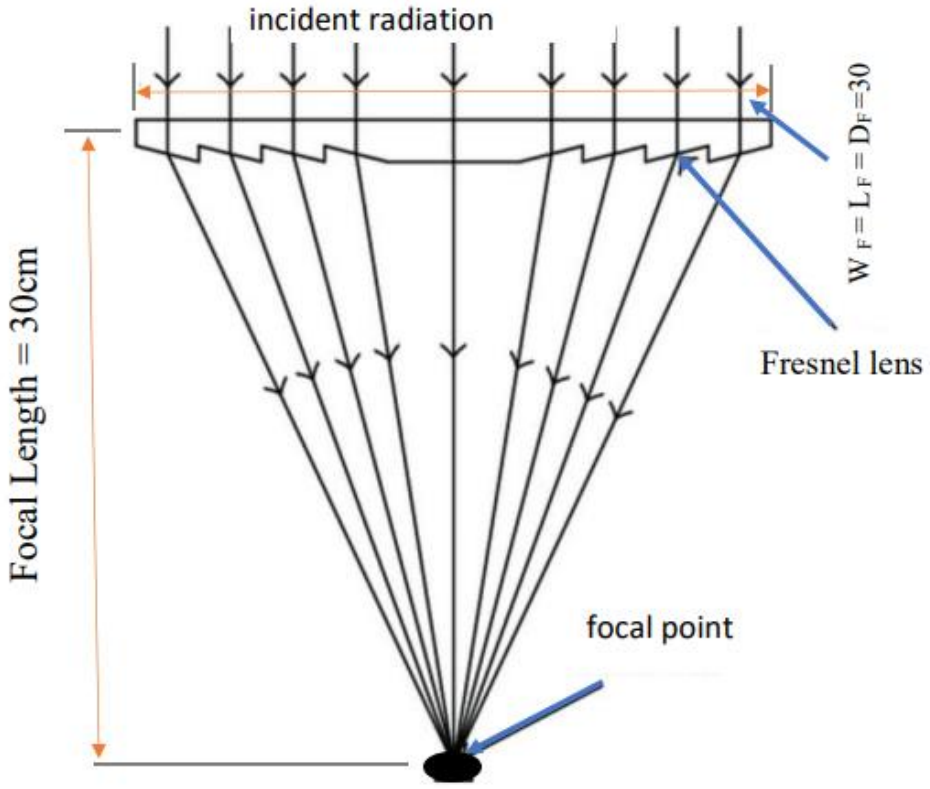

Figure (3.10): Schematic diagram dimension of Fresnel lens.

Table (3-2): Specifications of the Fresnel lenses used.

part	value	unit
Lens type	spot	
Length lens	30	cm
Width lens	30	cm
Area lens	0.09	m^2
Focal length	30	cm
Refractive angle	36.9°	dagree
refractive index	1.49	
largest diameter of the grooves	30	cm

3.2.4 The heat exchange unit

3.2.4.1 Heat exchanger

A heat exchanger with dimensions (58*36) cm was used, which is a winding copper tube with a length of 5.5 m and a diameter of 9.5 mm immersed in 2 cm of salt water inside the solar dweller basin. According to figure (3.11), the heat exchanger and galvanized sheet are coated black to absorb as much heat as possible.

Figure. (3.11): Images of heat exchanger with galvanized plate.

3.2.5 Flexible connection pipes

A set of plastic pipes insulated with glass wool is used to transfer the heat transfer fluid in a closed circulation loop between the solar still and the parabolic trough collector. These pipes are connected as follows:

1. Flexible pipe connecting the heat transfer fluid tank to the receiving tube.
2. Flexible pipe connect the outlet of the receiving tube to the inlet of the solar still.
3. Flexible pipe connects the outlet of the solar still to the heat transfer fluid tank. tank.

3.2.6 Heat transfer fluid circulation pump

The TM20-type pump is used to circulate the heat transfer fluid (water) inside the tubes in a closed cycle. The pump operates at a voltage of 220 volts, a frequency of 50 Hz, a capacity of 150W, and an electric current of 0.88A, with a protection level of IP 44. The pump can work under a maximum temperature of 110 °C for the conveyed liquid and a maximum flow rate of 25 liters per minute. The maximum working height of the pump is 12 m and the maximum pressure is 10 bar, as in Figure (3.12).

Figure (3.12): Flow pump picture.

3.2.7 Working fluid

In a closed cycle, water was used as a heat transfer medium between the parabolic trough and the solar still. A 1.5 liter tank filled with water was used as the heat transfer fluid. Water is transferred from the heat fluid tank by a low-speed pump to the receiving pipe and then to the solar still via flexible connecting pipes. It returns to the tank from the solar still, and the cycle is repeated. The flow meter, which will be mentioned later, determines the flow rate of the volume of water.

3.3 Parabolic trough calculations

The parabola used in the present work is a solar collector focused on a straight line in one dimension and curved as a parabola in the other two dimensions, lined with high reflectance mirrors. Parabola calculations include calculating the focal length (f_{Lp}), and solar radiation concentration ratio (CR_p) shown in Figure (3.13)

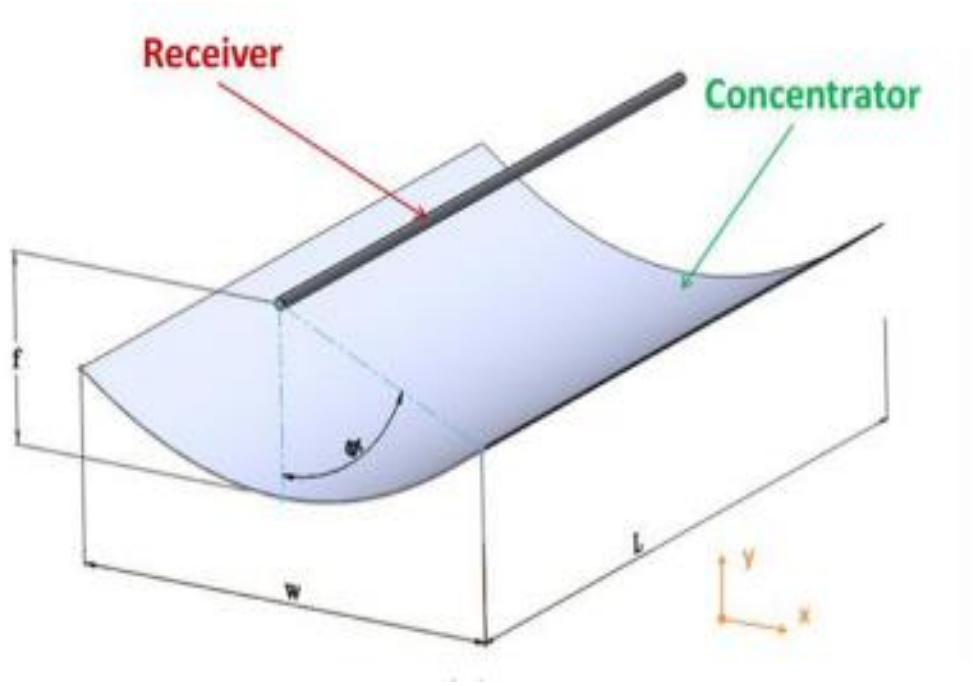

Figure (3.13): The schematic diagram of a reflective parabolic trough[53].

3.3.1 Focal length (f_{Lp}):

The focal length of the reflective parabolic trough (f_{Lp})can be found by the following equation[54]:

$$f_{Lp}=\frac{x^2}{4y} \tag{3.1}$$

Where x is the horizontal coordinate and y is the vertical coordinate of the focal length.

3.3.2 Solar radiation concentration ratio

The surface of the reflective mirrors of the solar concentrator (the larger area) reflects the incident radiation towards the receiving tube (the smaller area), to obtain the largest possible amount of solar radiation on the receiving as shown in Figure (3.14).

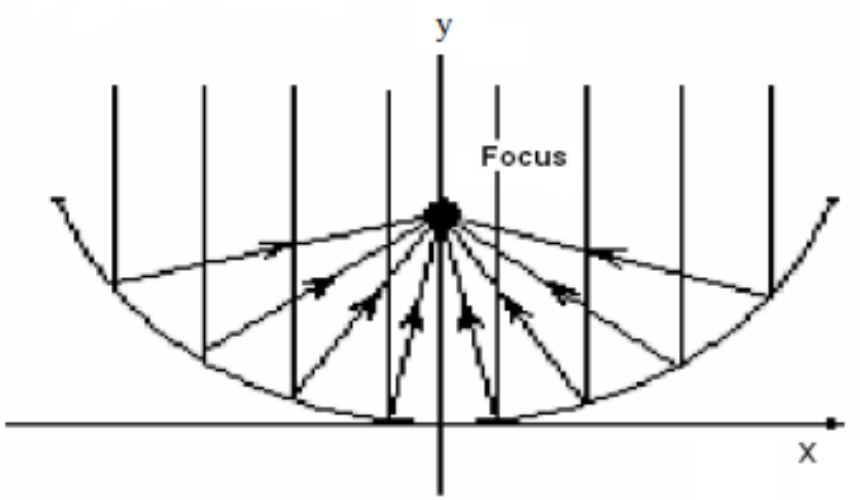

Figure. (3.14): Schematic diagram of a parabolic trough concentration[55]**.**

The concentration ratio (CR_p), which is the ratio of the effective aperture area (A_p) to the a area of focus on absorber tube (A_{foc}), is the most important feature of a PTC [56].

$$CR_p=\frac{A_p}{A_{foc}} \tag{3.2}$$

The area of the parabolic trough collector (A_p) is the product of the trough width (W_p) and the trough length (L_p). The following equation can be used as follow [57]: -

$$A_p = W_p \cdot L_p \quad (3.3)$$

To find the area of concentration of solar radiation at the focus point on the surface of the heat absorbing tube [57]:

$$A_{foc} = \pi D_{abs} \; L_{abs} \quad (3.4)$$

D_{abs}: is the diameter of the absorbent tube

L_{abs} : is the length of the absorbent tube

3.4 Fresnel lens calculations.

In this study, two spot-type Fresnel lenses were used, each side length equal to the diameter of its largest groove. A lens reflects the rays of the sun falling on the surface area of the lens vertically and focuses them toward a smaller area.

3.4.1 Focal length of a Fresnel lens (f_{LF}):

The calculation of the focal length of a Fresnel lens (f_{LF}) depends on the prism angle (α), refractive index (n), aperture area of Fresnel lens as length, width,and largest radius of the grooves (r_F), and the direction of the grooves (inward or outward) as shown in Figure (3.15).

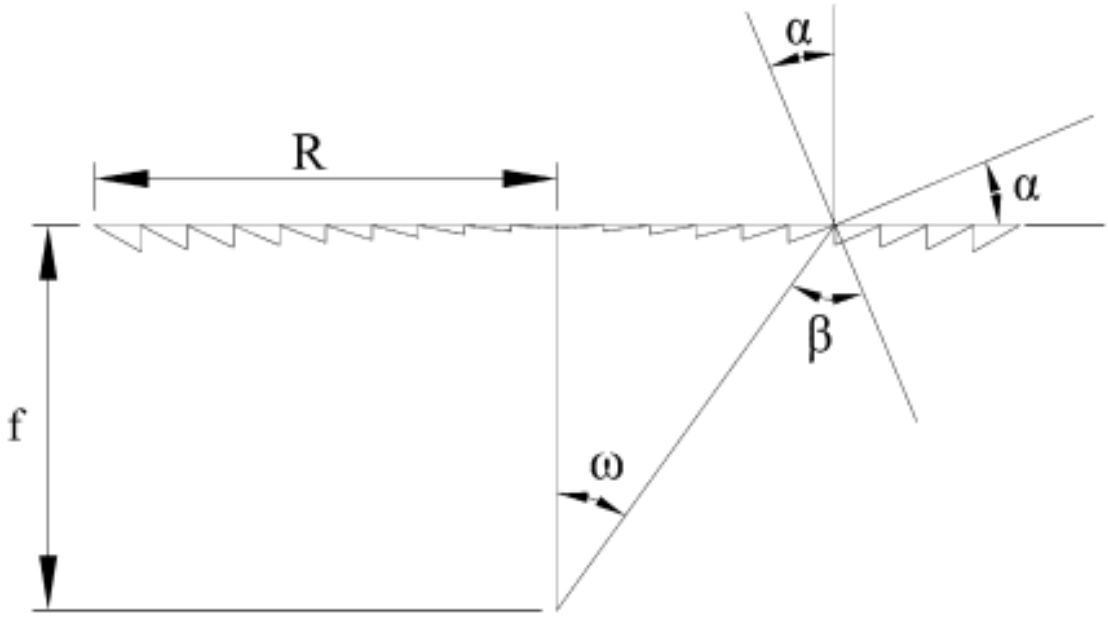

Figure (3.15): Schematic diagram dimension of Fresnel lens[58]**.**

The focal length equation can be calculated for the lenses used in this study that have grooves facing inward (towards the receiving tube)[59].

$$\tan\alpha = \frac{r_F}{n\sqrt{r_F^2+(f_{LF})^2}-f_{LF}} \tag{3.5}$$

3.4.2 Aperture area calculations of a Fresnel lens (A_F):

To calculate the effective Fresnel lens surface area (A_F), multiply the lens width (W_F) by the lens length (L_F) as shown in Figure (3.16). Since the lens used is square, its largest prism diameter (D_F) is equal to the length of one of its sides. The equation can be written as follows[60].

$$A_F = L_F * W_F = {D_F}^2 \tag{3.6}$$

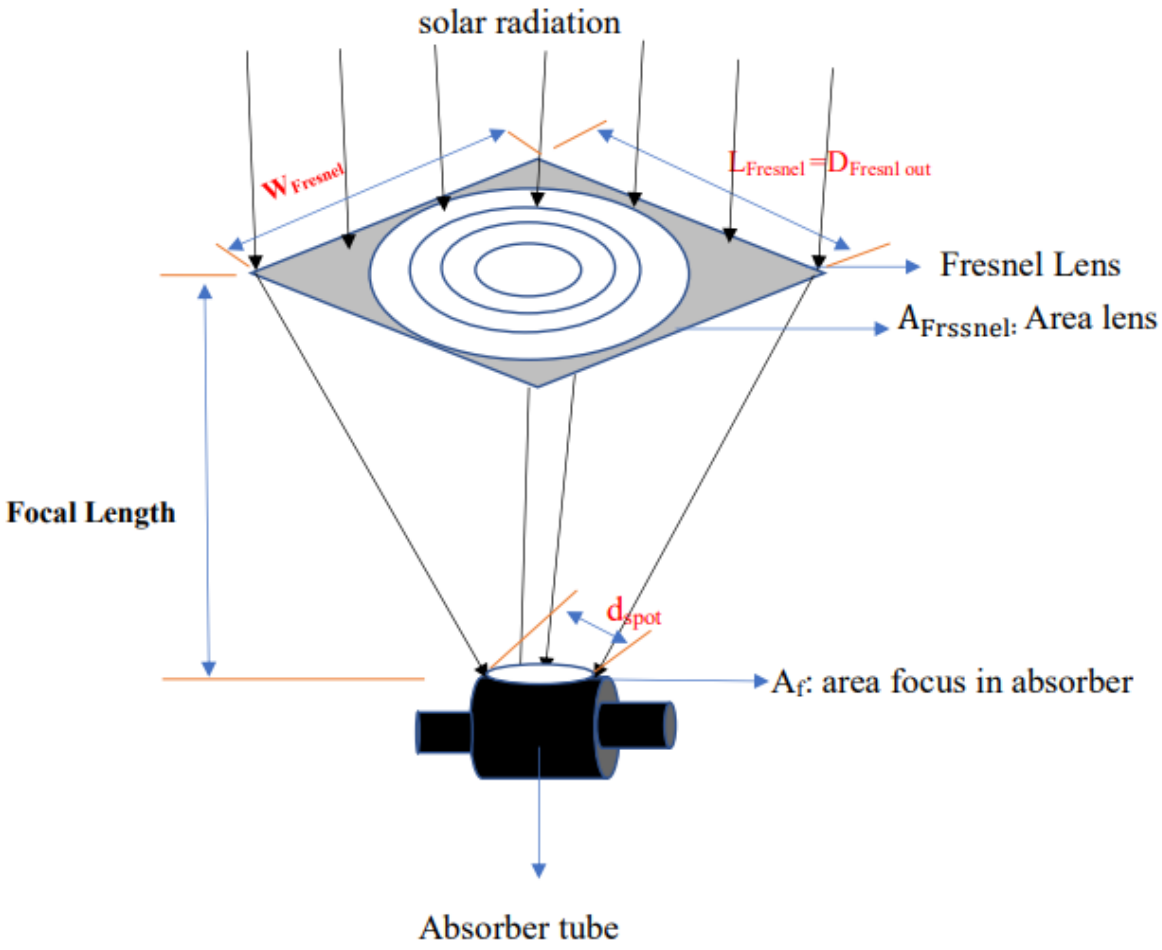

Figure. (3.16): Schematic diagram of effective Fresnel lens area and focus area.

3.5 Calculation of thermal efficiency.

Energy efficiency can be defined as the ratio of the useful energy to produce pure water per hour (Q_u) to the amount of energy input per hour ($Q_{s)}$ can be expressed by the equation (3.7) [61] [45].

$$\eta = \frac{Q_u}{Q_s} \tag{3.7}$$

$$Q_u = M_{ev} * h_{fg} \tag{3.8}$$

M_{ev}: is the amount of daily productivity of fresh water.

h_{fg}: is the latent heat of vaporization of water and is taken as an average value of 2335 J/kg to find daily energy efficiency[62]. The latent heat of water

vaporization per hour can also be calculated according to the following equation [63]:

$$h_{fg} = \left(2501.9 - 2.40706 * T_W + 1.192217 * 10^{-3} * {T_W}^2 - 1.5863 * 10^{-5} * {T_W}^3\right) * 10^3 \quad (3.9)$$

T_W : is the temperature basin water in solar still.

The available solar energy (input energy) that falls on all parts of the test device can be calculated by multiplying the area of solar energy receivers by the incident solar radiation according to the following equation[64].

$$Q_s = A_s \ I_S \quad (3.10)$$

Where (I_S) the incident solar radiation intensity (W/m^2). A_s is area of the surface for incident solar radiation (m^2)

3.5.1 Efficiency calculations of solar still only.

The daily efficiency of the solar still can be calculated by the following equation depending on the pure water productivity per hour (kg/s), the latent heat of evaporation of the basin water (h_{fg}) (J/kg), the average solar radiation per day (W/m^2), and aperture area of Solar still (m^2)[65].

$$\eta_{th} = \frac{\sum M_{ev} * h_{fg}}{\sum I_s * (A_b) * 3600} * 10^2 \quad (3.11)$$

A_b *:* is solar still basin area.

3.5.2 Efficiency calculations of the modified system

The energy efficiency of the single-slope solar still associated with a parabolic trough and Fresnel lenses can be calculated from the quotient of dividing the useful thermal energy by the total energy falling on the heat collecting surfaces (i.e. the area of the solar distiller in addition to the solar condensers area), considering the location of the lenses, as their area is not calculated when placed above the parabolic trough collector. According to equation (3.12), the energy efficiency is calculated for the solar still coupled with a parabolic trough only, or

for the solar still coupled with a parabolic trough with Fresnel lenses above the parabolic trough[66].

$$\eta_{th} = \frac{\sum M_{ev} * h_{fg}}{\sum [I_s * A_b + I_s * A_P] * 3600} * 10^2 \quad (3.12)$$

A_p *:* is parabolic trough area.

for the solar still coupled with a parabolic trough with Fresnel lenses out of the parabolic trough collector[66].

$$\eta_{th} = \frac{\sum M_{ev} * h_{fg}}{\sum [I_s * A_b + I_s * A_P + I_s * A_F] * 3600} * 10^2 \quad (3.13)$$

To calculate the percentage of pure water productivity enhancement ratio, the following equation is used[67]:

$$P_{Enh}\% = \left(\frac{P_M - P_C}{P_C}\right) * 100 \quad (3.14)$$

$P_{Enh}\%$: is the Productivity enhancement ratio.

P_{M} : is the modified water productivity.

P_C: is the Productivity conventional.

3.6 Measuring equipment

During all the experiments that were conducted, different measuring devices were used as follows:

3.6.1 Temperature measurement

The temperature was measured using 16 thermocouple K-type as in Fig. (3.17). They are calibrated with a margin of error (0.2% ± 1 °C) according to the calibration results in Appendix B. The thermocouples are fixed at different positions of the conventional still and the solar still is coupled to an equivalent solar concentrator as shown in Tables (3.3, and 3.4) and Figure (3.18). A thermocouple to measure the ambient air temperature in the shaded area and another to measure the temperature of the feed tank A thermocouple were

installed on the galvanized sheet. The two thermocouples were placed in the still basin water, and another thermocouple was placed to measure the steam temperature. The temperature of the inner and outer surfaces of the glass was monitored by installing a thermocouple on the inner surface of the glass and another on the outer surface. Two thermocouples were used to measure the temperature of the heat transfer fluid, one at the entrance of the PTC absorption tube and the other at the outlet. Sixteen thermal sensors were connected to a 32-channel digital recorder and data reader (CKT4000) as shown in Figure (3.19).

Figure (3.17): Images of thermocouple K-type

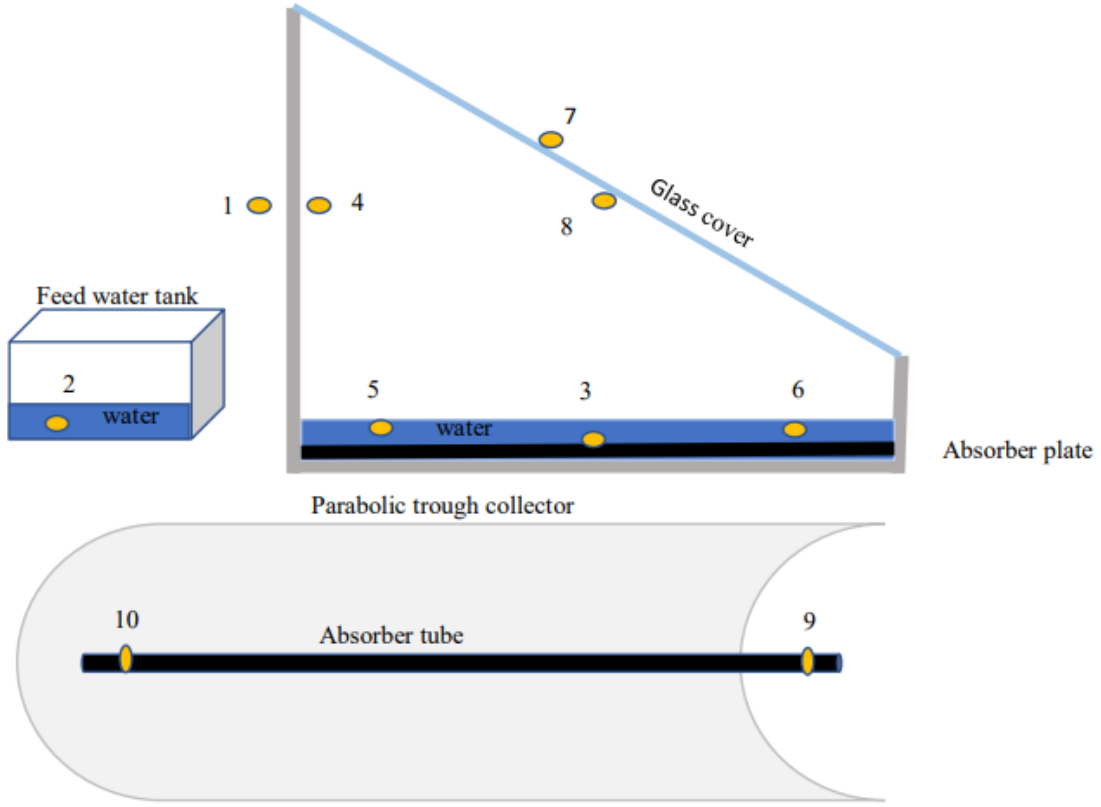

Figure (3.18): Distribution of the dual thermal sensors to theparts of the experiment.

Table (3-3): Distribution of dual thermal sensors on the experimental parts of the traditional still.

Thermocouple no.	1	2	3	4	5,6	7	8
Location	Ambient	Water feed temp.	Galvanized plate	Moist steam	Basin water temp.	Inner glass cover	Outer glass cover

Table (3-4): Distribution of dual thermal sensors on the experimental parts of the solar still with PTC.

Thermocouple no.	9	10	11	16	12,13	14	15
Location	Fluid temp in absorber tube	Fluid temp out absorber tube	Galvanized plate	Moist steam	Basin Water temp.	Inner Glass cover	Outer glass cover

Figure (3.19): Data logger type (CKT4000) with a capacity of 32 channels.

3.6.2 Measure the intensity of solar radiation

To calculate the intensity of the solar radiation falling on the parabolic trough, the lenses, and the solar still every hour, Solar power meter, model (SM206-solar), was used, with measurement range: 0.1-399.9W / m^2, 1-3999 W/m^2, as shown in the figure (3.20). Error percentage is (± 5% or ± 10 W/m^2) as shown in Appendix C for the calibration process for the solar power meter.

Figure (3.20): Measure the intensity of solar radiation.

3.6.3 Wind speed measurement

Using a digital anemometer (BTMETER BT-100-WM), the wind speed was measured hourly for its direct effect on solar distillation productivity. The device operates with a measurement range of 0.3 to 30 m/s, with a measurement accuracy of (+/- 5%) depending on the results. The device has been calibrated in the Ministry of Science and Technology / Department of Environment, Water and Renewable Energies, Department of Wind Energy, according to book numbered (979/3) dated 11/5/2023 as in Appendix D. Figure (3.21) shows the scale used to calculate wind speed.

Figure (3.21): Wind speed measurement.

3.6.4 Distilled water collector

To calculate the amount of water produced per hour and the cumulative yield of fresh water, a graduated flask with a volume of 1.2 liters and an accuracy of 5 ml was used.

3.6.5 Measurement of the amount of flowing liquid

The LZM-Z type liquid flow meter was used to calculate the amount of liquid flow (water) between the receiver tube and the heat exchanger. The measurement rate ranges from 0.38 to 4 liters per minute with an error rate of 4% as shown in Figure (3.22).

Figure (3.22): Flow meter image.

3.7 Experimental procedure

In this work, the experiments were carried out on different days for the first modified system (solar still combined with a parabolic trough collector) with conventional, the second modified system (still solar combined with a parabolic trough collector with Fresnel lenses over the parabola), and the third modified system (solar still combined with a parabolic trough collector with Fresnel lenses outside the parabola) with the conventional, as follows:

1. The work begins with the experiments by assembling the parts of the solar system, installing the necessary measuring devices and electrical connections, installing 16 thermocouples of type (K) in the positions mentioned in Tables (3-3 and 3-4), and connecting them to a reader and a digital data recorder to record the obtained thermal data.
2. Measurement of the solar radiation falling on the solar collector using an hourly radiation intensity meter.
3. Measureing the wind speed hourly with a digital scale and manually record the data.
4. Manually moving the parabola through south and north to track the sun's rays.

5. The quantity produced is calculated of pure condensed water per hour using a graduated vessel and record the results manually.
6. Work on all exams starts from 7 a.m to 5 p.m.

CHAPTER FOUR

Results and Discussions

CHAPTER FOUR

Results and Discussions

4.1. Introduction

This chapter discusses the results of experimental work conducted to improve the daily throughput of a single-slope solar system. All experiments were conducted from 7:00 AM to 5:00 PM, with a depth of 2 cm of still basin water, and within the climatic conditions of the city of Diwaniyah (31.99°N latitude, 44. 93°E longitude). In April and May, a volume flow rate of 0.5 L/min was used for the heat transfer fluid, and in June, volume flow rates of (0.38, 0.5, and 0.76) L/min were used. Based on the presented literature, several parameters affected the daily throughput of the system such as wind speed, solar radiation, and ambient temperature. A comparison was made between the results of a conventional single-slope solar distiller and a solar one equipped with a parabolic trough collector. The results were also compared between the use of Fresnel lenses as an enhancer to increase the concentration of solar radiation on the absorbent tube of the parabolic collector basin, and between the single solar still and the solar still associated with the parabolic trough collector. The effect of using Fresnel lenses inside and outside the parabolic basin on distilled water yield was studied. The amount of fresh water produced was calculated in L/m^2 by dividing by the area of only the solar still for all experiments

4.2. Experimental results

4.2.1. solar still only and solar still with PTC

The experiment was conducted on the 3rd of April 2023 for a single-slope conventional solar device and another with the same dimensions and specifications, integrated with a parabolic trough collector. The solar radiation intensity was 224 W/m^2, the wind speed was 0.9 m/s, and the ambient temperature was 19.7 °C at the beginning of the experiment. With time, the intensity of solar

radiation increased to reach its maximum intensity at 12:00 p.m to reach 984 W/m^2 and then decrease, while the ambient temperature continued to rise until 15:00 even after the decrease in solar radiation due to the nature of Earth storing heat. The maximum pure water production was 190 mL for the conventional device and 231 mL for the PTC-coupled device at 13:00, the total daily production was (4.74, 5.98) L/m^2 respectively, with an enhancement rate of 26.3% compared to the conventional one. The thermal efficiency obtained of conventional up to 44.7% and 17.05% for the solar still associated with a parabolic trough collector at an average solar radiation of 624.6 W/m^2 and an average wind speed of 1.5 m/s as in Figures (4.1, and 4.2). The effect of the overall performance of the system is observed in the solar collecting area when the solar energy collecting area increases. The sample temperature rises and the freshwater production increases while the thermal energy efficiency decreases as a result of heat loss to the surroundings. The purity of the water produced from the solar distiller was measured by a purity test device total dissolved solids (TDS) as it reached 20 parts per million while the purity of the water entering the distiller was 776 part per million (ppm).

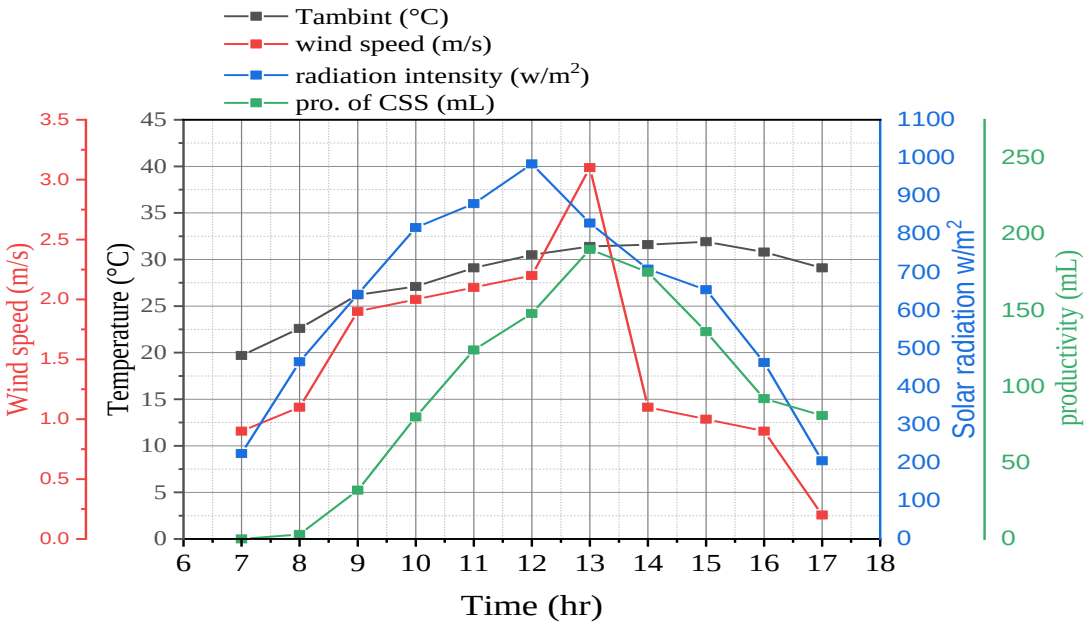

Figure (4.1): Variation of productivity and environmental conditions with time for conventional solar still in 3/4/2023.

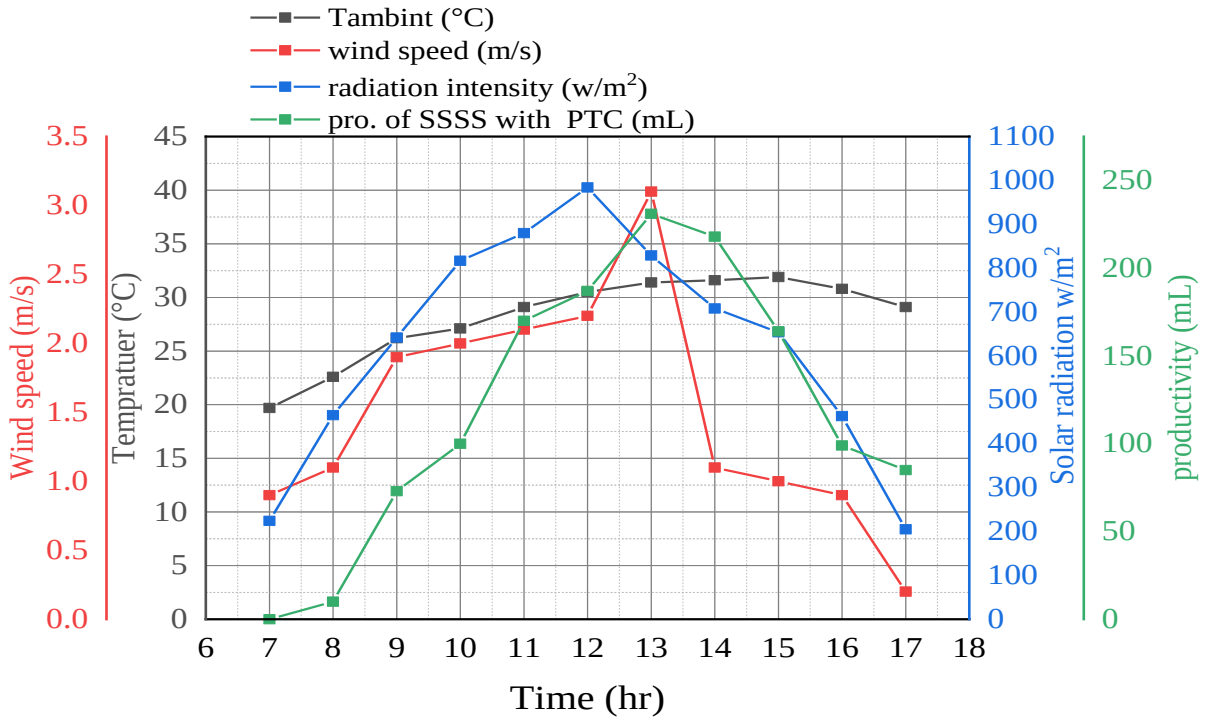

Figure (4.2): Variation of productivity and environmental conditions with time for solar energy associated with the parabolic trough collector in 3/4/2023.

Figure 4.3 shows temperature changes over time for a conventional solar dweller by measuring the temperatures of the galvanized plate, distillation water, the inner and outer surface of glass cover, steam temperature, feed water temperature, and ambient temperature. At the beginning of the experiment, the temperatures of the solar still are close, then they begin to rise as the intensity of the incident radiation increases. At 1:00 p.m, the maximum temperature of the still basin water reached 69.3 °C as a result of the sun's rays falling vertically on the distiller. the maximum temperature recorded of outer surface of the glass cover 57.6 °C at 1:00 p.m due to the effect of the wind speed on the surface of the glass. after 1:00 p.m. It was observed that temperatures decreased in parts of the still with a decrease in the intensity of solar radiation, while the ambient temperature remained high.

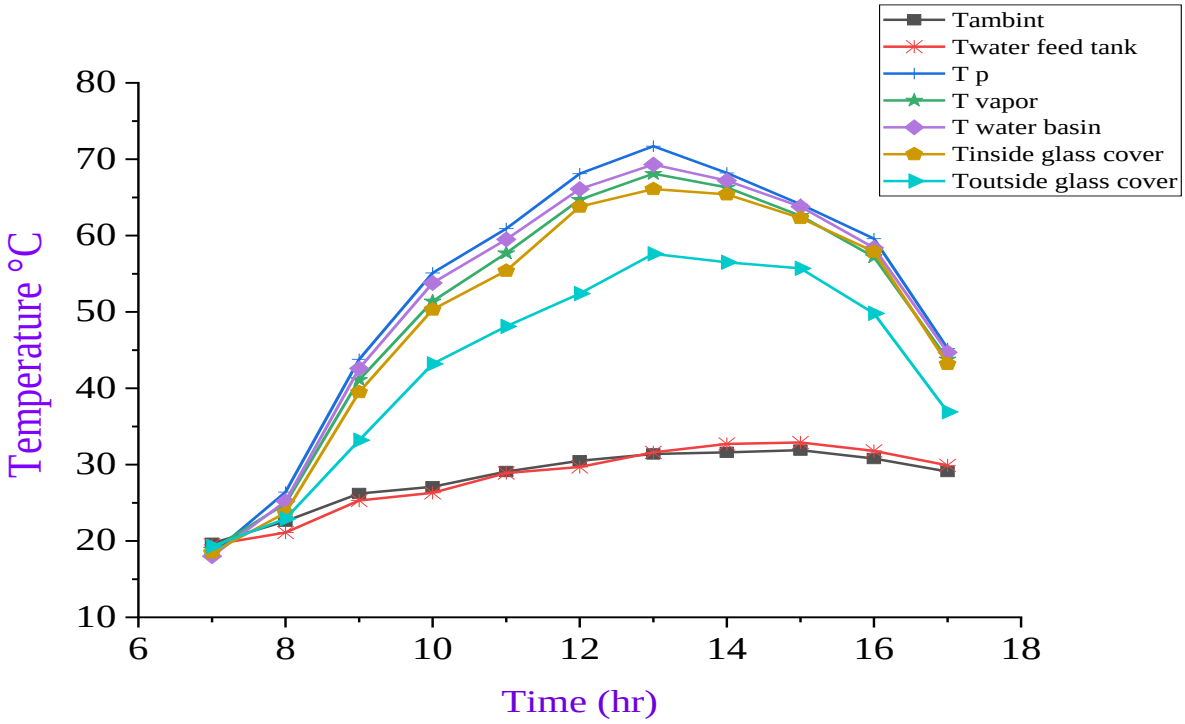

Figure (4.3): Conventional solar still temperature variation with time in 3/4/2023.

Figure 4.4 shows the changes in temperature with time for a single-slope solar still associated with a parabolic trough. The parabolic trough collector raises the water temperature in the solar trough and thus increases evaporation rates. At the beginning of the experiment, the temperatures of the solar still are close, then they begin to rise as the intensity of the incident radiation increases. At 1:00 p.m, the maximum temperature of the still basin water reached 72.3 °C as a result of the sun's rays falling vertically on the distiller. the maximum temperature recorded of outer surface of the glass cover 61.1 °C at 1:00 p.m due to the effect of the wind speed on the surface of the glass. after 1:00 p.m. It was observed that temperatures decreased in parts of the still with a decrease in the intensity of solar radiation, while the ambient temperature remained high.

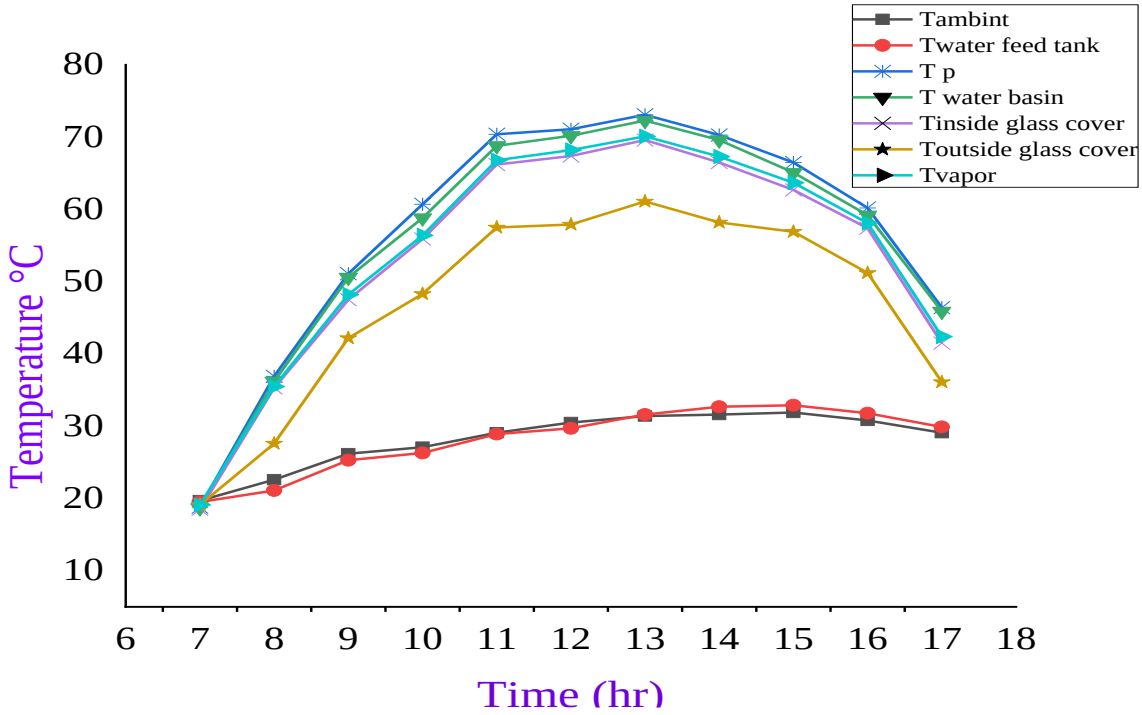

Figure (4.4): Temperatures variation with time for the single slope still solar with the PTC on 3/4/2023.

Figure 4.5 shows the freshwater yield of a single-slope solar still and distillation unit coupled to a parabolic trough on April 3, 2023. At 8:00 in the morning, the solar distillers begin to produce water and gradually increase until it reaches the greatest productivity at 13:00 p.m and then decrease after that. The intensity of solar radiation and wind speed have a significant impact on productivity, as with the increase in solar radiation intensity and wind speed, productivity increases. The daily cumulative output of the single solar distiller was 4.74 L/m^2 d and 5.98 L/m^2 d for the distiller combined with PTC. The highest productivity was at 13:00 p.m, 190 mL for the traditional one and 231 mL for 72.3 for the combined device with PTC.

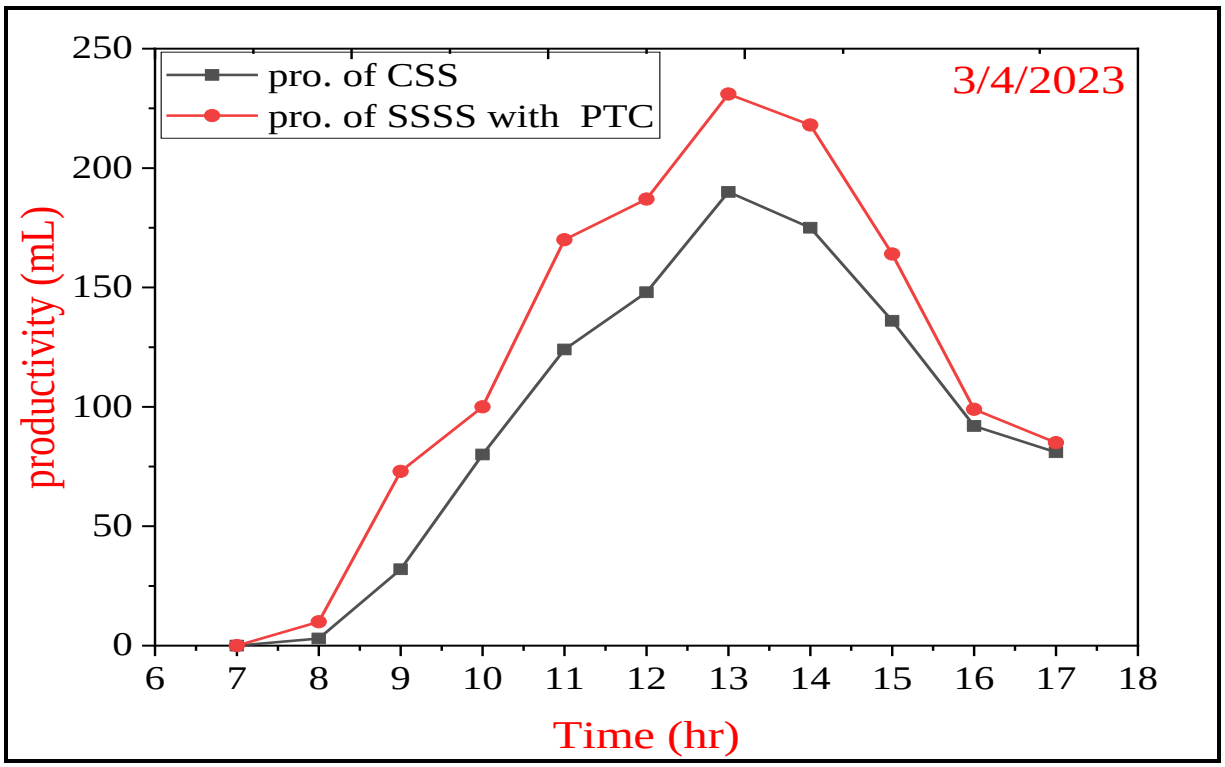

Figure (4.5): Variation of distilled water yield with time for the conventional solar distiller and the integrated distiller with PTC.

The second experiment was conducted on May 5, 2023 for a traditional single-slope solar device and another with the same dimensions and specifications linked to a parabolic basin within the climatic conditions of the city of Diwaniyah. At the solar radiation intensity starting from 201 W/m^2, the wind speed 1.9 m/s, and the ambient temperature 21.2 °C at the beginning of the experiment. With time, the solar radiation is at its peak at 12:00 p.m, when it reaches 1061 W/m^2, and then decreases after that with the ambient temperature continuing to rise. A cumulative output was reached for the day of the experiment, with an average solar radiation intensity of (672) W/m^2 and an average wind speed from (2.1) m/s is (6.85, and 5.34) L/m^2 per day, for the traditional and solar energy associated with a parabolic trough respectively, with an average 27.2% enhancement compared to conventional as in Figures (4.6, and 4.7). The system showed a thermal efficiency of up to 46.93% for conventional still and 18.1% for solar energy associated with a parabolic trough collector. It was noted that the purity of the produced water was measured by the TDS device, was at 20 ppm.

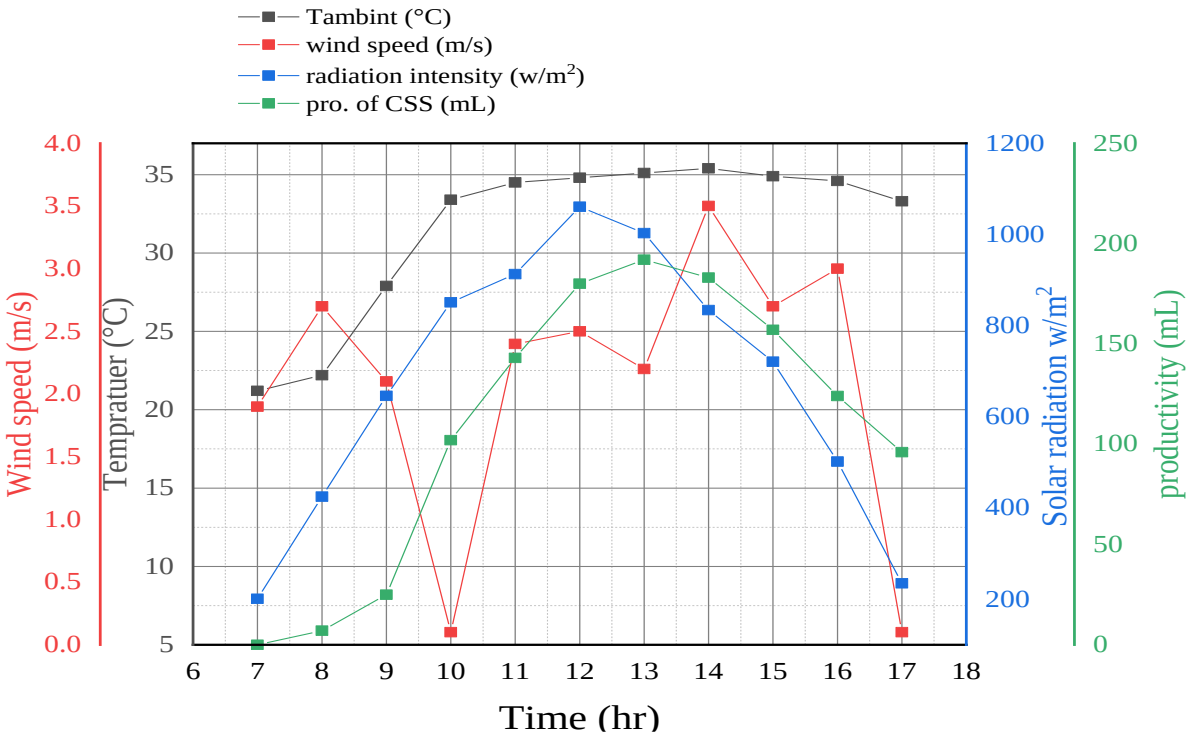

Figure (4.6): Variation of productivity and environmental conditions with time for conventional solar still in 5/5/2023.

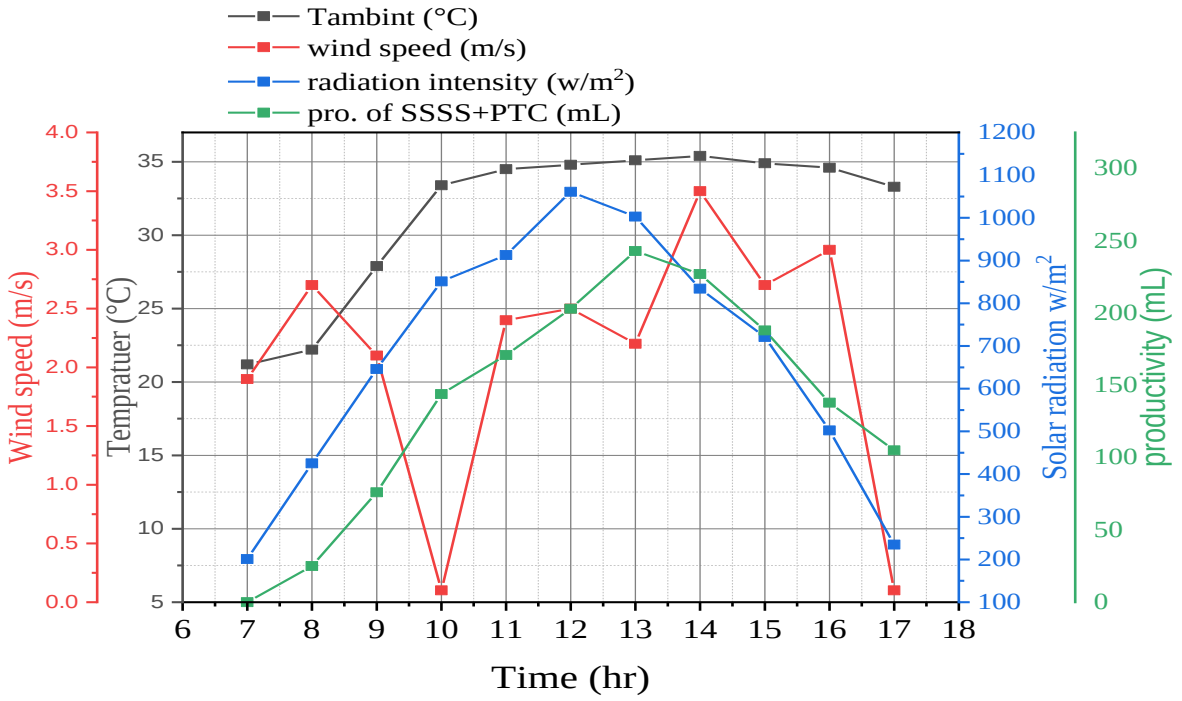

Figure (4.7): Variation of productivity and environmental conditions with time for solar energy associated with the parabolic trough collector on 5/5/2023.

Figure 4.8 shows temperature changes over time for a conventional solar still over time. At the beginning of the experiment, the temperatures of all parts

of the solar still are similar. The temperature of the parameters begins to rise with the increase in the intensity of incident solar radiation. At 1:00 p.m, the maximum temperature of the water still basin water reached 71.7 °C as a result of sunlight falling vertically on the distillation device. The maximum temperature of the outer surface of the glass cover was recorded at 59.1°C at 1:00 p.m. After 1:00 p.m, temperatures were observed to decrease in parts of the solar, with the intensity of solar radiation decreasing.

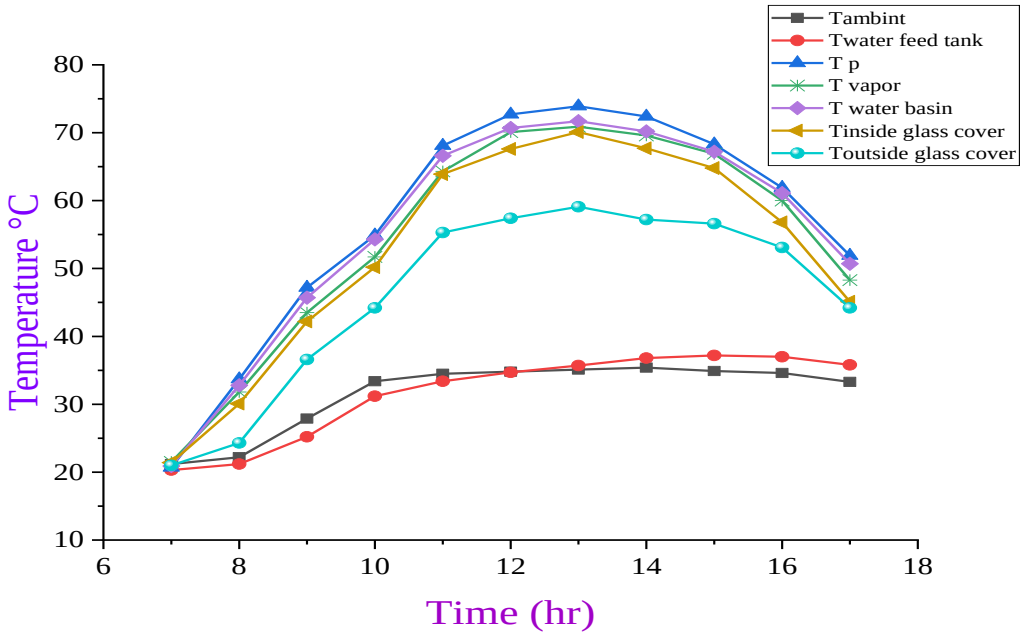

Figure (4.8): Conventional solar still temperature variation with time in 5/5/2023.

Figure 4.9 shows the temperature changes with time for a single-slope solar still associated with a parabolic trough. The system contributes to enhancing the water temperature in the solar basin. At the beginning of the experiment, the sun's temperatures are close, then they begin to rise as the intensity of the incident radiation increases. At 1:00 p.m , the maximum temperature of the solar basin water reached 74.2 °C as a result of sunlight falling vertically on the distillation device and the parabolic trough. The maximum temperature of the outer surface of the glass cover was recorded as 63.4 °C at 1:00 p.m due to the effect of wind speed on the glass surface. After 1:00 p.m was observed that temperatures decreased in parts of the solar still as a result of a decrease in the intensity of solar radiation.

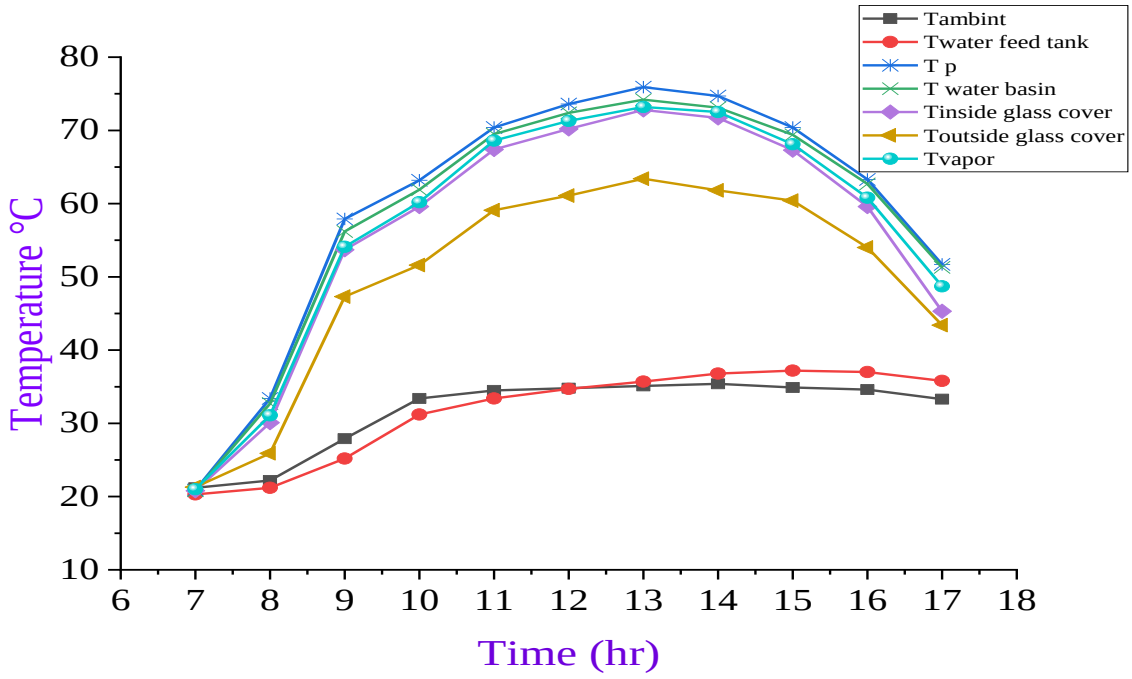

Figure (4.9): Temperatures variation with time for the single slope still solar with the PTC on 5/5/2023.

Figure 4.10 shows the freshwater yield of a single-slope solar still and distillation unit coupled to a parabolic trough on May 5, 2023. At 8:00 in the morning, the solar distillers begin to produce water and gradually increase until it reaches the greatest productivity at 13:00 p.m and then decrease after that. The effect of solar radiation intensity and wind speed on productivity has been observed. The greater the intensity of solar radiation and wind speed, the greater the productivity.The daily cumulative output of the single solar distiller was 1240 mL and 1590 mL for the distiller combined with PTC, where the highest productivity was at 13:00 pm, 192 mL for the conventional , and 243 mL for the SSSS with PTC.

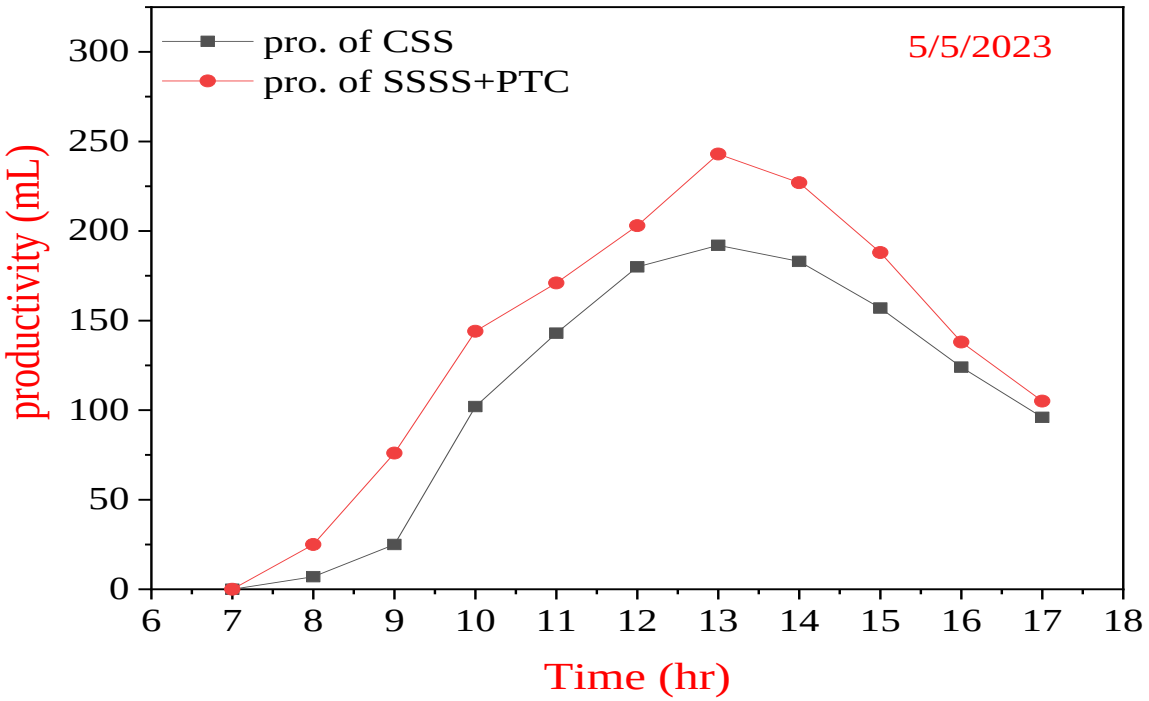

Figure (4.10): Variation of distilled water yield with time for the conventional solar distiller and the integrated distiller with PTC in 5/5/2023.

4.2.2. Solar still only and solar still with PTC and Fresnel lenses over PTC

The experiment was conducted on the 5th of April 2023 for a traditional single-slope solar device and another with the same dimensions and specifications, integrated with a parabolic trough and two Fresnel lenses above the PTC. The solar radiation intensity was 270.6 W/m^2, the wind speed was 0.1 m/s, and the ambient temperature was 18.9 °C at the beginning of the experiment. With time, the solar radiation intensity increased to reach its maximum at 12:00 p.m to reach 977 W/m^2, and then decreasing after that. The maximum pure water production was 188 mL for the conventional device and 242 mL for the PTC-coupled device and two lenses over the PTC at 13:00, and the total daily production was (4.7, 6.6) L/m^2 per day respectively, with an average solar radiation of 632.3 W/m^2. The average wind speed is 1.59 m/s as exhibited in Figures (4.11 and 4.12). The productivity improvement was 41% compared to conventional still. The system showed a thermal efficiency of 44.2% for conventional and 18.78% for solar still associated with a parabolic trough collector with lenses. The purity of the distilled water was 22 ppm.

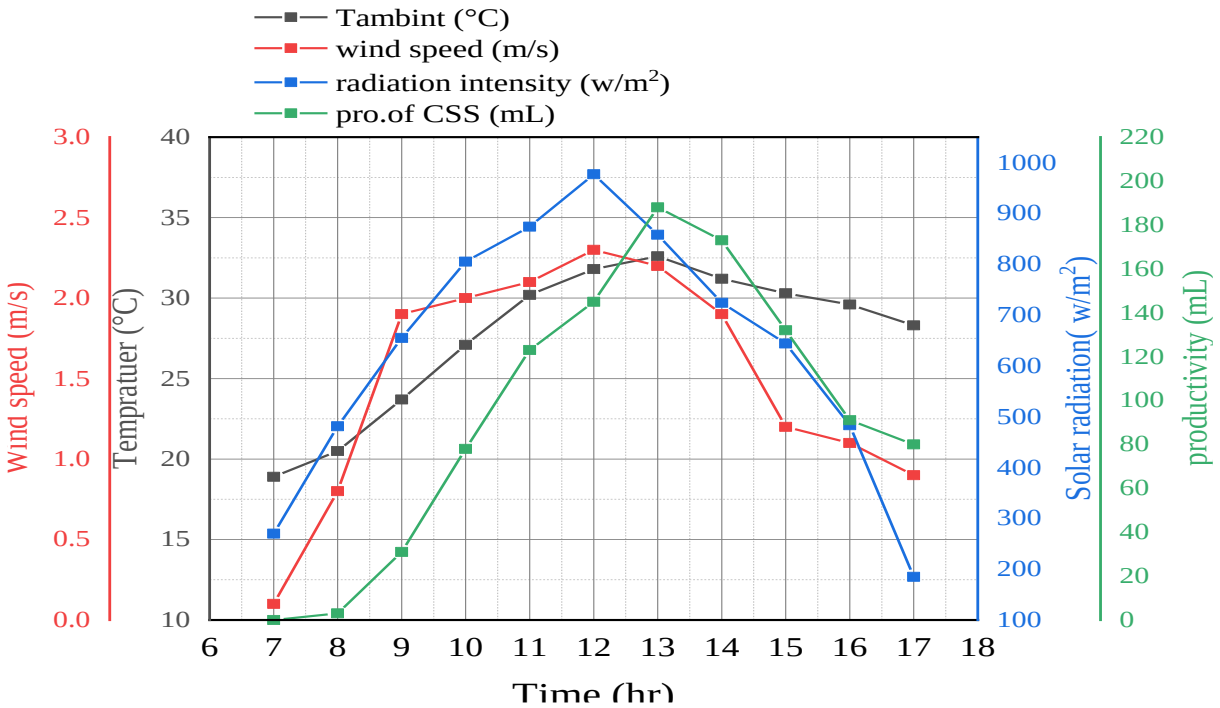

Figure (4.11): Variation of productivity and environmental conditions with time for conventional solar still on 5/4/2023.

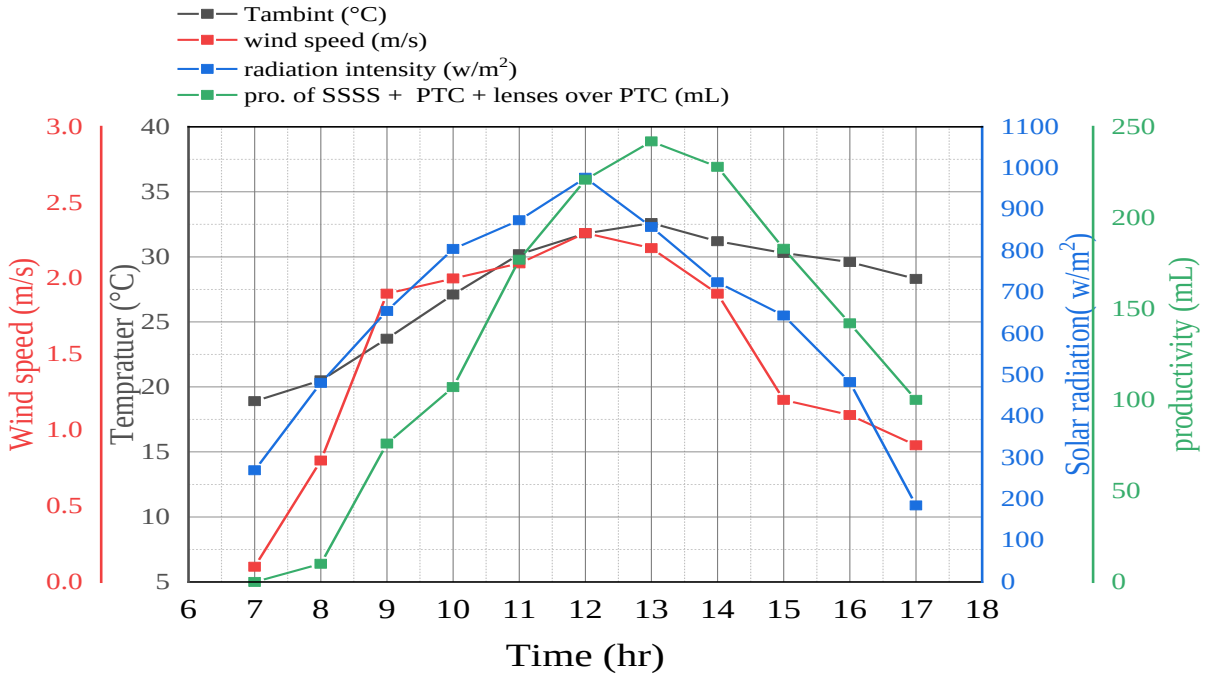

Figure (4.12): Variation of productivity and environmental conditions with time for solar energy associated with the parabolic trough collector and two lenses over PTC on 5/4/2023.

Figure 4.13 shows the temperature variation of conventional over time. Temperatures were observed for all parameters of the traditional solar still were

close at the beginning of the experiment, then it begins to rise as the intensity of the incident radiation increases. At 1:00 p.m, the maximum temperature of the water still basin water reached 69.1 °C as a result of sunlight falling vertically on the distillation device. The maximum temperature of the outer surface of the glass cover was recorded at 57.8°C at 1:00 p.m. After 1:00 p.m, temperatures were observed to decrease in parts of the solar, with the intensity of solar radiation decreasing.

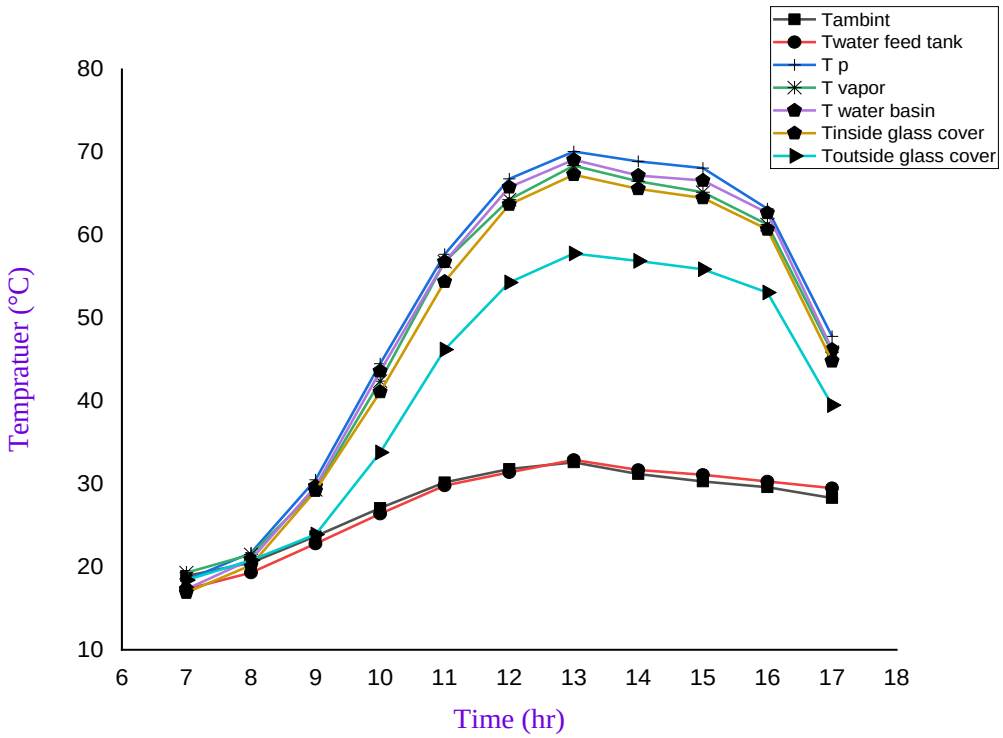

Figure (4.13): Conventional solar still temperature variation with time in 5/4/2023.

Figure 4.14 shows the temperature changes with time for a single-slope solar still associated with a parabolic trough with Fresnel lenses above the PTC. The system contributes to enhancing the water temperature in the solar still basin. At the beginning of the experiment, the sun's temperatures are similar, then they begin to rise as the intensity of the incident radiation increases. At 1:00 p.m , the maximum temperature of the solar basin water reached 74.2 °C as a result of sunlight falling vertically on the distillation device and the parabolic trough with the lenses. The maximum temperature of the outer surface of the glass cover was recorded as 62.8 °C at 1:00 p.m due to the effect of wind speed on the glass

surface. After 1:00 p.m observed that temperatures decreased in parts of the a solar still with a decrease in the intensity of solar radiation.

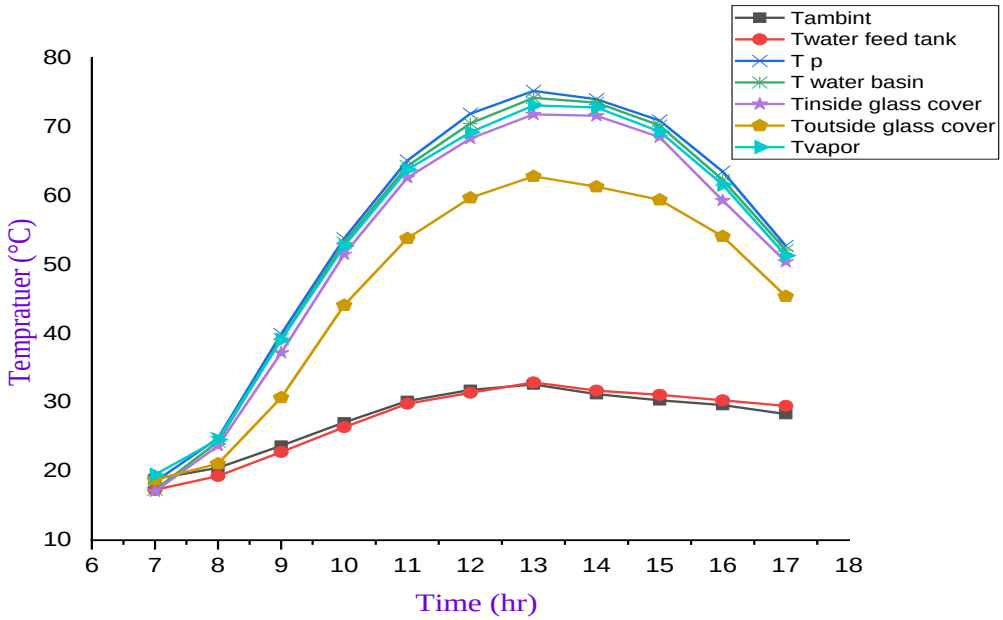

Figure (4.14): Temperatures variation with time for the single slope still solar with the PTC and two lenses over PTC on 5/4/2023.

Figure 4.15 shows the freshwater productivity of a single-slope solar still coupled with a parabolic trough with two Fresnel lenses over the parabolic trough on April 5, 2023. The performance of solar stills in terms of productivity has been observed as it starts at 8:00 a.m. and reaches its maximum value at the daily cumulative output of the single solar distiller was 1099 mL and 1550 mL for the combined distiller with PTC and lenses over PTC. The highest yield was at 13:00, 188 mL for the conventional still, and 242 mL for SSSS with PTC and lens.

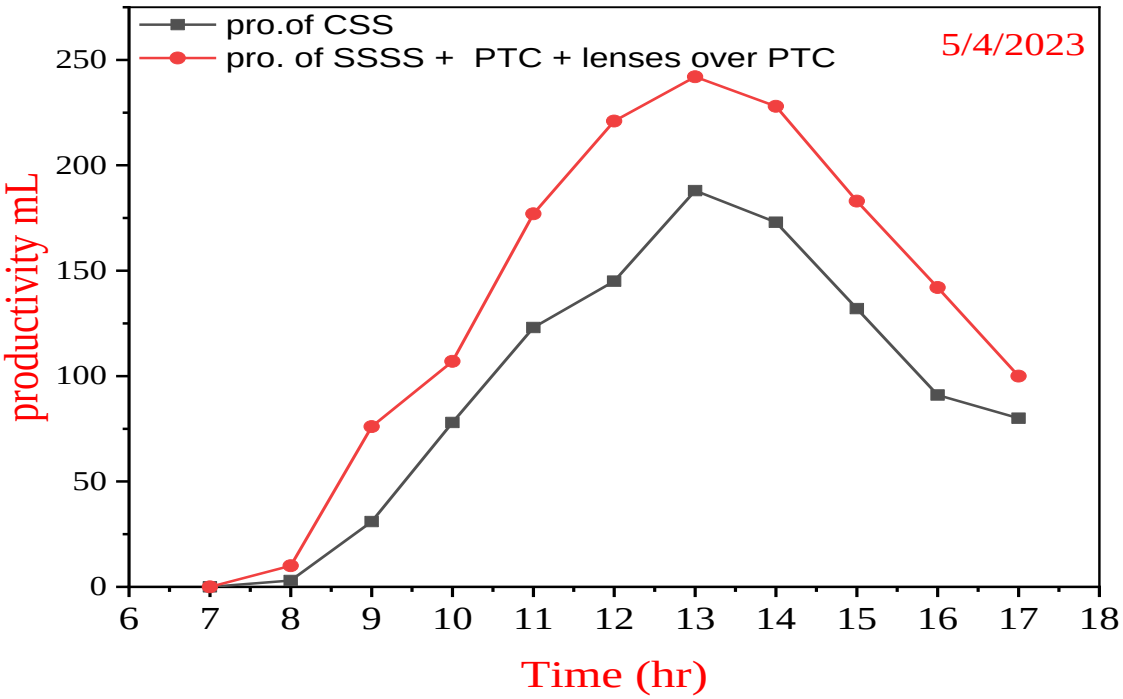

Figure (4.15): Variation of distilled water yield with time for the conventional solar distiller and the integrated distiller with PTC and two Fresnel lenses over PTC on 5/4/2023.

The second experiment was conducted on May 6, 2023, for a conventional solar still and another with the same dimensions and specifications integrated to a parabolic trough and two Fresnel lenses that were placed above the parabolic trough. At the beginning of the experiment, the solar radiation was 241 W/m^2, the wind speed was 0.6 m/s, and the ambient temperature was 20.6 °C. With time, the solar radiation is at its peak at 12 p.m, reaching 1057.6 W/m^2. Then, it decreases as the ambient temperature continues to rise. The average radiation intensity was (670.7) W/m^2 and an average wind speed was (1.19) m/s. The cumulative output of freshwater reached 5.3 L/m^{2}d and 7.5 L/m^{2}d for conventional devices and solar still connected to a parabolic trough with lenses in front of the parabola, respectively, as in Figures (4.16, 4.17). The improvement in productivity was 43.3% compared to conventional energy, and the thermal energy efficiency was 47% for conventional still and 20.3% for solar still associated with a parabolic trough collector with lenses above the a parabolic trough. Experiments, a purity

of up to 20 ppm has been obtained using river water as a feed source for solar stills.

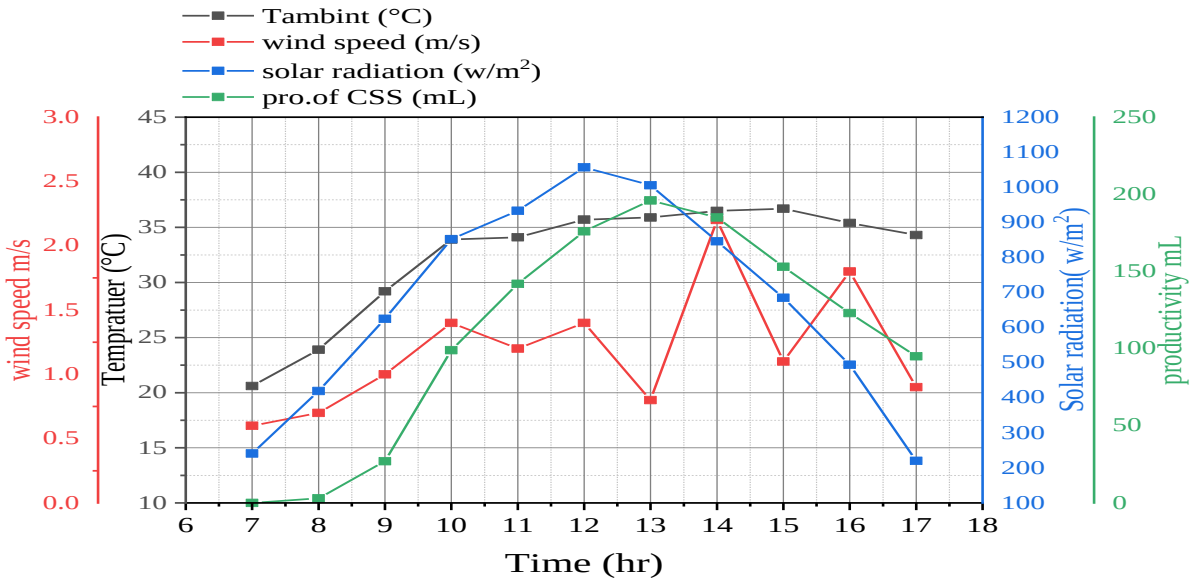

Figure (4.16): Variation of productivity and environmental conditions with time for conventional solar is still on 6/5/2023.

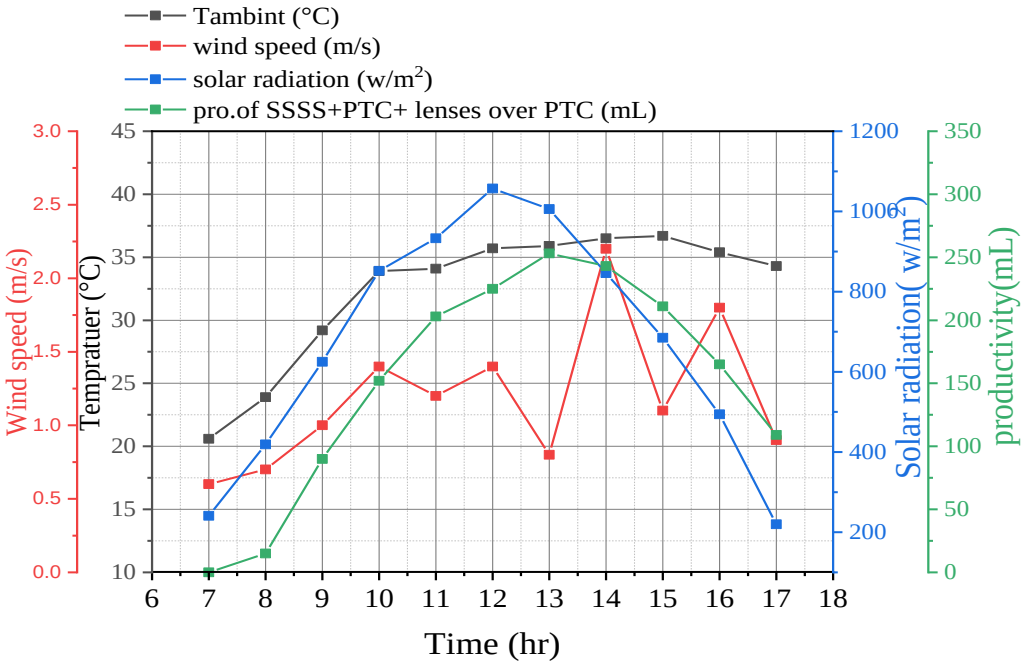

Figure (4.17): Variation of productivity and environmental conditions with time for solar energy associated with the parabolic trough collector and two lenses over PTC on 6/5/2023.

Figure 4.18 shows the temperature variation of conventional over time. Temperatures were observed for all parameters of the traditional solar still were close at the beginning of the experiment, then it begins to rise as the intensity of

the incident radiation increases. At 1:00 p.m, the maximum temperature of the water still basin water reached 71.9°C as a result of sunlight falling vertically on the distillation device. The maximum temperature of the outer surface of the glass cover was recorded at 59.8°C at 1:00 p.m. After 1:00 p.m, temperatures were observed to decrease in parts of the solar, with the intensity of solar radiation decreasing.

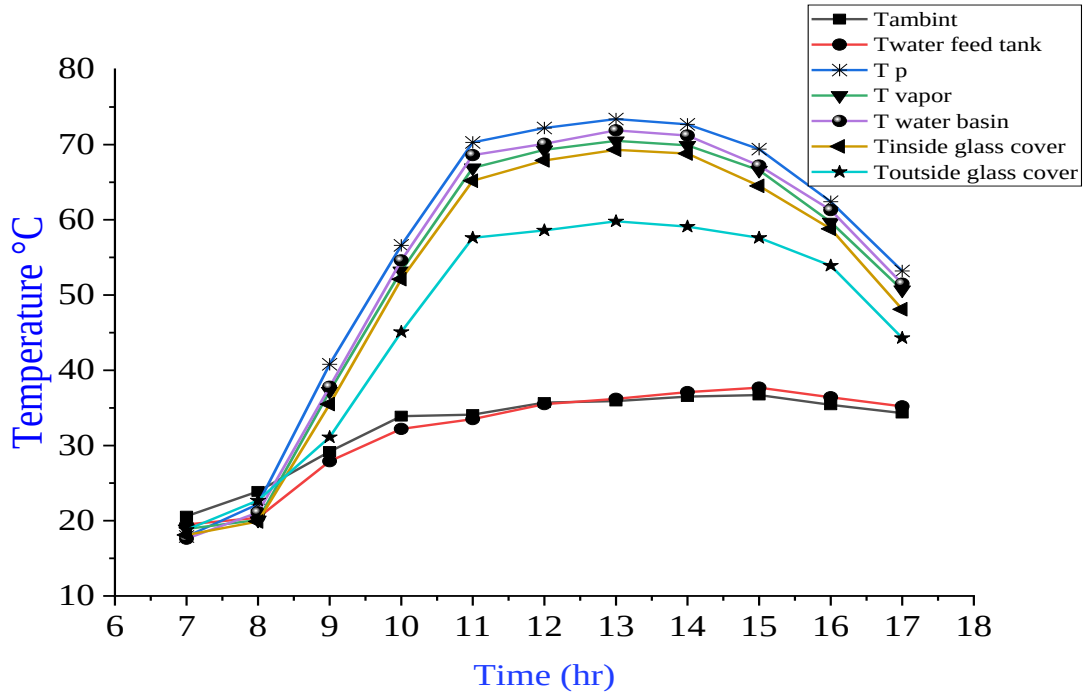

Figure (4.18): Conventional solar still temperature variation with time in 6/5/2023.

Figure 4.19 shows the temperature changes with time for a single-slope solar still associated with a parabolic trough with Fresnel lenses above the PTC. The system contributes to enhancing the water temperature in the solar still basin. At the beginning of the experiment, the sun's temperatures are similar, then they begin to rise as the intensity of the incident radiation increases. At 1:00 p.m, the maximum temperature of the solar basin water reached 75.5 °C as a result of sunlight falling vertically on the distillation device and the parabolic trough with the lenses. The maximum temperature of the outer surface of the glass cover was recorded as 64.4 °C at 1:00 p.m due to the effect of wind speed on the glass surface. After 1:00 p.m observed that temperatures decreased in parts of the a solar still with a decrease in the intensity of solar radiation.

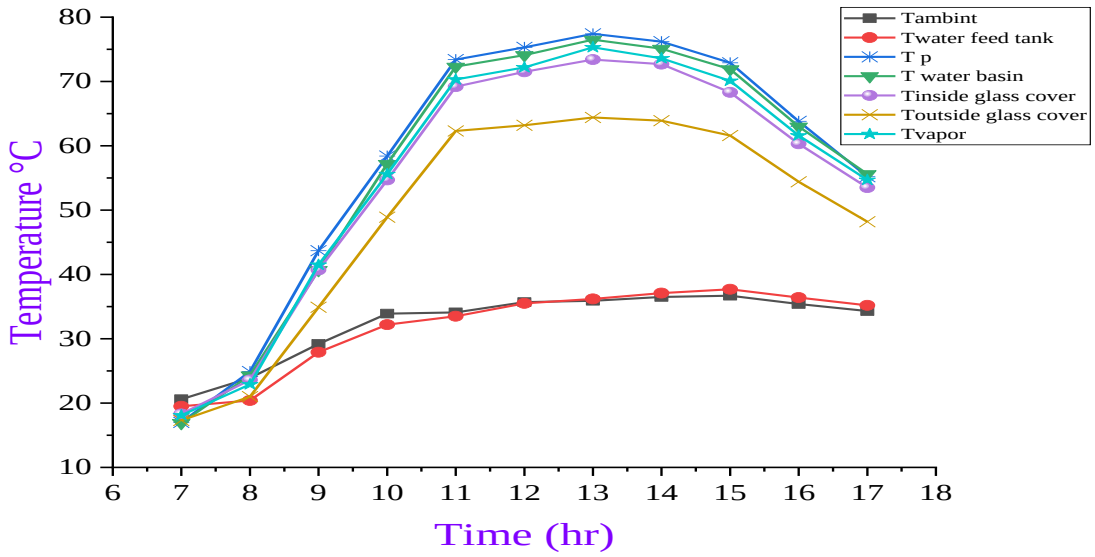

Figure (4.19): Variation of distilled water yield with time for the conventional solar distiller and the integrated distiller with PTC and Fresnel lenses over PTC on 6/5/2023.

Figure 4.20 shows the freshwater productivity of a conventional solar still and a solar still coupled to a parabolic trough and two Fresnel lenses above the parabolic trough, on May 6, 2023. The productivity was observed from the start of operation at 08:00 a.m until 17:00 p.m. The maximum productivity was reached at 13:00, reaching 196 mL for the traditional, and 253 mL of solar energy with PTC and lenses inside.

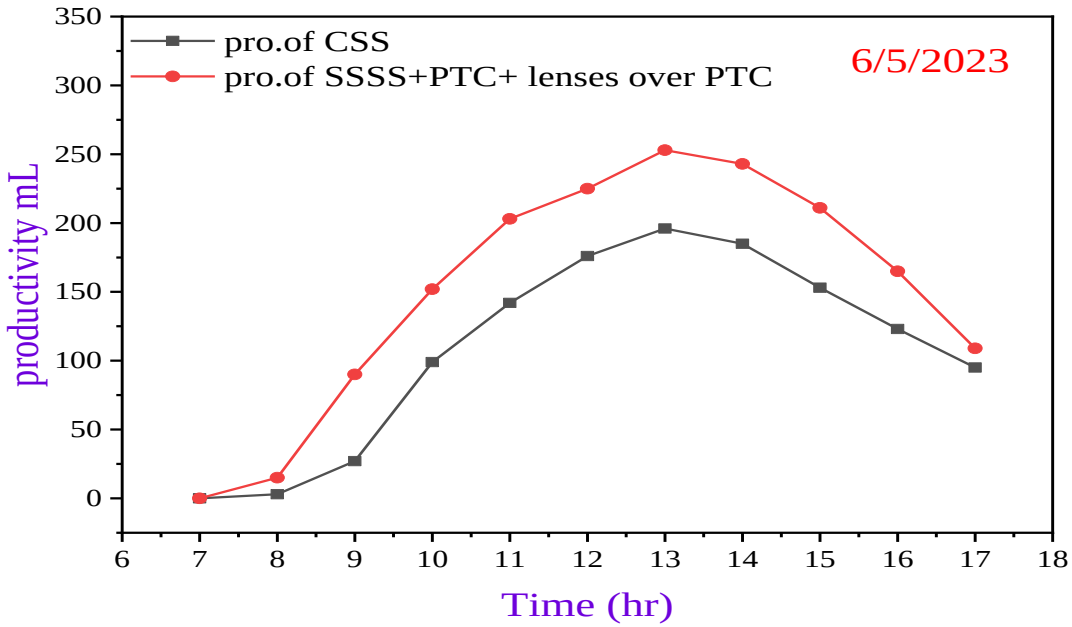

Figure (4.20): Variation of productivity with time for the conventional solar distiller and the integrated distiller with PTC and Fresnel lenses over PTC on 6/5/2023.

4.2.3. Solar still only and solar still with PTC and lenses outside PTC

The experiment was conducted on April 27, 2023, for a single-slope conventional solar device and another with the same dimensions and specifications, integrated with a parabolic trough and two Fresnel lenses outside the PTC. Fresnel lenses focus the sun's rays on a node that was designed in the receiving tube with specifications as mentioned in Chapter Four. The solar radiation intensity was 221 W/m^2, the wind speed was 0.2 m/s, and the ambient temperature was 20.9 °C at the beginning of the experiment. With time, the intensity of solar radiation increased, reaching its maximum at 12:00 p.m, reaching 949 W/m^2, and then decreasing thereafter. The cumulative output per day reached an average intensity of solar radiation (623.9) W/m^2 and an average wind speed was between (1.34) m/s (4.7, 6.7) L/m^2 per day, for the traditional and static distillers associated with a parabolic trough and Fresnel lenses on the parabolic trough collector side, respectively as in Figures (4.21 and 4.22). In this experiment, the increase in productivity amounted to 42.7% compared to the conventional energy, and the thermal efficiency was at 45.2% for the conventional still and 18.41% for the solar still associated with a parabolic trough collector with lenses outside the parabolic trough. The purity of the distilled water was 25 ppm.

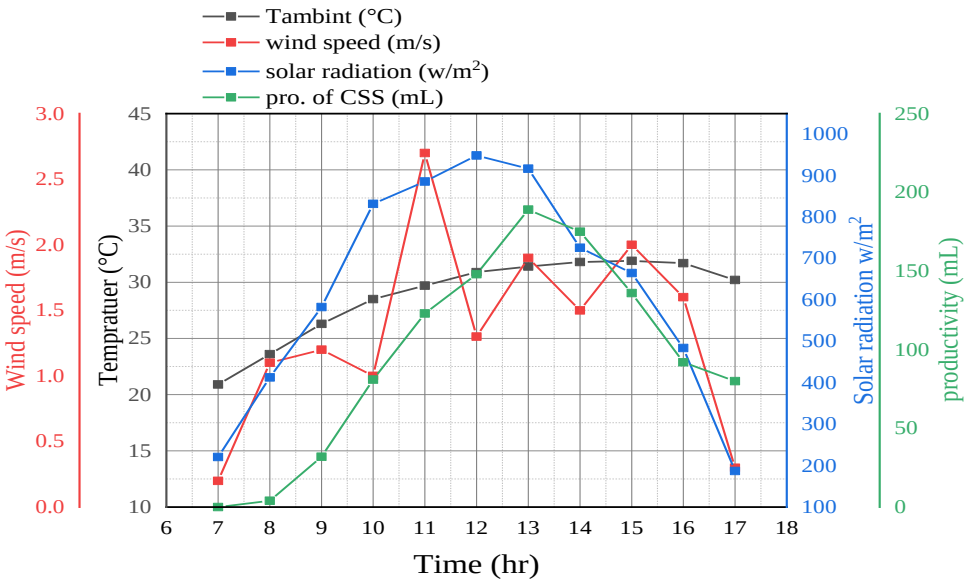

Figure (4.21): Variation of productivity and environmental conditions with time for conventional solar still on 27/4/2023.

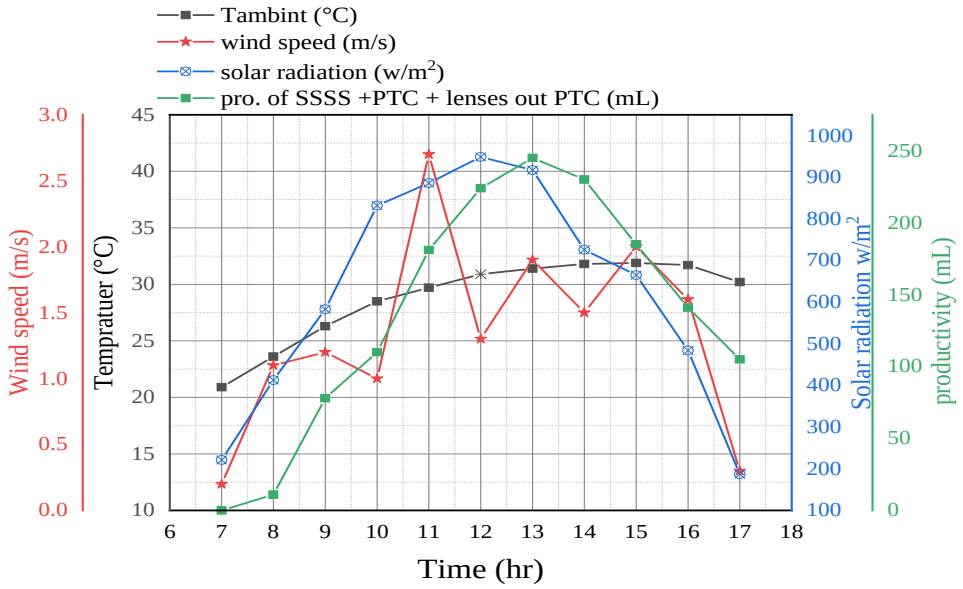

Figure (4.22): Variation of productivity and environmental conditions over time for solar still associated with a parabolic basin collector with lenses placed on either side of the parabolic trough on 4/27/2023.

Figure 4.23 shows the temperature variation of conventional over time. Temperatures were observed for all parameters of the traditional solar still were close at the beginning of the experiment, then it begins to rise as the intensity of the incident radiation increases. At 1:00 p.m, the maximum temperature of the water still basin water reached 69.5 °C as a result of sunlight falling vertically on the distillation device. The maximum temperature of the outer surface of the glass cover was recorded at 57.9°C at 1:00 p.m. After 1:00 p.m, temperatures were observed to decrease in parts of the solar, with the intensity of solar radiation decreasing..

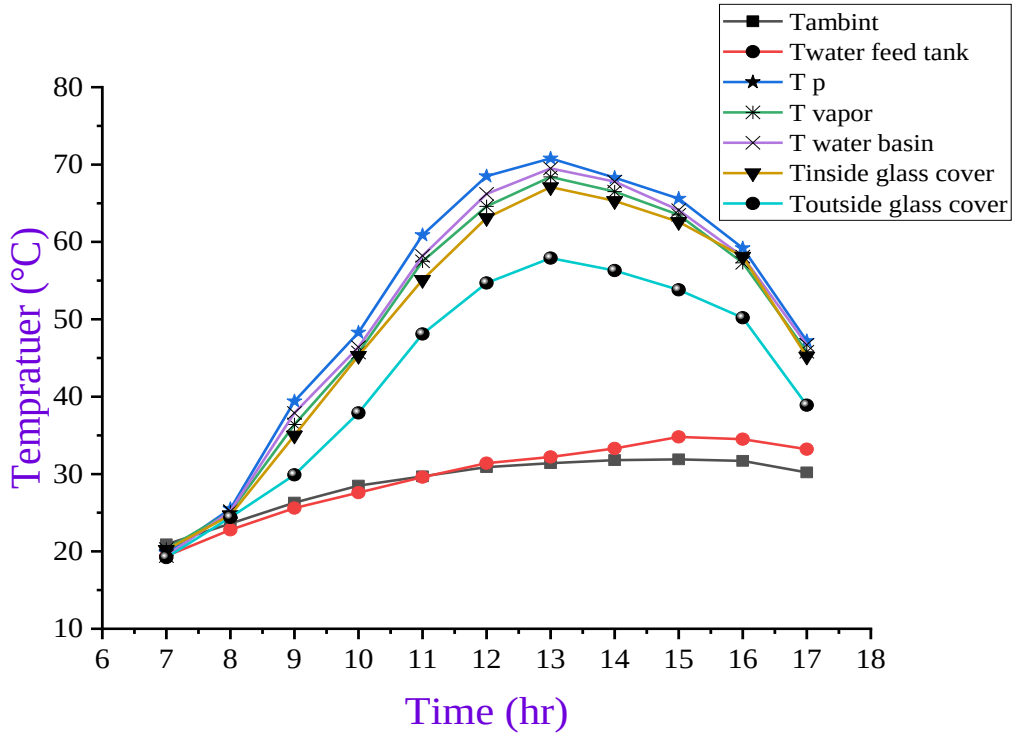

Figure (4.23): Conventional solar still temperature variation with time in 27/4/2023.

Figure 4.24 shows the temperature changes with time for a single-slope solar still associated with a parabolic trough with Fresnel lenses outside the PTC. The system contributes to enhancing the water temperature in the solar still basin. At the beginning of the experiment, the sun's temperatures are similar, then they begin to rise as the intensity of the incident radiation increases. At 1:00 p.m, the maximum temperature of the solar basin water reached 74.6°C as a result of sunlight falling vertically on the distillation device and the parabolic trough with the lenses. The maximum temperature of the outer surface of the glass cover was recorded as 62.1 °C at 1:00 p.m due to the effect of wind speed on the glass surface. After 1:00 p.m observed that temperatures decreased in parts of the a solar still with a decrease in the intensity of solar radiation.

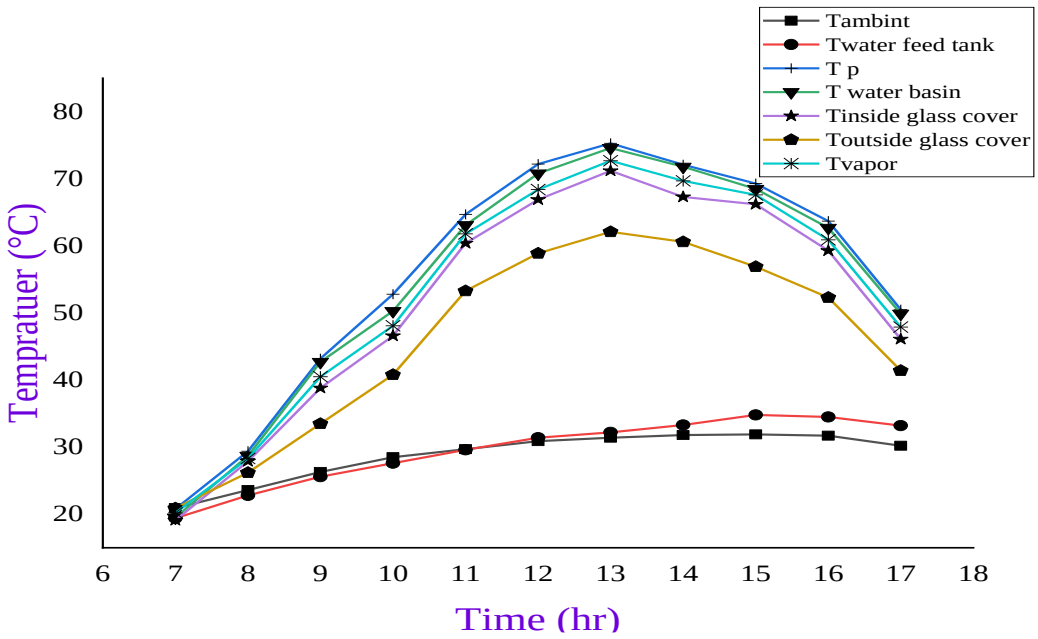

Figure (4. 24): Temperatures variation with time for the single slope still solar with the PTC and lenses out PTC on 27/4/2023.

Figure 4.25 shows the freshwater production over time of solar still and solar still associated with a parabolic trough with two Fresnel lenses on either side of the parabolic trough on April 27, 2023. Productivity was observed from the beginning of the experiment 8:00 am until 17:00, with maximum productivity of 189 mL for the traditional and 245 mL for the solar with PTC and lenses out PTC at 13:00.

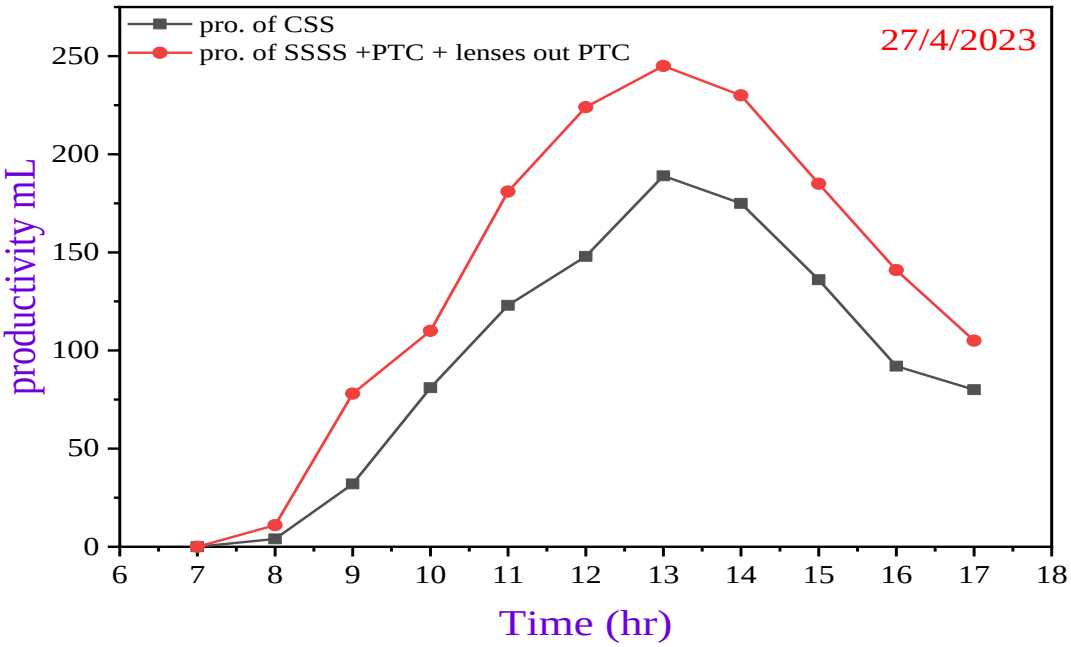

Figure (4.25): Variation of productivity with time for CSS and SSSS integrated with PTC and Fresnel lenses out PTC on 27/4/2023.

The second experiment was conducted on May 7, 2023, for conventional solar trains and distillers combined with a parabolic trough and two Fresnel lenses placed on both sides of the parabolic trough. At the solar radiation intensity starting from 259 W/m^2, wind speed was 0.5 m/s, and ambient temperature was 20.2 °C at the beginning of the experiment. The radiation intensity reached its peak at 12 pm, reaching 1025 W/m^2, and then decreased as the ambient temperature continued to rise. The cumulative output of the day, with an average solar radiation intensity of (673.2) W/m^2 and an average wind speed of (1.55) m/s is (5.3, 7.7) L/m^2 d for conventional and solar still associated with a parabolic trough with lenses outside the parabolic trough, on respectively as shown in Figures (4.26, 4.27). The increase in productivity amounted to 44.1% compared to the conventional, and the thermal efficiency was at 47% for the conventional and 19.32% for the solar energy associated with a parabolic trough collector with lenses outside PTC. A purity of up to 21 ppm has been obtained using river water as a feed source for solar still.

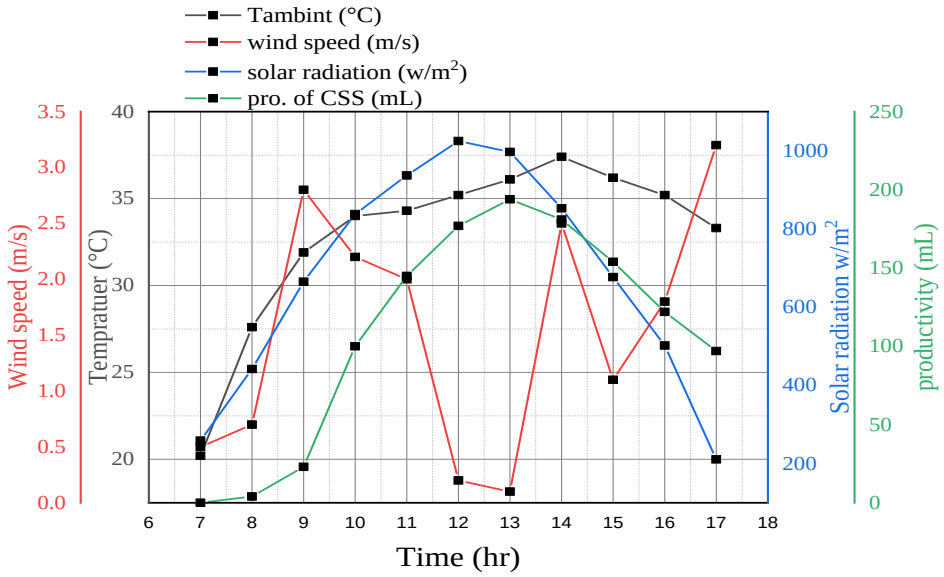

Figure (4.26): Variation of productivity and environmental conditions with time for conventional solar still on 7/5/2023.

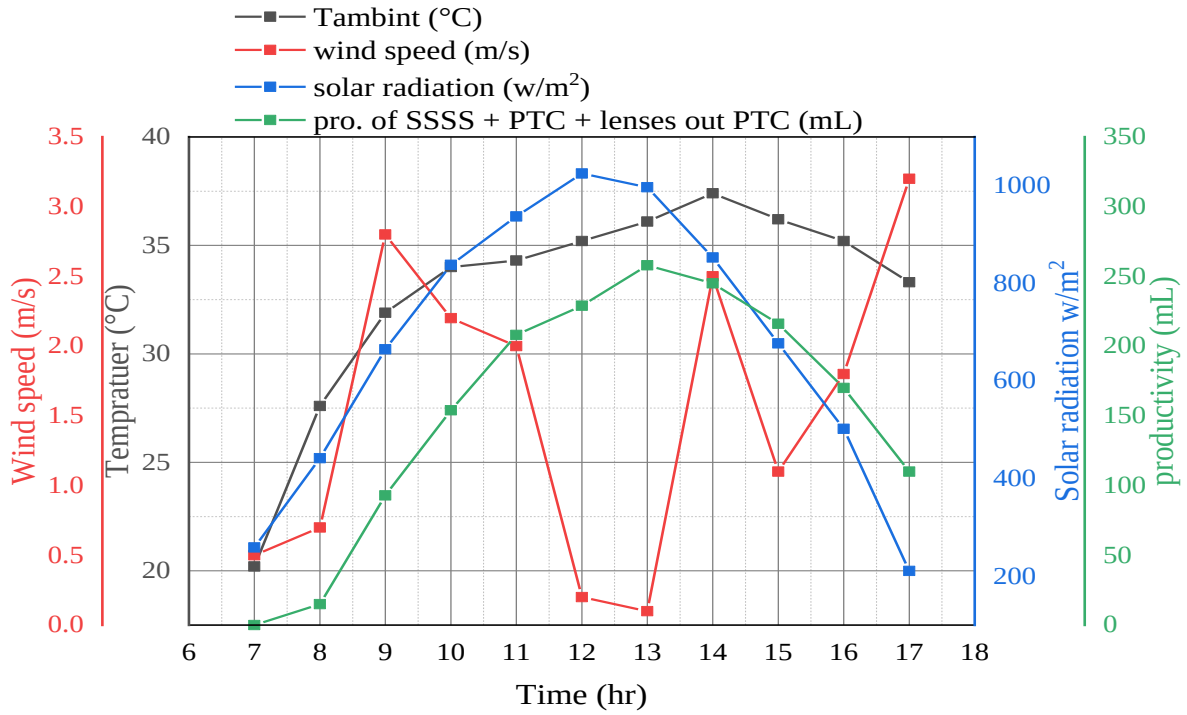

Figure (4.27): Variation of productivity and environmental conditions over time for solar still associated with PTC with lenses placed on either side of PTC on 7/5/2023.

Figure 4.28 shows the temperature variation of conventional over time. Temperatures were observed for all parameters of the traditional solar still were close at the beginning of the experiment, then it begins to rise as the intensity of the incident radiation increases. At 1:00 p.m, the maximum temperature of the water still basin water reached 71.8 °C as a result of sunlight falling vertically on the distillation device. The maximum temperature of the outer surface of the glass cover was recorded at 60.1°C at 1:00 p.m. After 1:00 p.m, temperatures were observed to decrease in parts of the solar, with the intensity of solar radiation decreasing.

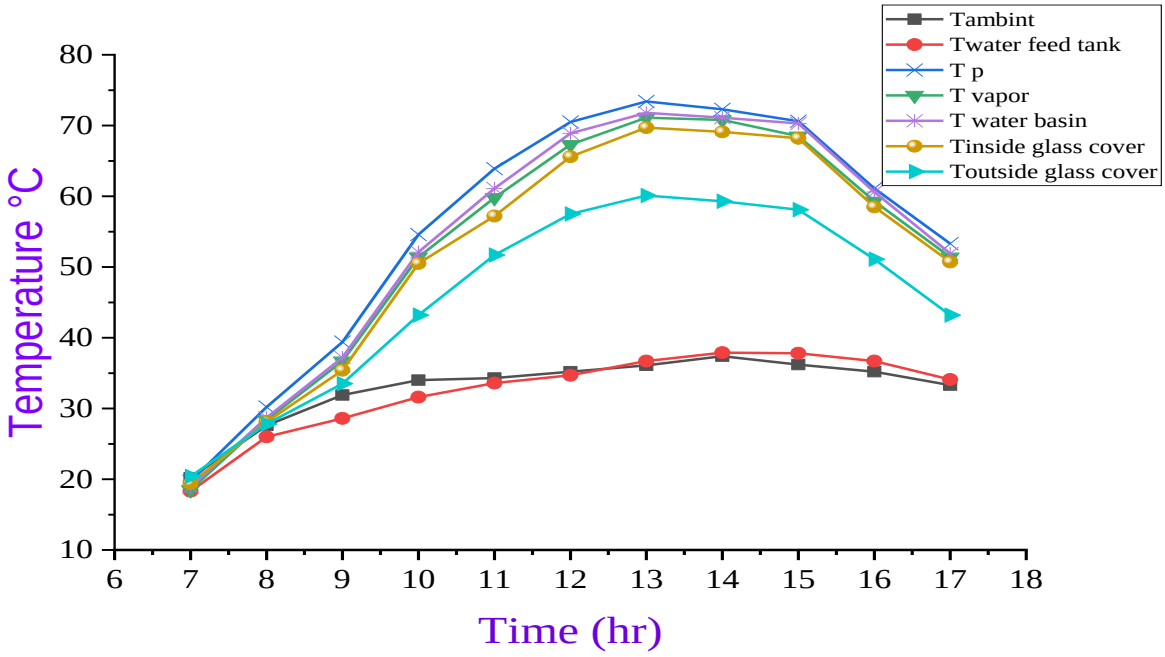

Figure (4.28): Conventional solar still temperature variation with time on 7/5/2023.

Figure (4.29) shows the temperature changes with time for a single-slope solar still associated with a parabolic trough with Fresnel lenses outside the PTC. The system contributes to enhancing the water temperature in the solar still basin. At the beginning of the experiment, the sun's temperatures are similar, then they begin to rise as the intensity of the incident radiation increases. At 1:00 p.m , the maximum temperature of the solar basin water reached 76.8°C as a result of sunlight falling vertically on the distillation device and the parabolic trough with the lenses. The maximum temperature of the outer surface of the glass cover was recorded as 64.2 °C at 1:00 p.m due to the effect of wind speed on the glass surface. After 1:00 p.m observed that temperatures decreased in parts of the a solar still with a decrease in the intensity of solar radiation.

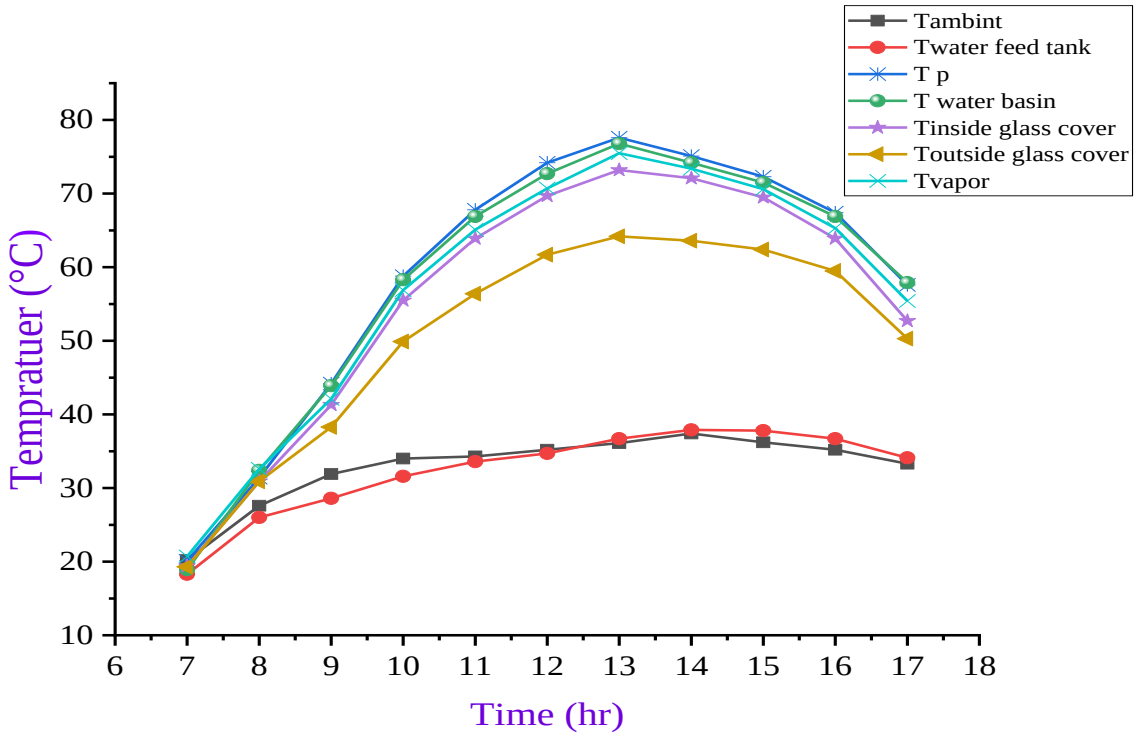

Figure (4.29): Temperatures variation with time for the single slope still solar with the PTC and lenses out PTC on 7/5/2023.

Figure 4.30 shows freshwater production over time from solar static and solar energy associated with a parabolic trough with two Fresnel lenses on either side of the parabolic trough on May 7, 2023. Productivity was observed from the beginning of the experiment 7:00 a.m until 17:00, with maximum productivity per hour 13:00 About 194 mL for the traditional model, and 258 mL for solar still with a parabolic trough and lenses on both sides PTC.

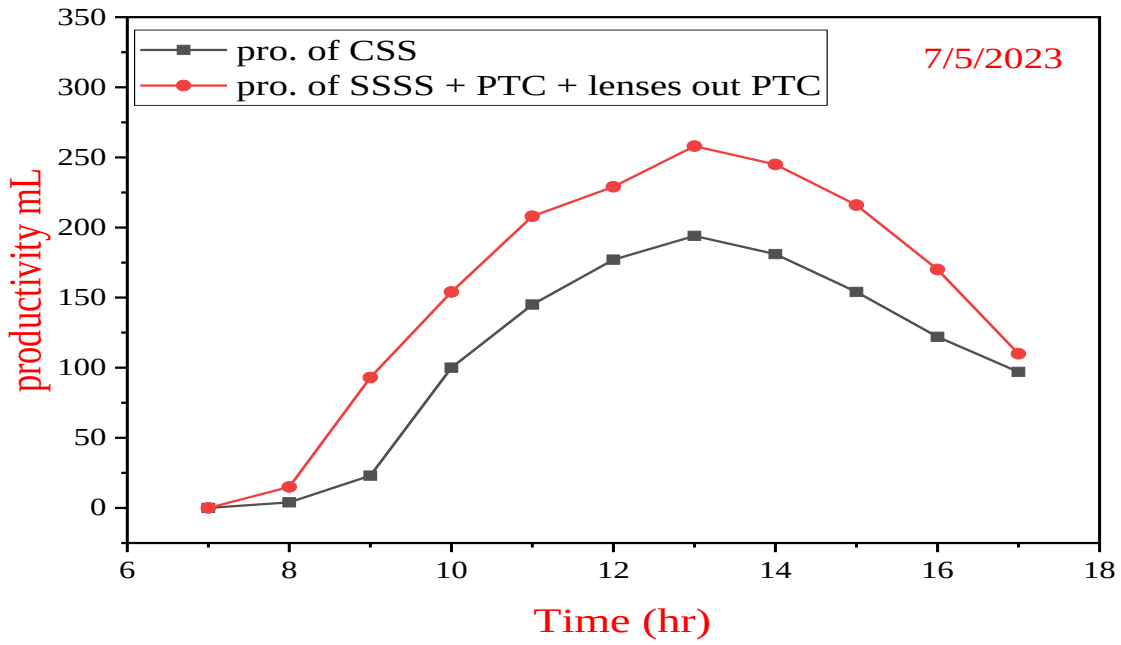

Figure (4.30): Variation of productivity with time for the conventional solar distiller and the integrated distiller with PTC and Fresnel lenses out PTC on 7/5/2023.

4.3 Comparison

4.3.1. Comparison of water productivity in experiments

In April and under close weather conditions for days 3, 5, and 27, a comparison was made between the productivity of the conventional solar and the solar energy associated with a parabolic trough collector, the solar energy associated with a parabolic trough collector with two Fresnel lenses over the trough, and the solar energy associated with a parabolic trough with two Fresnel lenses on both sides of the parabolic trough. The solar stills begin production for all experiments at 8:00 a.m, then begin to increase, reaching a maximum cumulative production at the end of the experiment of about 4.3, 5.76, 6.4, and 6.5 L/m^2 for all, respectively, as in Figure (4.31). Variation was noted in the amount of pure water obtained as a result of the different types of solar concentrators and the degree of similarity of climatic conditions.

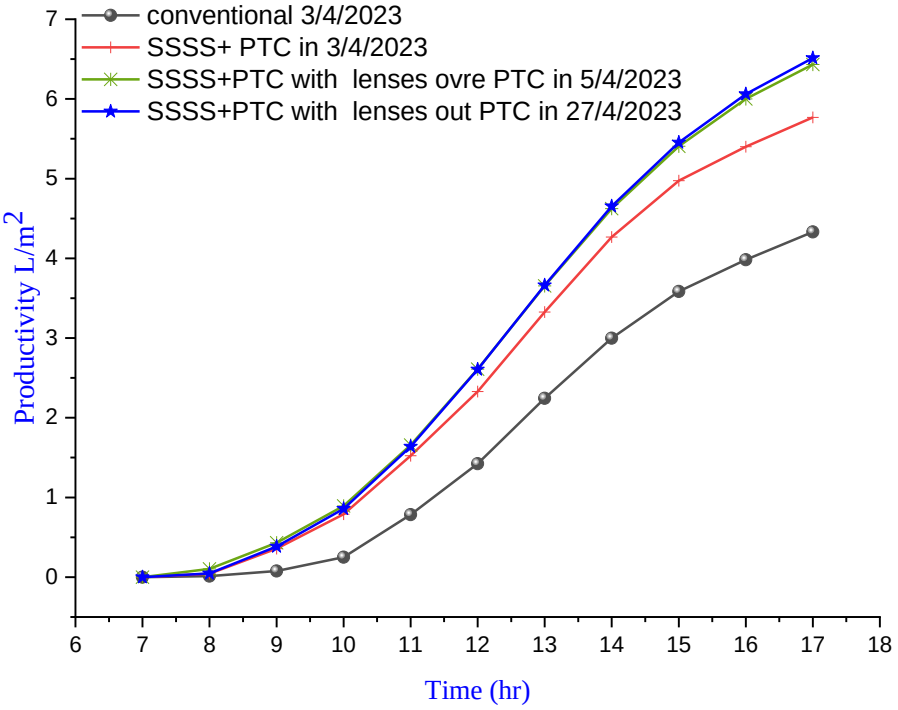

Figure (4.31): Production of pure water in April.

In May and under close weather conditions for days 5, 6, and 7, a comparison was made between the productivity of the conventional solar and the solar energy associated with a parabolic trough collector, the solar energy associated with a parabolic trough collector with two Fresnel lenses over the trough, and the solar energy associated with a parabolic trough with two Fresnel lenses on both sides of the parabolic trough. The solar stills begin production for all experiments at 8:00 a.m, then begin to increase, reaching a maximum cumulative production at the end of the experiment of about 5.1, 6.5, 7.1, and 7.3 L/m^2 for all, respectively, as in Figure (4.31). Variation was noted in the amount of pure water obtained as a result of the different types of solar concentrators and the degree of similarity of climatic conditions.

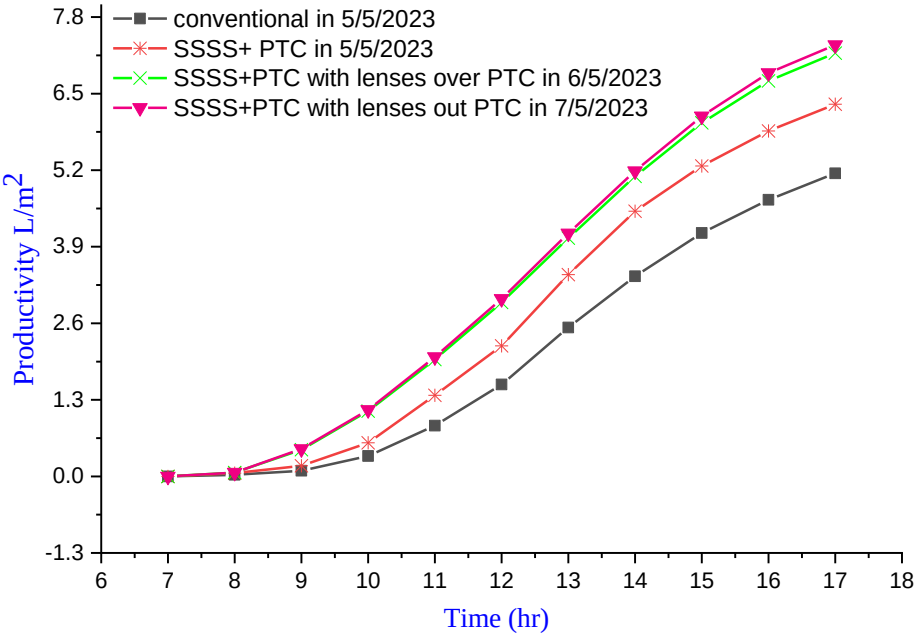

Figure (4.32): Production of pure water in May.

Figure (4.33) shows a comparison of the cumulative daily productivity from pure water for all practical experiments conducted in April and May of 2023. Observed the daily cumulative productivity for solar still associated with a parabolic trough collector with Fresnel lenses outside the parabolic trough is higher compared to the rest of the other cases. the maximum daily cumulative production was recorded at 1100 ml, 1390 ml, 1550 ml, and 1583 ml in April, and 1240 ml, 1590 ml, 1778 ml, and 1793 ml in May for the conventional CSS, SSSS with PTC, SSSS with PTC and lenses over PTC, and SSSS with PTC and lenses outside PTC respectively.

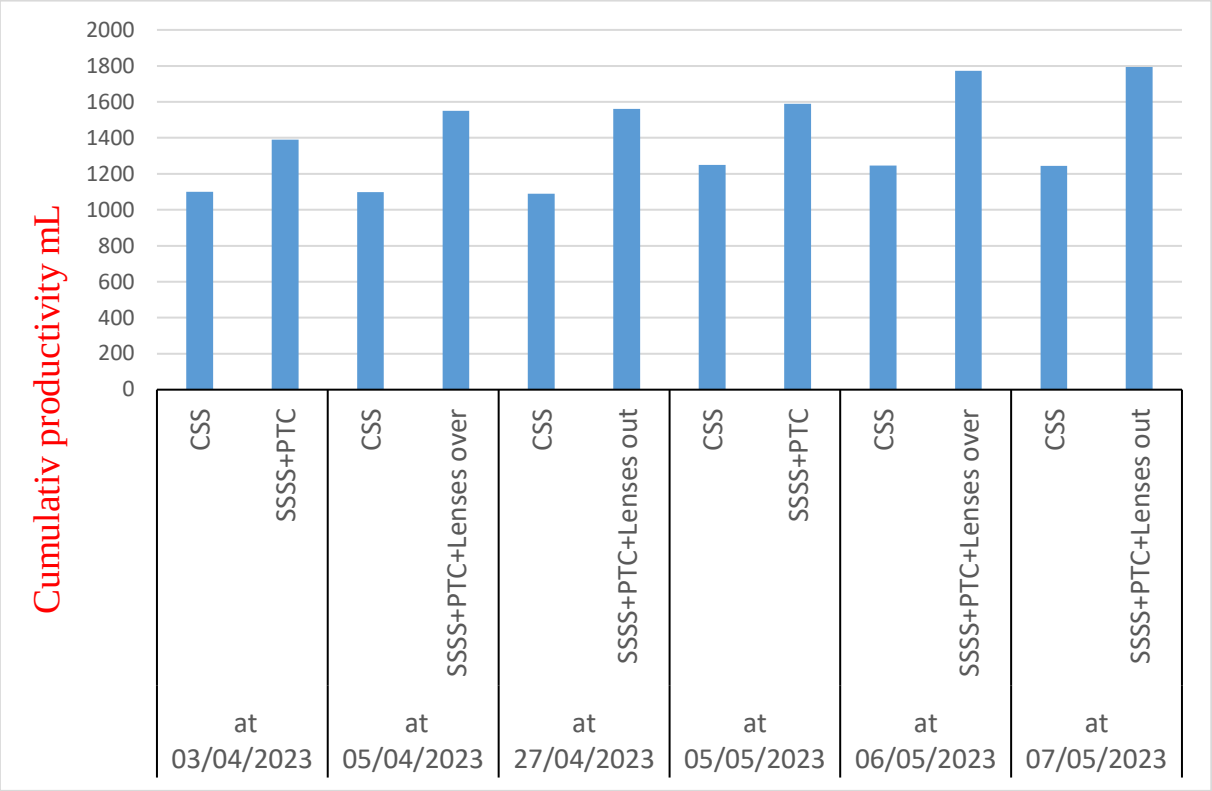

Figure (4.33): Comparing the daily cumulative productivity for all cases in this study.

4.3.2. Comparing the productivity and temperatures of the basin water with changing flow rates.

The system productivity was compared for different flow rates under similar climatic conditions in Al-Diwaniyah City during June. Experimental results show that using a lower volume flow rate increases the brine temperatures inside the solarium and thus increases the rates of evaporation and condensation. Figure 4.34 shows the variation in freshwater productivity over time for a solar still coupled to a parabolic trough collector. Experiments were conducted for days (1, 2, and 6) in June 2023, using volume flow rates of (0.5, 0.76, and 0.38) L/min, respectively. Experiments showed that the use of a volume flow rate (0.38) L/min reached the maximum productivity of pure water at 13:00 p.m is 252 mL, and at use of a volume flow rates (0.5, 0.76) L/min showed maximum productivity of about (247, 243) mL, respectively. Variation was observed in the amount of pure water obtained as a result of the difference in the discharge of heat transfer fluids and the degree of similarity of climatic conditions.

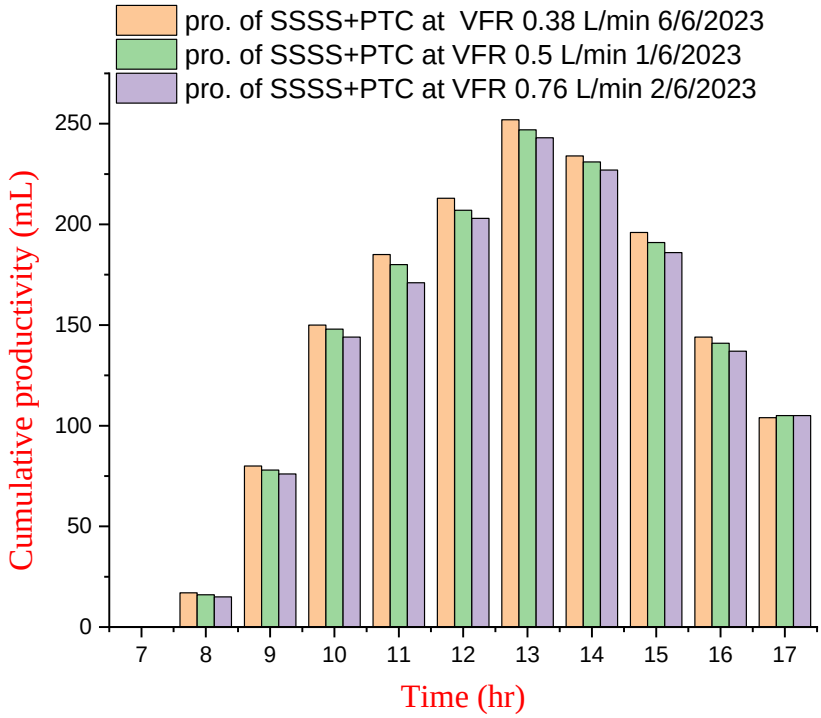

Figure (4.34): Productivity diagram of the solar collector with a parabolic trough at three volume flow rates.

Figure (4.35) shows the variation in freshwater productivity over time for a solar still coupled to a parabolic trough collector with Fresnel lenses over a parabolic trough. Experiments were conducted for days (8, 9, and 11) in June 2023, using volume flow rates of (0.5, 0.76, and 0.38) L/min, respectively. Experiments showed that the use of a volume flow rate (0.38) L/min reached the maximum productivity of pure water at 13:00 p.m is (262) mL, and at use of a volume flow rates (0.5, 0.76) L/min showed maximum productivity of about (257, and 249) mL, respectively. Variation was observed in the amount of pure water obtained as a result of the difference in the discharge of heat transfer fluids and the degree of similarity of climatic conditions.

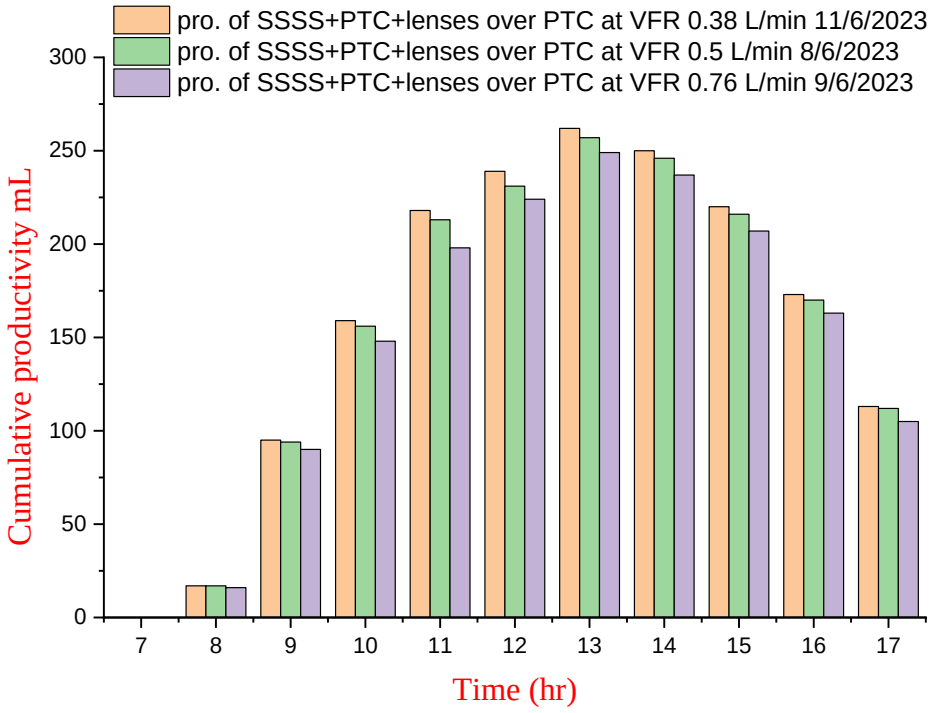

Figure (4.35): Productivity diagram of the solar collector with a parabolic trough and lenses inside at three volume flow rates.

Figure (4.36) shows the variation in freshwater productivity over time for a solar still coupled to a parabolic trough collector with Fresnel lenses outside a parabolic trough. Experiments were conducted for days (13, 15, and 16) in June 2023, using volume flow rates of (0.5, 0.76, and 0.38 L/min, respectively. Experiments showed that the use of a volume flow rate (0.38) L/min reached the maximum productivity of pure water at 13:00 p.m is (267) mL, and at use of a volume flow rates (0.5, 0.76) L/min showed maximum productivity of about (262, and 250) mL, respectively. Variation was observed in the amount of pure water obtained as a result of the difference in the discharge of heat transfer fluids and the degree of similarity of climatic conditions.

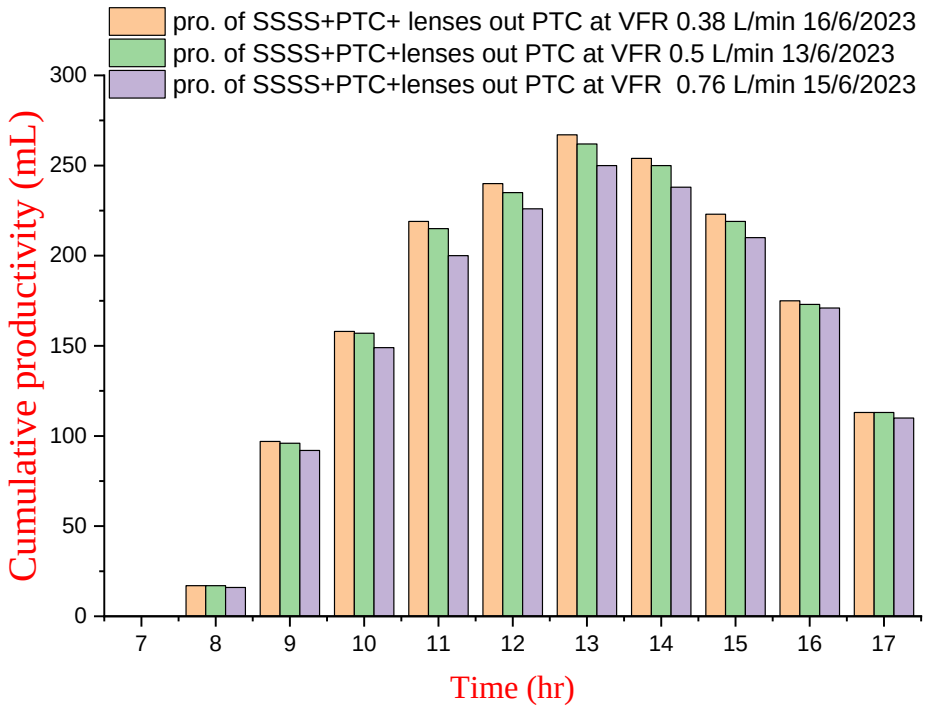

Figure (4.36): Productivity diagram of the solar collector with a parabolic trough and lenses outside at three volume flow rates.

Temperature results for the water basin of the conventional still and the solar still PTC were compared for days (1, 2, and 6) in June 2023, using volume flow rates of (0.5, 0.76, 0.38) L/min, respectively. The results showed that using a lower volume flow rate gave higher temperatures compared to other rates. Figure (4.37) shows that the temperature of all stills was close at 7:00 a.m began to rise, reaching the greatest value at 1:00 p.m, and then it began to decrease after that. The maximum temperature of the distillation basin water reached (81.9)°C at a volume flow rate of (0.38) L/min, while the basin water temperature was (76.8, 79.1) °C at volume flow rates of (0.76, and 0.5) L/min, respectively. while conventional solar still shows a maximum temperature basin still of 75.5 °C at the same time. Variation in solar still water temperatures resulting from the use of solar concentrators, variation in the discharge of heat transfer fluids, and similarity in climatic conditions were observed.

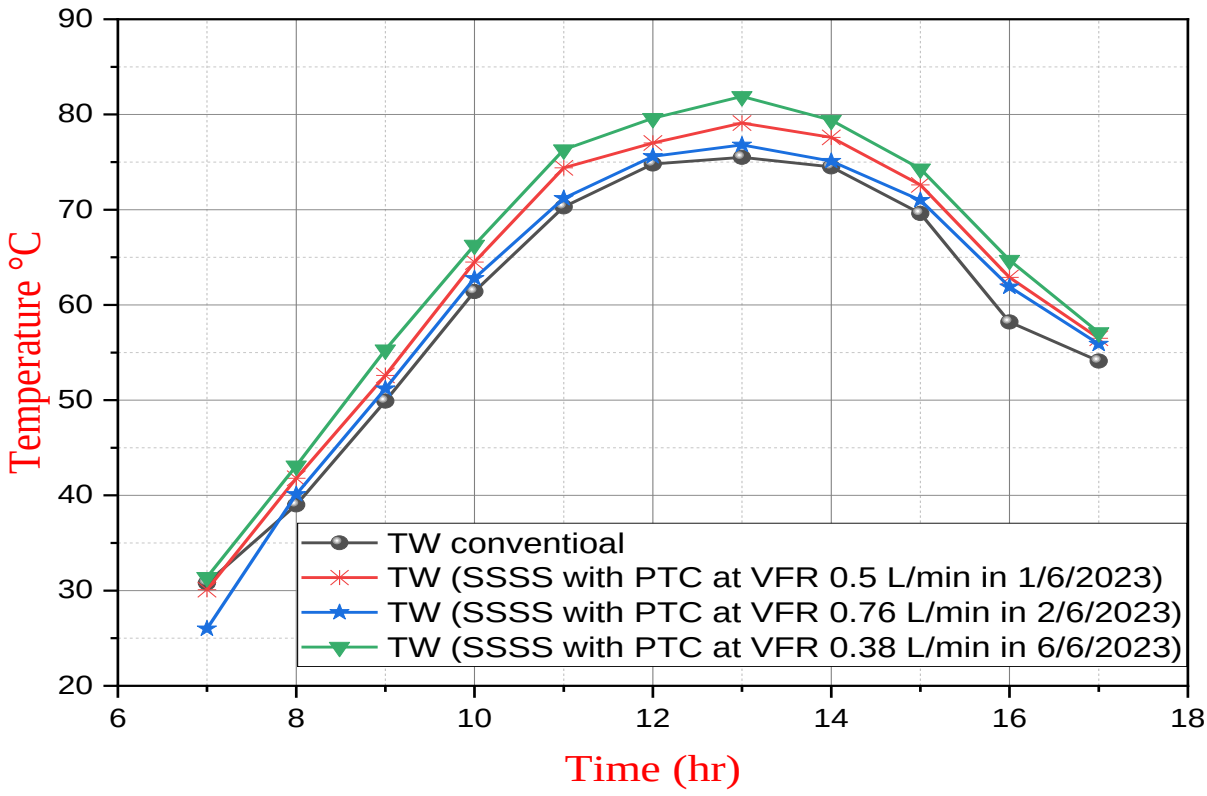

Figure (4.37): Variation of basin water temperatures over time for conventional and PTC-coupled distillation for three flow rates.

Figure (4.38) shows the variation of temperature water basin for the conventional still and solar still with PTC with Fresnel lenses over PTC were compared for days (8, 9, and 11) in June 2023, using volume flow rates of (0.5, 0.76, 0.38) L/min, respectively. The results showed that using a lower volume flow rate gave higher temperatures compared to other rates. It was observed that the basin water temperatures for all distillers were close at 7:00 a.m, then began to rise, reaching the highest value at 1:00 p.m, and then began to decrease after that. The maximum temperature of the distillation basin water reached (83.3) °C at a volume flow rate of (0.38) L/min, while the basin water temperature was (81.7, and 79.1) °C at volume flow rates of (0.5, 0.76) L/min, respectively. while conventional solar still shows a maximum temperature basin still of 75.5 °C at the same time. Variation in solar still water temperatures resulting from the use of solar concentrators, variation in the discharge of heat transfer fluids, and similarity in climatic conditions were observed.

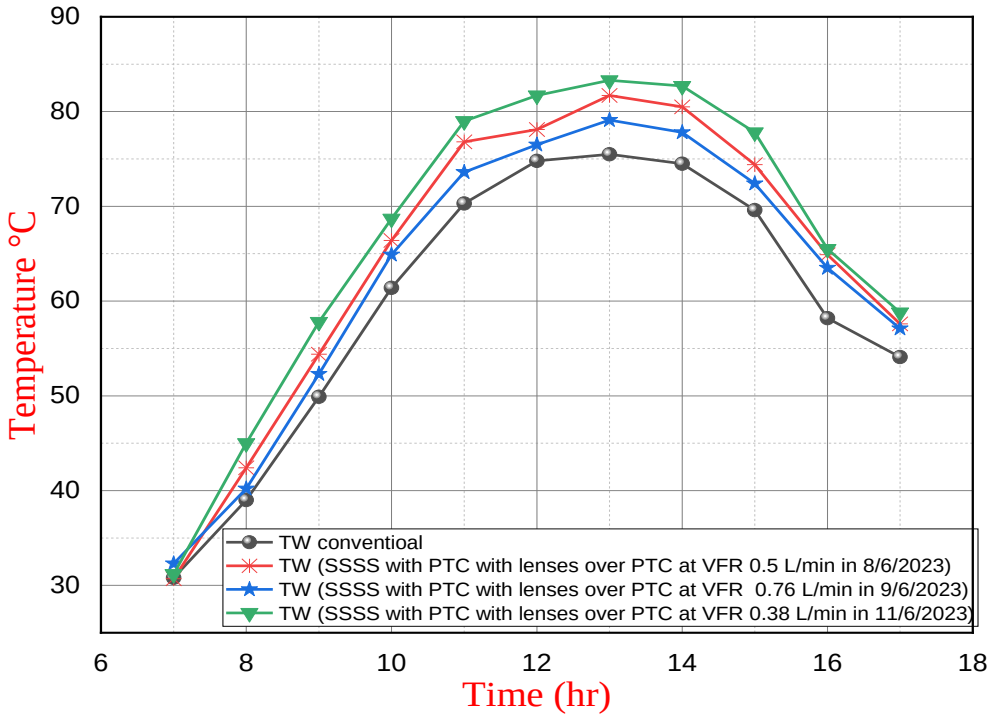

Figure (4.38): Variation of basin water temperatures over time for conventional and PTC-coupled distillation and lenses inside at three flow rates.

Figure (4.39) shows the variation of temperature water basin for the conventional still and solar still with PTC with Fresnel lenses outside PTC were compared for days (13, 15, and 16) in June 2023, using volume flow rates of (0.5, 0.76, 0.38) L/min, respectively. The results showed that using a lower volume flow rate gave higher temperatures compared to other rates It was observed that the basin water temperatures for all distillers were close at 7:00 a.m, then began to rise, reaching the highest value at 1:00 p.m, and then began to decrease after that. The maximum temperature of the distillation basin water reached (84.3) °C at a volume flow rate of (0.38) L/min, while the basin water temperature was (82.7 and 80.1) °C at volume flow rates of (0.5, 0.76) L/min, respectively. while conventional solar still shows a maximum temperature basin still of 75.5 °C at the same time. Variation in solar still water temperatures resulting from the use of solar concentrators, variation in the discharge of heat transfer fluids, and similarity in climatic conditions were observed.

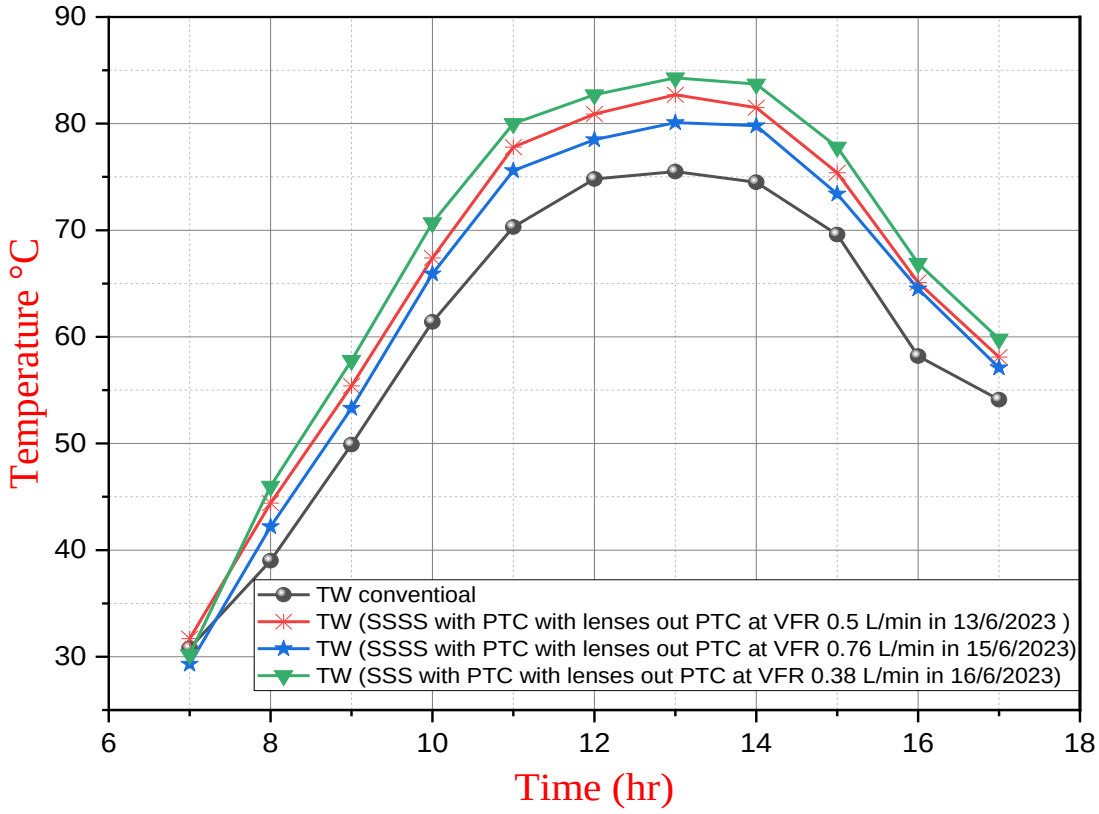

Figure (4.39): Variation of basin water temperatures over time for conventional and PTC-coupled distillation and lenses out for three flow rates.

4.3.3 Comparison of energy efficiency experiments.

The thermal efficiency of the system is the ratio between the useful energy (Qu) and the energy input (Qs). Energy efficiency depends on many factors such as the amount of fresh water, the amount of incident solar radiation, and the ambient temperature. In April the daily efficiencies were (44.7%, 17.05%, 18.78%, and 18.41%). In May they were (46.9%, 18.1%, 20.3%, 19.32%) for conventional devices, SSSS + PTC, SSSS + PTC with lenses in the side, SSSS + PTC with external lenses, respectively. A decrease in the daily thermal energy efficiency of the system associated with a solar concentrator was observed in Figure (4.40) as a result of the large heat loss when the area of the solar radiation fall aperture increased[68].

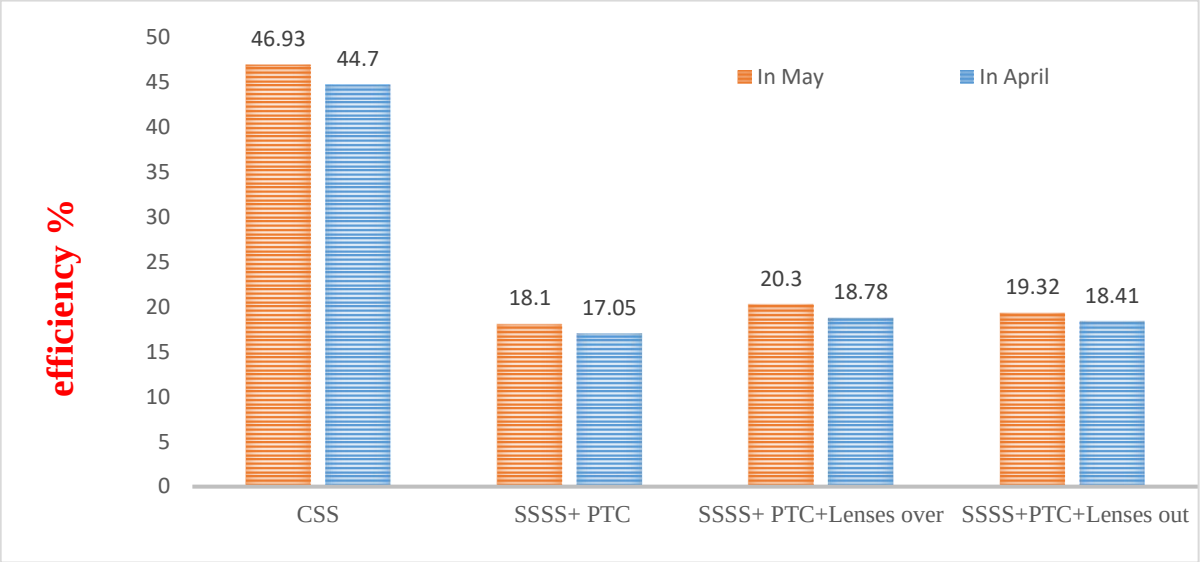

Figure (4.40): Thermal efficiency comparison chart.

4.3.4 Comparison with previous works.

4.3.4.1 Comparison of basin water temperatures and productivity for solar still.

To validate the experimental results of the conventional distillation apparatus, they were compared with the experimental results of previous researchers. Fadil (2022) [52] reported on an experimental work on a traditional single-slope solar distiller, with an area of about 0.159 m^2 made of cork, with a transparent glass cover 4 mm thick, with an inclination angle of 32 degrees with the horizon. The results on April 3 showed an acceptable agreement between them in terms of temperature and productivity, as shown in Figure (4.41). The error is only 17% for water temperature and it is only 18.2% when it comes to productivity. The presence of a difference in the temperatures of the basin water is the result of the difference in the type of absorbent plate, where galvanized iron with a thickness of 2 mm was used in this study, while [52] an absorbent plate combined with pipes (heat exchanger) with a thickness of 1 mm was used, which becomes more effective when combined with a parabolic trough.

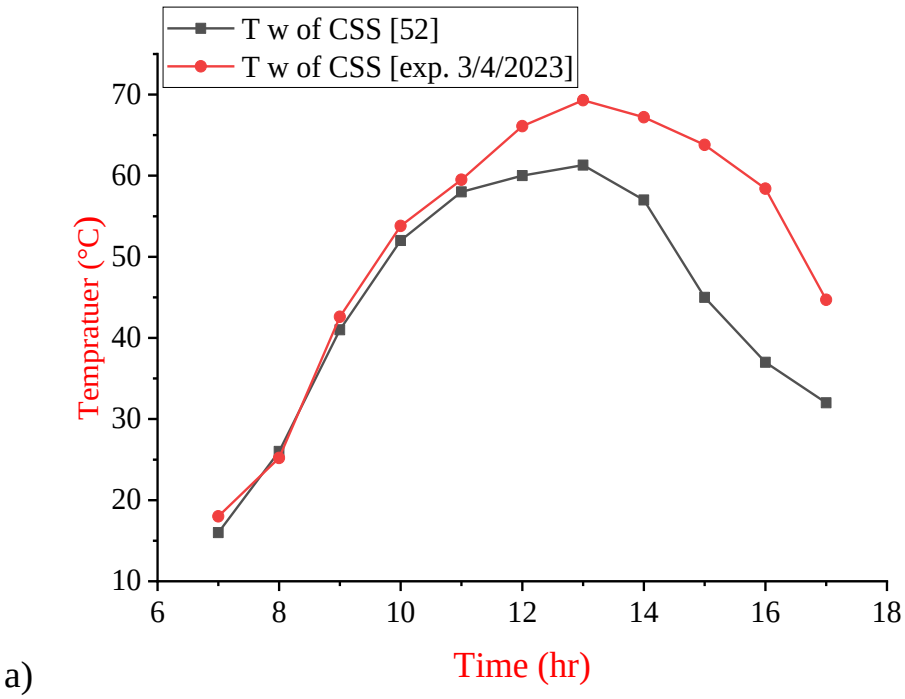

a)

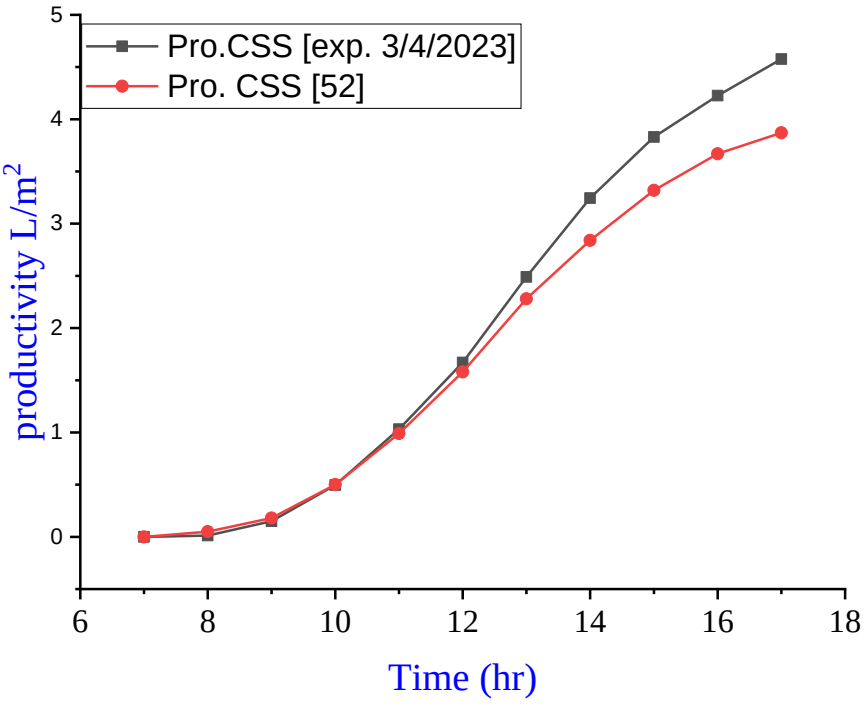

b)

Figure (4.41): a) Comparing experimental results for water temperatures inside the solar still (Tw). b) Comparing experimental results for productivity.

However, it is necessary to consider more than one case to ensure reliable work. Thus, other works were considered to validate the results obtained. Zahraa Abbas [29] reported an experimental work of a traditional solar distiller. The area of the basin used was 0.39 m^2 made of cork material, with a transparent glass

cover of 4 mm thickness, at an angle of inclination of 32 degrees with the horizon. Figure (4.42-a) shows a comparison of the basin water temperatures of the obtained results with the results recorded by Abbas (2021) [29], as well as Figure (4.42-b) shows the acquired daily return. The results on May 5 showed that there was a good agreement between them in terms of temperature and productivity. The error does not exceed 3.4%, and for the temperature of the basin water, the error does not exceed 6.8% for productivity.

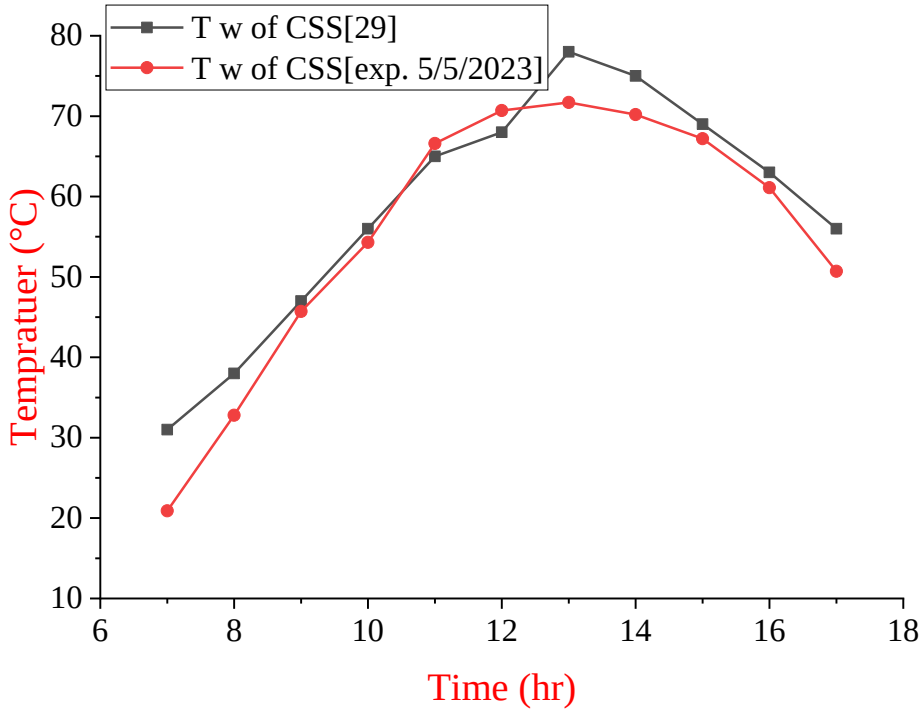

a)

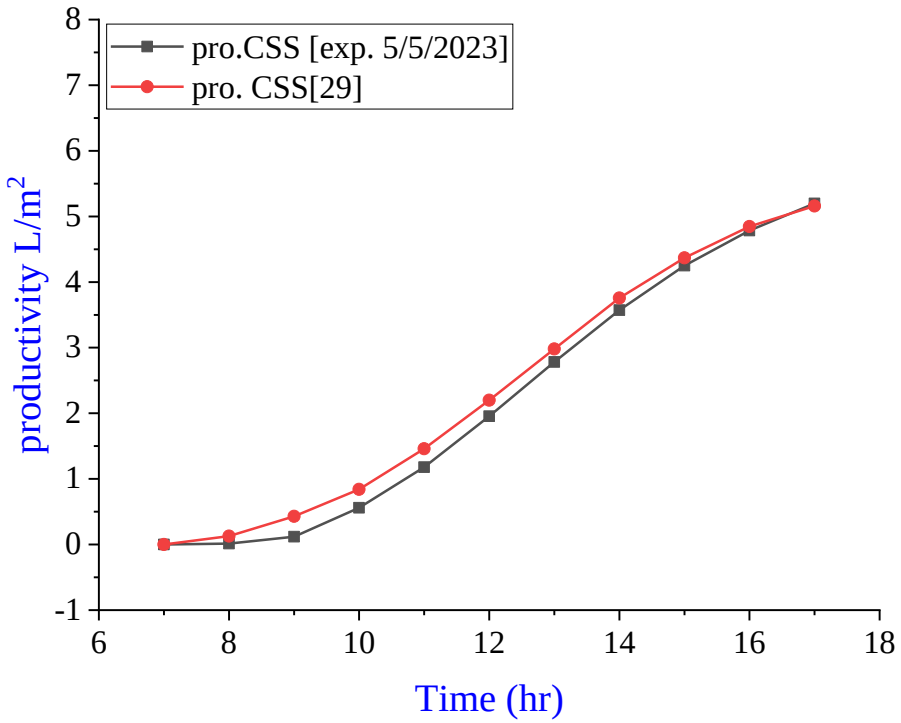

b)

Figure (4.42): a) Comparing experimental results for water temperatures inside the solar still (Tw). b) Comparing experimental results for productivity.

4.3.4.2 Comparison of basin water temperatures and productivity for parabolic trough collector.

The thermal performance and productivity of the parabolic trough-coupled solar distiller were compared with previous experimental studies to validate the results obtained. Fadel and colleagues [52] tested an experimental solar still working coupled to a 1.12 square meter parabolic trough oriented to the south with a manual tracking system. Figure (4.43-a) shows a comparison between the basin water temperatures of the distillation apparatus used in the experiment with the results recorded by Fadel. Figure (4.43-b) shows a comparison of the productivity of pure water during May with the results recorded by Fadel. The results showed a good agreement between them in terms of temperature and productivity. The error does not exceed 1%, and for aquarium water temperature the error does not exceed 1% for productivity.

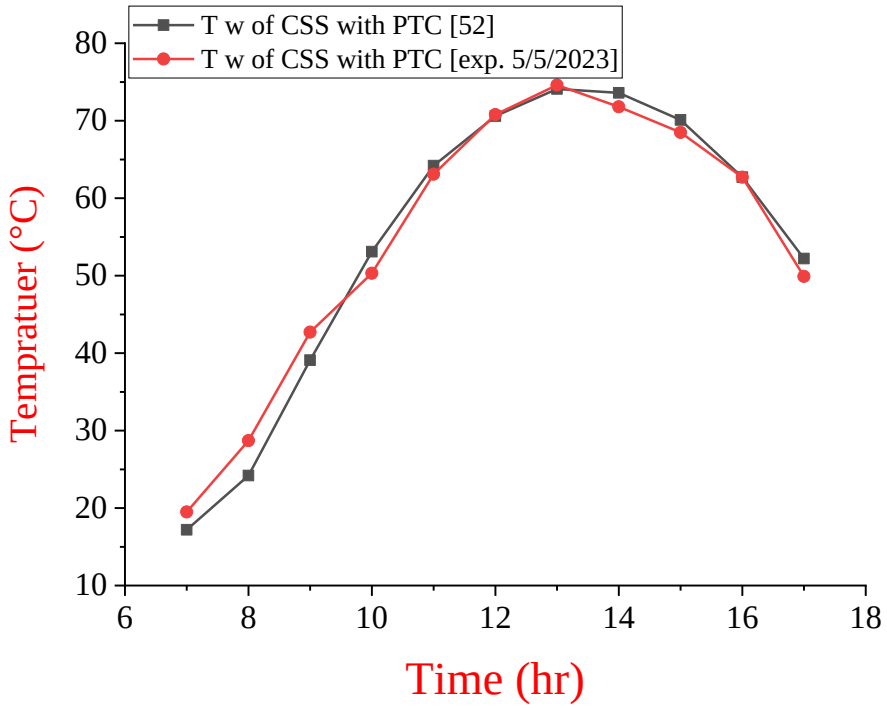

a)

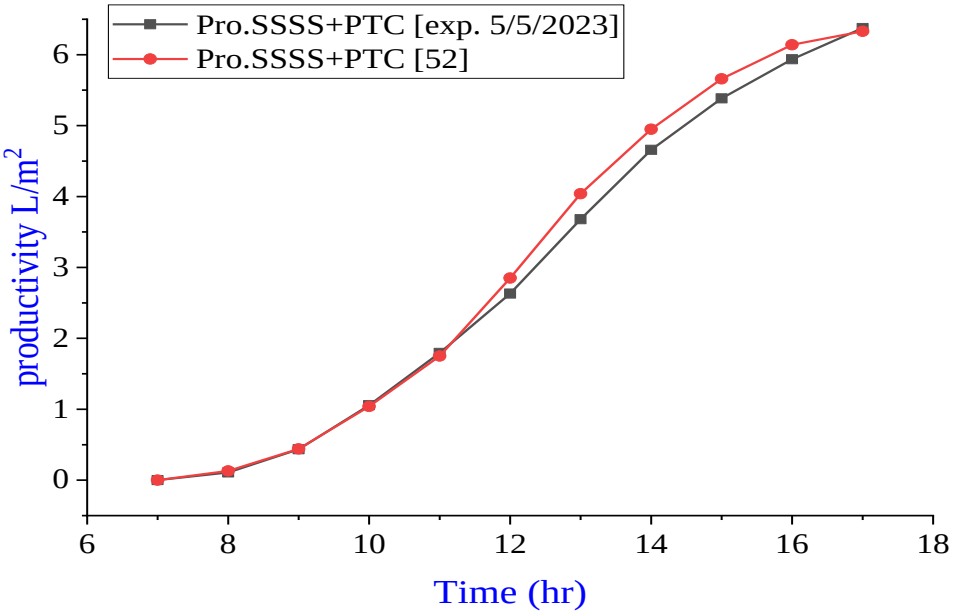

b)

Figure (4.43): a) Comparison of experimental results for water temperatures inside a basin of solar still (Tw) coupled with a PTC. b) Comparison of experimental results for productivity.

4.3.4.3 Comparison of cumulative productivity and daily thermal efficiency.

Many researchers have studied the performance of solar stills combined with a parabolic trough collector and have used several techniques to obtain better

results. Results in this study was compared in terms of the daily productivity of pure water with the results of previous researchers, as shown in figure (4.44).

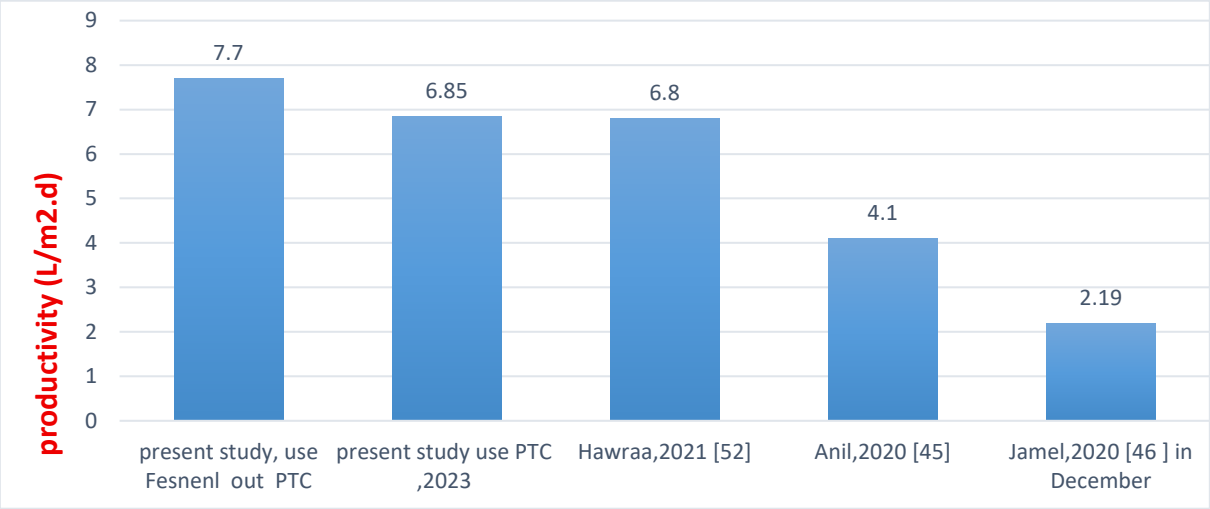

Figure (4.44): Comparison of the current study with other studies.

Table (4-1) Indicates a comparison of the efficiency and productivity of the current work with the previous work. It is clear from the comparison that the current work has a lower thermal efficiency and productivity than the previous literature for the solar distiller associated with a parabolic basin. This is due to the small area of the opening of the parabolic basin and the glass cover of the absorption tube and the difference in the heat transfer fluid used inside the tubes. oil was used as a heat transfer fluid with high thermal conductivity compared to water.

Table (4-1): Comparison of efficiency in the current work with previous work.

system	Freshwater Productivity, L/m^2 /day	Daily efficiency	Ref.
CSS	4.7	44.7%	present work
SSSS+PTC	5.9	17.05%	present work
CSS	4.03	32.59%	[48]

SSSS +PTC	8.2	22.2%	[48]
CSS	4.51	36.87%	[51]
SSSS+PTC	8.53	23.26%	[51]

CHAPTER FIVE

Conclusion and Recommendation

CHAPTER FIVE

Conclusion and Recommendation

5.1 Conclusion

All experiments were conducted in Iraq-Diwaniyah city (31.99°N, 44.93°E) during April and May, 2023. This research aimsed to enhance the production of static solar energy and to study the effect of using thermal condensers on the performance of solar distillation. A fixed solar distillation device was used towards the south with an inclination of 32 degrees and a linear thermal condenser (PTC) facing south in addition to Fresnel lenses placed either inside or outside the solar concentrator aperture area. Results showed that the use of Fresnel lenses increased in evaporation rates, which greatly contributed to improving the productivity of the solar distillation system, and the conclusions can be summarized as follows:

1. The proposed solar energy yield is still affected by many factors, including environmental factors and design factors. Environmental factors include wind speed, radiation intensity, and ambient temperature. The solar still design factors include solar distillation area, galvanized sheet thickness type, inclination angle, glass transmittance, thermal insulation, and saltwater height inside the solar housing. For PTC, the reflective surface type, equivalent aperture area, receiving tube material, heat transfer medium, insulation, and solar tracking accuracy play a major role in the enhancement process. For condenser lenses, aperture area, focal length, and focus intensity are important design factors to consider when using condenser lenses.
2. The results showed that the use of Fresnel lenses inside or outside the parabolic trough has an effective role in the performance of the monoclinic solar distillation system.
3. The maximum productivity obtained from the solar system using Fresnel lenses outside the PTC aperture area was 7.7 L/m^2, while the productivity of

the conventional distiller was 5.31 L/m^2 on May 7, with an average wind speed was 1.55 m/s and average solar radiation intensity was 673.2 W/m^2.

4. On the 6th of May, when an average solar radiation intensity was 670.7 W/m^2 and average wind speed was 1.19 m/s, a maximum productivity was obtained from the solar system using Fresnel lenses within the PTC aperture area was 7.5 L/m^2, while the productivity of the traditional distiller was 5.32 L/m^2.
5. The solar distiller associated with the parabolic trough collector on the 5th of May, when an average wind speed was 2.1 m/s and average solar radiation intensity was 663.8 W/m^2 showed the maximum productivity obtained 6.7 L/m^2, while the productivity of the traditional distiller was 5.34 L/m^2
6. In May Fresnel lenses and a parabolic trough improved the solar still yield by (44.1%, 43.3%, and 28.2%) for solar stills with lenses outside the PTC aperture area, solar stills with lenses inside the PTC aperture area, and for solar stills combined with the parabolic trough, respectively.
7. The solar system showed daily thermal energy efficiency in April (44.7%, 17.05%, 18.78%, 18.41%) in May (46.9%, 18.1%, 20.3%, 19.32%) for conventional devices, SSSS + PTC, SSSS + PTC with Lenses in side, SSSS + PTC with external lenses, respectively. When comparing the thermal energy efficiency results obtained from previous researchers' experiments using a parabolic sump collector, it is considered acceptable. The thermal efficiency ratio of modified solar energy is lower than that of conventional energy due to the increase in the area of the solar collector.

5.2 Recommendations

Several recommendations can be used in future work:

1. Using the solar tracking system of the parabolic basin collector to focus the solar radiation with high accuracy towards the absorption tube using thermal condensers.
2. Fabrication of a vacuum glass tube to cover the receiver tube to contribute to reducing heat loss.
3. Increasing the paraboloid orifice area and distillation orifice area, which enhances the productivity of the solar system.
4. Using the highly reflective surfaces of the parabolic trough to increase the concentration of sunlight towards the absorber tube.

REFERENCES

REFERENCES

[1] R. Sathyamurthy, P. K. Nagarajan, S. A. El-Agouz, V. Jaiganesh, and P. Sathish Khanna, “Experimental investigation on a semi-circular trough-absorber solar still with baffles for fresh water production,” Energy Convers. Manag., vol. 97, pp. 235–242, 2015, doi: 10.1016/j. enconman. 2015.03.052.

[2] K. V. Modi and K. H. Nayi, “Efficacy of forced condensation and forced evaporation with thermal energy storage material on square pyramid solar still,” Renew. Energy, vol. 153, pp. 1307–1319, 2020, doi: 10.1016/j. renene. 2020. 02.095.

[3] J. J. Feria-Díaz, M. C. López-Méndez, J. P. Rodríguez-Miranda, L. C. Sandoval-Herazo, and F. Correa-Mahecha, “Commercial thermal technologies for desalination of water from renewable energies: A state of the art review,” Processes, vol. 9, no. 2, pp. 1–22, 2021, doi: 10. 3390/pr 9020262.

[4] S. Shanmugan, V. Manikandan, K. Shanmugasundaram, B. Janarathanan, and J. Chandrasekaran, “Energy and exergy analysis of single slope single basin solar still,” Int. J. Ambient Energy, vol. 33, no. 3, pp. 142–151, 2012, doi: 10.1080/01430750.2012.686194.

[5] A. F. Muftah, M. A. Alghoul, A. Fudholi, M. M. Abdul-Majeed, and K. Sopian, “Factors affecting basin type solar still productivity: A detailed review,” Renew. Sustain. Energy Rev., vol. 32, pp. 430–447, 2014, doi: 10.1016/j.rser.2013.12.052.

[6] S. A. Kalogirou, Solar thermal collectors and applications, Progress in Energy and Combustion Science, vol. 30, no. 3. 2004. doi: 10.1016/j. pecs.2004.02.001.

[7] F. Muhammad-sukki, R. Ramirez-iniguez, S. G. Mcmeekin, B. G. Stewart, and B. Clive, “Solar Concentrated,” nternational Journal of Applied

Sciences (IJAS), Volume (1): Issue (1), no. 1, pp. 1–15, 2010.

[8] H. A. Kazem and M. T. Chaichan, “Status and future prospects of renewable energy in Iraq,” Renew. Sustain. Energy Rev., vol. 16, no. 8, pp. 6007–6012, 2012, doi: 10.1016/j.rser.2012.03.058.

[9] M. S. Sachit, H. Z. M. Shafri, A. F. Abdullah, and A. S. M. Rafie, “Combining Re-Analyzed Climate Data and Landcover Products to Assess the Temporal Complementarity of Wind and Solar Resources in Iraq,” Sustain., vol. 14, no. 1, 2022, doi: 10.3390/su14010388.

[10] V. V. Tyagi, S. C. Kaushik, and S. K. Tyagi, “Advancement in solar photovoltaic/thermal (PV/T) hybrid collector technology,” Renew. Sustain. Energy Rev., vol. 16, no. 3, pp. 1383–1398, 2012, doi: 10.1016/j. rser.2011.12.013.

[11] K. Ravi Kumar, N. V. V. Krishna Chaitanya, and N. Sendhil Kumar, “Solar thermal energy technologies and its applications for process heating and power generation – A review,” J. Clean. Prod., vol. 282, p. 125296, 2021, doi: 10.1016/j.jclepro.2020.125296.

[12] S. Suman, M. K. Khan, and M. Pathak, “Performance enhancement of solar collectors - A review,” Renew. Sustain. Energy Rev., vol. 49, pp. 192–210, 2015, doi: 10.1016/j.rser.2015.04.087.

[13] V. Kumar, R. L. Shrivastava, and S. P. Untawale, “Fresnel lens: A promising alternative of reflectors in concentrated solar power,” Renew. Sustain. Energy Rev., vol. 44, pp. 376–390, 2015, doi: 10.1016/j. rser. 2014.12.006.

[14] E. Bellos, Z. Said, and C. Tzivanidis, “The use of nanofluids in solar concentrating technologies: A comprehensive review,” J. Clean. Prod., vol. 196, pp. 84–99, 2018, doi: 10.1016/j.jclepro.2018.06.048.

[15] Q. Xiong et al., “A comprehensive review on the application of hybrid

nanofluids in solar energy collectors," Sustain. Energy Technol. Assessments, vol. 47, no. March, 2021, doi: 10.1016/j.seta.2021.101341.

[16] L. Wang, Z. Yuan, Y. Zhao, and Z. Guo, "Review on Development of Small Point-Focusing Solar Concentrators," J. Therm. Sci., vol. 28, no. 5, pp. 929–947, 2019, doi: 10.1007/s11630-019-1134-4.

[17] A. Asrori, S. Suparman, S. Wahyudi, and D. Widhiyanuriyawan, "Investigation of Steam Generation Performance on Conical Cavity Receiver By Different Geometric Concentration Ratios for Fresnel Lens Solar Concentrator," Eastern-European J. Enterp. Technol., vol. 4, no. 8–106, pp. 6–14, 2020, doi: 10.15587/1729-4061.2020.209778.

[18] K. Awasthi, D. S. Reddy, and M. K. Khan, "Design of Fresnel lens with spherical facets for concentrated solar power applications," Int. J. Energy Res., vol. 44, no. 1, pp. 460–472, 2020, doi: 10.1002/er.4947.

[19] W. T. Xie, Y. J. Dai, R. Z. Wang, and K. Sumathy, "Concentrated solar energy applications using Fresnel lenses: A review," Renew. Sustain. Energy Rev., vol. 15, no. 6, pp. 2588–2606, 2011, doi: 10.1016/j .rser. 2011.03.031.

[20] T. T. Pham, N. H. Vu, and S. Shin, "Novel design of primary optical elements based on a linear fresnel lens for concentrator photovoltaic technology," Energies, vol. 12, no. 7, 2019, doi: 10.3390/en12071209.

[21] G. A. Madhugiri and S. R. Karale, "High solar energy concentration with a Fresnel lens: A Review," Int. J. Mod. Eng. Res. www.ijmer.com, vol. 2, no. 3, pp. 1381–1385, 2012, [Online]. Available: www.ijmer.com

[22] M. A. Sharaf, A. S. Nafey, and L. García-Rodríguez, "Exergy and thermo-economic analyses of a combined solar organic cycle with multi effect distillation (MED) desalination process," Desalination, vol. 272, no. 1–3, pp. 135–147, 2011, doi: 10.1016/j.desal.2011.01.006.

[23] E. Kabir, P. Kumar, S. Kumar, A. A. Adelodun, and K. H. Kim, "Solar energy: Potential and future prospects," Renew. Sustain. Energy Rev., vol. 82, no. September 2017, pp. 894–900, 2018, doi: 10.1016/j. rser. 2017. 09. 094.

[24] V. K. Chauhan, S. K. Shukla, J. V. Tirkey, and P. K. Singh Rathore, A comprehensive review of direct solar desalination techniques and its advancements, vol. 284. Elsevier Ltd, 2021. doi: 10.1016/j. jclepro. 2020. 124719.

[25] A. E. Kabeel, Z. M. Omara, and M. M. Younes, "Techniques used to improve the performance of the stepped solar still-A review," Renew. Sustain. Energy Rev., vol. 46, pp. 178–188, 2015, doi: 10.1016/j.rser. 2015. 02.053.

[26] T. Abderachid and K. Abdenacer, "Effect of orientation on the performance of a symmetric solar still with a double effect solar still (comparison study)," Desalination, vol. 329, pp. 68–77, 2013, doi: 10.1016/j.desal.2013.09.011.

[27] A. Muthu Manokar, K. Kalidasa Murugavel, and G. Esakkimuthu, "Different parameters affecting the rate of evaporation and condensation on passive solar still - A review," Renew. Sustain. Energy Rev., vol. 38, pp. 309–322, 2014, doi: 10.1016/j.rser.2014.05.092.

[28] K. Kalidasa Murugavel, P. Anburaj, R. Samuel Hanson, and T. Elango, "Progresses in inclined type solar stills," Renew. Sustain. Energy Rev., vol. 20, pp. 364–377, 2013, doi: 10.1016/j.rser.2012.10.047.

[29] Z. A. Faisal, H. G. Hameed, "Investigation The Effects Of Preheating Water And Cooling Of Glass Cover On The Performance Of Single Slope Solar Still," A thesis submitted to the Department of Mechanical Power Engineering Technologies To obtain a master's degree at Al-Furat Al-Awsat University - College of Engineering Technology/Najaf vol. 10, p. 6,

2021.

[30] D. Nagasundaram and K. Karuppasamy, “Desalination of Sea Water By Using Solar Still With Fresnel,” International Journal of Advanced Research in Biology Engineering Science and Technology (IJARBEST), vol. 2, no. 6, 2016.

[31] V. R. Rajesh, K. Harikrishnan, K. K. Chaithanya, and S. Salim, “Performance evaluation of a solar desalination system integrated with a Fresnel lens concentrator,” Int. J. Renew. Energy Res., vol. 6, no. 1, pp. 250–253, 2016, doi: 10.20508/ijrer.v6i1.3092.g6781.

[32] A. E. D. I. Owaid, S. M. Hadi, R. A. Ahmmed, and K. Alwan, “Studying of Performance Enhancement for Classic Solar Still Using Solar Concentrator By Fresnel Lens Technique With Hot Water Production,” International Journal of Research in Engineering & Technology (IMPACT: IJRET) , vol. 5, no. 10, pp. 29–40, 2017.

[33] R. Sathyamurthy and E. El-Agouz, “Experimental analysis and exergy efficiency of a conventional solar still with Fresnel lens and energy storage material,” Heat Transf. - Asian Res., vol. 48, no. 3, pp. 885–895, 2019, doi: 10.1002/htj.21412.

[34] L. Mu et al., “Enhancing the performance of a single-basin single-slope solar still by using Fresnel lens: Experimental study,” J. Clean. Prod., vol. 239, pp. 1–27, 2019, doi: 10.1016/j.jclepro.2019.118094.

[35] A. Johnson et al., “A thermal model for predicting the performance of a solar still with fresnel lens,” Water (Switzerland), vol. 11, no. 9, 2019, doi: 10.3390/w11091860.

[36] R. Borase, J. Gawande, S. Pawar, and S. Jadhav, “Solar Powered Water Desalination Using Fresnel Lens Tracking System,” 2019 IEEE Pune Sect. Int. Conf. PuneCon 2019, pp. 14–17, 2019, doi: 10.1109/PuneCon46936. 2019 .9105668.

[37] M. Muraleedharan, H. Singh, M. Udayakumar, and S. Suresh, "Modified active solar distillation system employing directly absorbing Therminol 55–Al2O3 nano heat transfer fluid and Fresnel lens concentrator," Desalination, vol. 457, no. August 2018, pp. 32–38, 2019, doi: 10.1016/j. desal.2019.01.024.

[38] M. H. R. Alktranee, Q. Al-Yasiri, and A. E. Kabeel, "Improving the productivity of a single-slope solar still using fresnel lenses under iraq climatic conditions," Desalin. Water Treat., vol. 205, pp. 22–30, 2020, doi: 10.5004/dwt.2020.26424.

[39] P. S. Bhambare, D. K. Kaithari, and S. A. R. AI Hosni, "Performance enhancement of a single slope solar still with single basin using Fresnel lens," J. Mech. Eng. Sci., vol. 15, no. 1, pp. 7781–7791, 2021, doi: 10.15282/jmes.15.1.2021.14.0614.

[40] D. G. Subhedar, K. V. Chauhan, K. Patel, and B. M. Ramani, "Performance improvement of a conventional single slope single basin passive solar still by integrating with nanofluid-based parabolic trough collector: An experimental study," Mater. Today Proc., vol. 26, no. xxxx, pp. 1478–1481, 2019, doi: 10.1016/j.matpr.2020.02.304.

[41] H. Amiri, M. Aminy, M. Lotfi, and B. Jafarbeglo, "Energy and exergy analysis of a new solar still composed of parabolic trough collector with built-in solar still," Renew. Energy, vol. 163, pp. 465–479, 2021, doi: 10.1016/j.renene.2020.09.007.

[42] R. Bellatreche, M. Ouali, D. Tassalit, and M. Balistrou, "Thermal efficiency improvement of a solar desalination process by parabolic trough collector," Water Supply, vol. 21, no. 7, pp. 3698–3709, 2021, doi: 10.2166/ws. 2021.131.

[43] A. K. Thakur et al., "Sea-water desalination using a desalting unit integrated with a parabolic trough collector and activated carbon pellets as

energy storage medium," Desalination, vol. 516, no. July, p. 115217, 2021, doi: 10.1016/j.desal.2021.115217.

[44] H. Hassan, M. S. Yousef, M. Fathy, and M. S. Ahmed, "Assessment of parabolic trough solar collector assisted solar still at various saline water mediums via energy, exergy, exergoeconomic, and enviroeconomic approaches," Renew. Energy, vol. 155, pp. 604–616, 2020, doi: 10.1016/j.renene.2020.03.126.

[45] A. Kumar, S. Vyas, and D. Nchelatebe Nkwetta, "Experimental study of single slope solar still coupled with parabolic trough collector," Mater. Sci. Energy Technol., vol. 3, pp. 700–708, 2020, doi: 10.1016/j.mset. 2020. 07.005.

[46] J. Madiouli, C. A. Saleel, A. Lashin, I. A. Badruddin, and A. Kessentini, "An experimental analysis of single slope solar still integrated with parabolic trough collector and packed layer of glass balls," J. Therm. Anal. Calorim., vol. 146, no. 6, pp. 2655–2665, 2021, doi: 10.1007/s10973-020-10320-x.

[47] T. Nabil and M. M. K. Dawood, "Numerical and experimental investigation of parabolic trough collector with focal evacuated tube and different working fluids integrated with single slope solar still," Heat Transf., vol. 50, no. 3, pp. 2007–2032, 2021, doi: 10.1002/htj.21966.

[48] H. Hassan, "Comparing the performance of passive and active double and single slope solar stills incorporated with parabolic trough collector via energy, exergy and productivity," Renew. Energy, vol. 148, pp. 437–450, 2020, doi: 10.1016/j.renene.2019.10.050.

[49] M. A. Al-Amir Khadim, W. A. A. Al-Wahid, D. M. Hachim, and K. Sopian, "Experimental Study of the Performance of Cylindrical Solar Still with a Hemispherical Dome," Smart Sci., vol. 9, no. 1, pp. 30–39, 2021, doi: 10.1080/23080477.2021.1876298.

[50] H. Hassan, M. S. Ahmed, and M. Fathy, “Experimental work on the effect of saline water medium on the performance of solar still with tracked parabolic trough collector (TPTC),” Renew. Energy, vol. 135, pp. 136–147, 2019, doi: 10.1016/j.renene.2018.11.112.

[51] M. Fathy, H. Hassan, and M. Salem Ahmed, “Experimental study on the effect of coupling parabolic trough collector with double slope solar still on its performance,” Sol. Energy, vol. 163, no. January, pp. 54–61, 2018, doi: 10.1016/j.solener.2018.01.043.

[52] H. F. A. Hassan, “Experimental Study and Evaluation of Single Slope Solar Still Combined With Parabolic Trough Using Nanofluid, A thesis submitted to the Department of Mechanical Power Engineering Technologies To obtain a master’s degree at Al-Furat Al-Awsat University - College of Engineering Technology/Najaf” 2022.

[53] E. Bellos and C. Tzivanidis, “Alternative designs of parabolic trough solar collectors,” Prog. Energy Combust. Sci., vol. 71, pp. 81–117, 2019, doi: 10.1016/j.pecs.2018.11.001.

[54] İ. Halil, “Modeling , simulation and performance analysis of parabolic trough solar collectors : A comprehensive review,” Applied Energy, vol. 225, no. May, pp. 135–174, 2018, doi: 10.1016/j.apenergy.2018.05.014.

[55] A. B. Auti, “Energy Procedia Domestic Solar Water Desalination System,” Energy Procedia, vol. 14, no. 2011, pp. 1774–1779, 2012, do10.1016/j. egypro. 2011.12.1166.

[56] W. Fuqiang, C. Ziming, T. Jianyu, Y. Yuan, S. Yong, and L. Linhua, “Progress in concentrated solar power technology with parabolic trough collector system: A comprehensive review,” Renew. Sustain. Energy Rev., vol. 79, no. May, pp. 1314–1328, 2017, doi: 10.1016/j.rser.2017.05.174.

[57] N. Abed, I. Afgan, A. Cioncolini, H. Iacovides, and A. Nasser, “Assessment and Evaluation of the Thermal Performance of

VariousWorking Fluids in Parabolic Trough Collectors of Solar Thermal Power Plants under Non-Uniform Heat Flux Distribution Conditions," Energies, vol. 13, no. 15, pp. 1–27, 2020, doi: 10.3390/en13153776.

[58] Y. C. Chen and C. H. Su, "Integrated opto-mechanical analysis of a PMMA Fresnel lens for a concentrated photovoltaic system," Microsyst. Technol., vol. 19, no. 11, pp. 1725–1729, 2013, doi: 10.1007/s00542-013-1813-0.

[59] Y. A. Alamri, S. Mahmoud, R. Al-dadah, S. Sharma, J. N. Roy, and Y. Ding, "Optical Performance of Single Point-Focus Fresnel Lens Concentrator System for Multiple Multi-Junction Solar Cells — A Numerical Study," Energies 2021.

[60] S. I. Palomino-Resendiz, D. A. Flores-Hernández, N. Lozada-Castillo, L. Guzmán-Vargas, and A. Luviano-Juárez, "Design and implementation of a robotic active solar distiller based on a Fresnel concentrator and a photovoltaic system," Energy Convers. Manag., vol. 166, no. May, pp. 637–647, 2018, doi: 10.1016/j.enconman.2018.04.069.

[61] E. Bellos, C. Tzivanidis, K. A. Antonopoulos, and G. Gkinis, "Thermal enhancement of solar parabolic trough collectors by using nanofluids and converging-diverging absorber tube," Renew. Energy, vol. 94, pp. 213–222, 2016, doi: 10.1016/j.renene.2016.03.062.

[62] S. W. Sharshir, G. Peng, N. Yang, M. O. A. El-Samadony, and A. E. Kabeel, "A continuous desalination system using humidification - Dehumidification and a solar still with an evacuated solar water heater," Appl. Therm. Eng., vol. 104, pp. 734–742, 2016, doi: 10.1016/j.applthermaleng.2016.05.120.

[63] A. E. Kabeel and M. Abdelgaied, "Observational study of modified solar still coupled with oil serpentine loop from cylindrical parabolic concentrator and phase changing material under basin," Sol. Energy, vol.

144, pp. 71–78, 2017, doi: 10.1016/j.solener.2017.01.007.

[64] E. Bellos, C. Tzivanidis, and Z. Said, “A systematic parametric thermal analysis of nanofluid-based parabolic trough solar collectors,” Sustain. Energy Technol. Assessments, vol. 39, no. May, 2020, doi: 10.1016/j.seta. 2020.100714.

[65] S. W. Sharshir, G. Peng, N. Yang, M. A. Eltawil, M. K. A. Ali, and A. E. Kabeel, “A hybrid desalination system using humidification-dehumidification and solar stills integrated with evacuated solar water heater,” Energy Convers. Manag., vol. 124, pp. 287–296, 2016, doi: 10.1016/j.enconman.2016.07.028.

[66] G. N. Tiwari, J. K. Yadav, D. B. Singh, I. M. Al-helal, and A. M. Abdel-ghany, “Exergoeconomic and enviroeconomic analyses of partially covered photovoltaic fl at plate collector active solar distillation system,” DES, vol. 367, pp. 186–196, 2015, doi: 10.1016/j.desal.2015.04.010.

[67] O. Bait and M. Si-Ameur, “Enhanced heat and mass transfer in solar stills using nanofluids: A review,” Sol. Energy, vol. 170, no. May, pp. 694–722, 2018, doi: 10.1016/j.solener.2018.06.020.

[68] H. Muhammad et al., “Performance analysis of nanofluid - based water desalination system using integrated solar still , flat plate and parabolic trough collectors,” J. Brazilian Soc. Mech. Sci. Eng., no. August, 2022, doi: 10.1007/s40430-022-03734-1.

Appendix

Appendix A

Theoretical Calculations

Apply theoretical calculations in chapter three equations according to the following steps.

1. Calculation of the focal length of the parabolic trough

$$f_{Lp} = \frac{x^2}{4y} = \frac{0.4^2}{4*0.194} = 21.05 \text{ cm}$$

2. Calculation of the aperture area of the reflector parabolic trough

$$A_p = W_p \cdot L_p = 0.8 * 1.4 = 1.12\ m^2$$

3. Calculation of the aperture area of the focus area on the absorbent tube

$$A_{foc} = \pi D_{abs}\ L_{abs} = \pi * (D_{knot} * L_{knot} * 2 + D_{abs} * L_{abs})$$

$$= \pi * (0.05 * 0.1 * 2 + 0.019 * 1.38) = 0.113\ m^2$$

4. Calculation of the Solar Radiation Concentration Ratio of parabolic trough

$$CR_p = \frac{A_p}{A_{foc}} = \frac{1.12}{0.113} = 9.91$$

5. Calculation of the focal length of the lenses used in this study, which have a diameter of 30 cm and a prism angle of 36.9° with a refractive index of 1.49.

$$\tan \alpha = \frac{r_F}{n\sqrt{{r_F}^2 + (f_{LF})^2} - f_{LF}}$$

$$\tan 36.9 = \frac{0.15}{(1.49)\sqrt{0.15^2 + (f_L)^2} - f_L} \rightarrow f_{LF} = 0.30\ m$$

6. Calculation of the aperture area of the Fresnel lenses.

$$A_F = {D_F}^2 = 0.3^2 = 0.09\ m^2$$

7. Calculation of thermal efficiency of conventional.

$$\eta_{th} = \frac{\sum M_{ev} * h_{fg}}{I_s * (A_b) * 3600} * 10^2$$

$$A_b = w_b * L_b = 0.61 * 0.38 = 0.2318$$

$$\eta_{th\,day} = \frac{\sum_0^{24} M_{ev} * h_{fg}}{\sum_0^{24} I_s * A_b * 3600} = \frac{\sum_0^{24} 1.1 * 2335000 * 100}{\sum_0^{24} 6871 * 0.2318 * 3600} = 44.7\%$$

8. Calculation of thermal efficiency of the modified system.

When using SSSS + PTC.

$$\eta_{th} = \frac{\sum_0^t M_{ev} * h_{fg}}{\sum_0^t (A_b + A_p) * I_s * 3600} * 10^2$$

$$\eta_{th\,day} = \frac{\sum_0^{24} M_{ev} * h_{fg}}{(\sum_0^{11} A_p + \sum_0^{24} A_b) * I_s * 3600}$$

$$= \frac{\sum_0^{24} 1.39 * 2335000 * 100}{(\sum_0^{11} 1.12 + \sum_0^{24} 0.2318) * 6871 * 3600} = 17.05\%$$

When using SSSS with PTC and Lenses inside.

$$\eta_{th} = \frac{\sum M_{ev} * h_{fg}}{\sum_0^t (A_b + A_p) * I_s * 3600} * 10^2$$

In this case, the lens area is not calculated because it falls within the area of the parabola basin.

$$\eta_{th\,day} = \frac{\sum_0^{24} M_{ev} * h_{fg}}{(\sum_0^{11} A_p + \sum_0^{24} A_b) * I_s * 3600}$$

$$= \frac{\sum_0^{24} 1.55 * 2335000 * 100}{(\sum_0^{11} 1.12 + \sum_0^{24} 0.2318) * 6956 * 3600} = 18.78\%$$

When using SSSS with PTC and Lenses outside.

$$\eta_{th} = \frac{\sum_0^t \sum M_{ev} * h_{fg}}{\sum_0^t (A_b + A_p + A_F) * I_s * 3600} * 10^2$$

$$\eta_{th\,day} = \frac{\sum_0^{24} M_{ev} * h_{fg}}{(\sum_0^{11} A_p + \sum_0^{24} A_b) * I_s * 3600}$$

$$= \frac{\sum_0^{24} 1.583 * 2335000 * 100}{(\sum_0^{11} 1.12 + \sum_0^{11} 0.09 + \sum_0^{24} 0.2318) * 6863 * 3600}$$

$$= 18.41\%$$

9. Calculating the productivity enhancement ratio of the developed model compared to conventional.

$$P_{Enh}\% = \left(\frac{P_{\mathrm{M}} - P_C}{P_C}\right) * 100$$

Table (A-1): Productivity enhancement of solar stills for all experiments compared to conventional.

Experiment date	system	Productivity (mL per day)	$P_{Enh}\%$
3/4/2023	CSS	1100	26.3%
	SSSS +PTC	1390	
5/4/2023	CSS	1099	41%
	SSSS +PTC+lenses inside	1550	
27/4/2023	CSS	1109	42.7%
	SSSS+PTC+lenses outside	1583	
5/5/2023	CSS	1240	28.2%
	SSSS +PTC	1590	
6/5/2023	CSS	1240	43.3%
	SSSS +PTC+lenses inside	1778	
7/5/2023	CSS	1244	44.1%
	SSSS+PTC+lenses outside	1793	

Appendix. B

Thermocouple Calibration

Thermocouples are one of the pieces of equipment that are used to measure temperatures in various locations from engineering experiments. 16 K-type thermocouples were calibrated using a mercury thermometer and a type (CTK4000) data logger. The thermocouples were connected to the data logger while the other end of it was placed in a container containing water whose temperature was controlled. Calibration was carried out with temperatures starting from zero ^{o}C and ending with 100 ^{o}C. As shown in Figure and Table B.1.

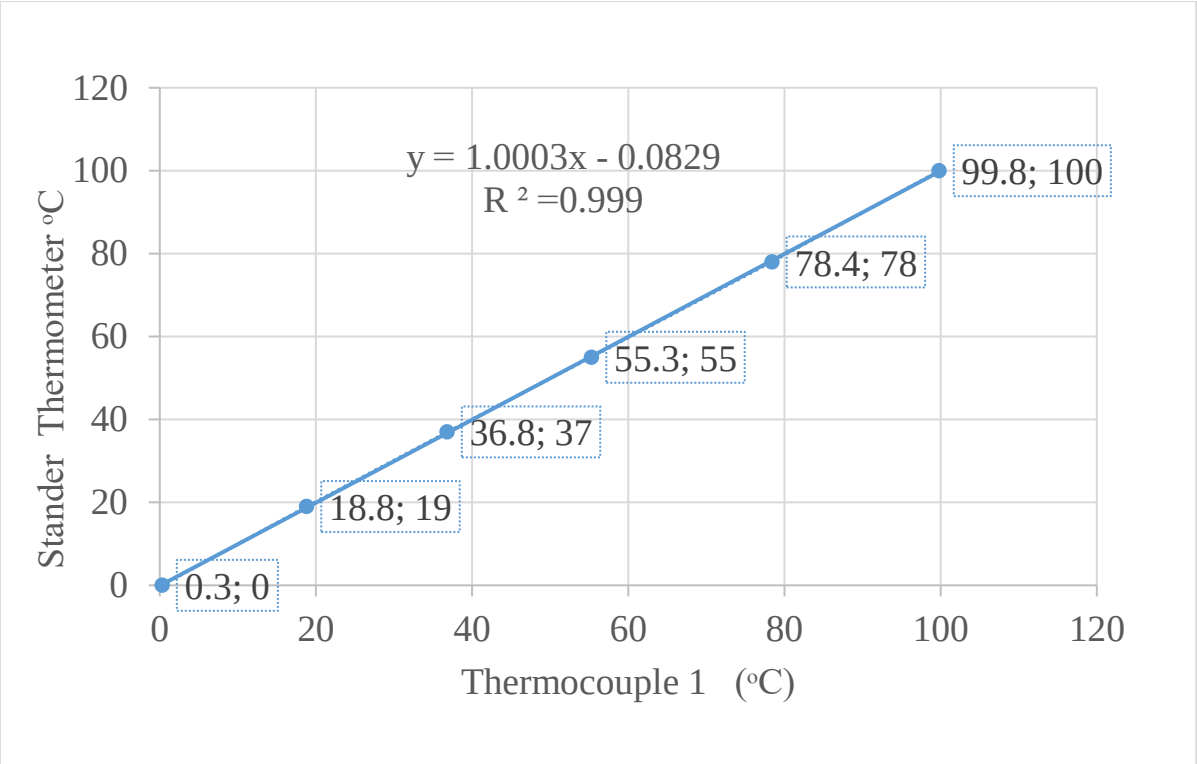

Figure (B.1): Results of thermocouples calibration

Table (B-1): Calibration equations for thermocouples.

Thermocouple no.	location thermocouple		Correction formula
T1	Ambient	Behind PTC	y = 1.0003x-0.08295
T2	water feed tank	tank level	y = 1.004582x -0.28768

T3	Galvanized plate	solar still traditional	y = 0.9923x +0.6202
T4	Most stream	solar still traditional	y = 0.9945x + 0.0513
T5	basin water	solar still traditional	y = 0.9997x + 0.098
T6	basin water	solar still traditional	y = 0.9965x + 0.1964
T7	Inner glass cover	solar still traditional	y = 0.9863x + 0.8255
T8	Outer glass cover	solar still traditional	y = 1.0113x - 0.2068
T9	inlet absorber tube	PTC	y = 0.9901x+ 0.8226
T10	out let absorber tube	PTC	y = 0.9788x+ 0.5959
T11	Galvanized plate	CSS+PTC	y = 1.0091x - 0.5892
T12	basin water	CSS+PTC	y = 0.9985x + 0.107
T13	basin water	CSS+PTC	y = 1.0038x + 0.369
T14	Inner glass cover	CSS+PTC	y = 0.9943x +0.0112
T15	Outer glass cover	CSS+PTC	y = 0.9897x + 0.3318
T16	Most stream	CSS+PTC	y = 1.0052x + 0.7029

Appendix. C

A solar radiation device model (SM206 - solar) was used every hour during the duration of the experiment. The accuracy of the measured results was calibrated with the solar radiation data obtained by the Ministry of Science and Technology / Department of Environment, Water and Renewable Energies for the same day and time of conducting the experiments and the results were identical as in Figure C-1.

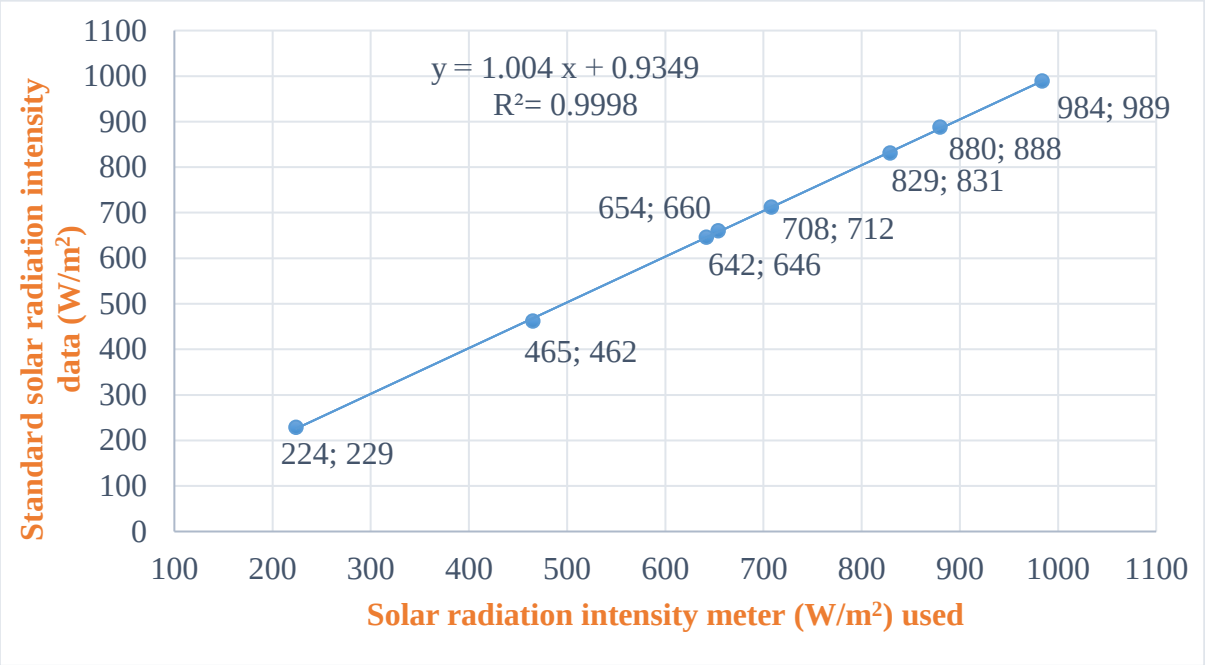

Figure (C.1) The results of calibration of the solar radiation intensity device

Appendix. D

The wind speed was documented every hour during the duration of the experiment using a digital device type (BTMETER BT-100-WM) to measure the intensity of the wind speed. The device was calibrated by the Ministry of Science and Technology /Department of Environment, Water and Renewable Energies in Baghdad, Iraq. Calibration results were identical as in the book picture.

Appendix

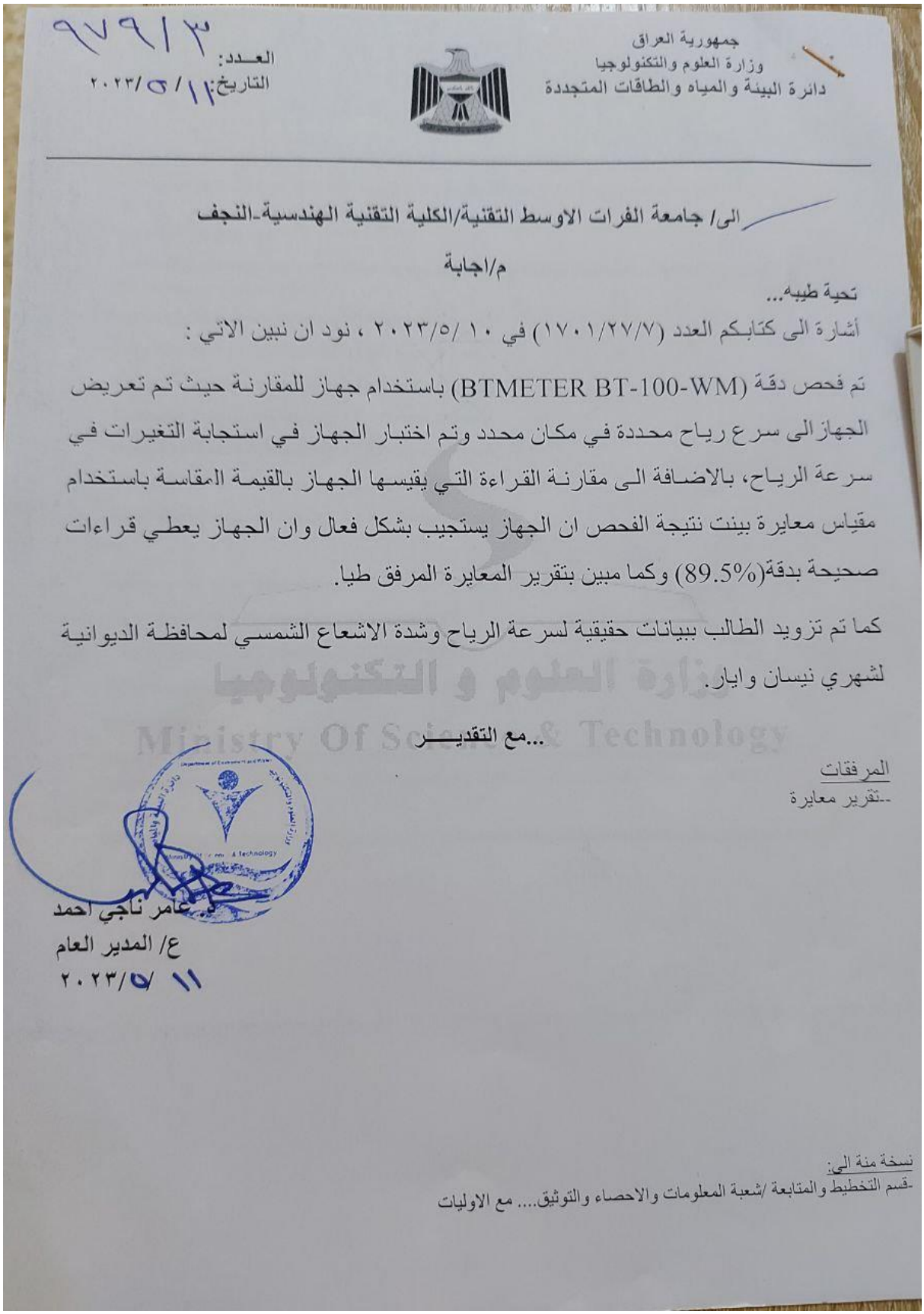

جمهورية العراق
وزارة العلوم والتكنولوجيا
دائرة البيئة والمياه والطاقات المتجددة

العـدد: ٩٧٩/٣
التاريخ: ١١/٥/٢٠٢٣

الى/ جامعة الفرات الاوسط التقنية/الكلية التقنية الهندسية-النجف

م/اجابة

تحية طيبه...

أشارة الى كتابكم العدد (١٧٠١/٢٧/٧) في ١٠ /٢٠٢٣/٥ ، نود ان نبين الاتي :

تم فحص دقة (BTMETER BT-100-WM) باستخدام جهاز للمقارنة حيث تم تعريض الجهاز الى سرع رياح محددة في مكان محدد وتم اختبار الجهاز في استجابة التغيرات في سرعة الرياح، بالاضافة الى مقارنة القراءة التي يقيسها الجهاز بالقيمة المقاسة باستخدام مقياس معايرة بينت نتيجة الفحص ان الجهاز يستجيب بشكل فعال وان الجهاز يعطي قراءات صحيحة بدقة(89.5%) وكما مبين بتقرير المعايرة المرفق طيا.

كما تم تزويد الطالب ببيانات حقيقية لسرعة الرياح وشدة الاشعاع الشمسي لمحافظة الديوانية لشهري نيسان وايار.

...مع التقديـــر

المرفقات
-تقرير معايرة

د. عامر ناجي احمد
ع/ المدير العام
١١/٥/٢٠٢٣

نسخة منة الى:
-قسم التخطيط والمتابعة /شعبة المعلومات والاحصاء والتوثيق.... مع الاوليات

ANEMOMETER CALIBRATION REPORT

Equipment calibrated: Air Flow Anemometer Model: BTMETER –BT-100WM Calibration date: May 11, 2023

CALIBRATION RESULTS:

The following results were obtained during the calibration of the Air Flow Anemometer BT100WM
Measurement of air velocity:

Calibration Point: 0 m/s Reading: 0.0 m/s Error: 0.0 m/s

Calibration Point: 1 m/s Reading: 1.2 m/s Error: 0.2 m/s

Calibration Point: 2 m/s Reading: 2.4 m/s Error: 0.4 m/s

Calibration Point: 3 m/s Reading: 3.2 m/s Error: 0.2 m/s

Calibration Point: 4 m/s Reading: 3.8 m/s Error: 0.20 m/s

Calibration Point: 5 m/s Reading: 4.6 m/s Error: 0.40 m/s

Calibration Point: 6 m/s Reading: 5.4 m/s Error: 0.60 m/s

Measurement of air temperature:

Calibration Point: 20°C Reading: 20.5°C Error: 0.5°C

Calibration Point: 25°C Reading: 25.5°C Error: 0.5°C

Calibration Point: 30°C Reading: 30.5°C Error: 0.5°C

CONCLUSION:

Based on the calibration results obtained, the Air Flow Anemometer BT100WM has been found to comply with the requirements for the measurement of air velocity and temperature with **89.5%** Accuracy.

The calibration certificate is valid until the next calibration date, which is recommended to be performed every 12 months.

Appendix E

1. Akeel Salman Hammoud, Ahmed Hashem Yousef, Improved the productivity of solar distillers through modifying designs: Review. Posted in.
2. Akeel Salman Hammoud, Ahmed Hashem Yousef, An experimental study to improve the productivity of a solar still using a parabolic trough collector with Fresnel lenses. Posted in.

3rd International Conference on Engineering & Science (ICES2023)
3 -4 MAY 2023 | Al-SAMAWA | IRAQ

Final Acceptance Letter

Manuscript Number: 45_Salman_ICES2023

Decision ID : 004_FAL_ICES
Date : 1/3/2023

Dear Akeel Salman ,

Co-Authors : Ahmed M. Hashim .

Congratulations!

It's a great pleasure to inform you that, after the peer review process, your manuscript entitled **Improved the Productivity of Solar Distillers through Modifying Designs: Review**

Has been **ACCEPTED** for participating in the **3rd International Conference on Engineering and Science,** and considered for publication in **AIP Conference Proceedings.**

Thank you for your valuable participation in the ICES2023 conference.

Prof. Dr. Sabah Mohammed Mlkat
Head of ICES2023 Scientific Committee
Dean of Al-Samawa Technical Institute

Dr.Ahmed Razzaq H. Al-Manea
ICES2023 Scientific Committee
AIP Conference Proceedings Editor

ATU
Tomorrow starts today

2nd International Conference on Engineering, and Science to Achieve the Sustainable Development Goals
(9th – 10th) July 2023 in Tabriz - Iran

Final Acceptance Letter

Manuscript Number: 574

Dear: Akeel. Salman

Co-Authors: Ahmed M. Hashim

Congratulations!

It is a great pleasure to inform you that, following the peer review process, your manuscript titled

(An experimental study to improve the productivity of a solar still using a parabolic trough collector with Fresnel lenses.)

Had been **ACCEPTED** for participating in the **2nd International Conference on Engineering, and Science to Achieve the Sustainable Development Goals,** and considered for publication in **(AIP Conference proceeding).**

Thank you for your significant contribution to the ICASDG2023 conference.

Prof. Dr. Ahmed G. Wadday
ICASDG2023 Scientific Committee Chair | AIP Conference Proceeding Editor
9th – 10th July 2023 | Tabriz | Iran

الخلاصة

تعتبر الطاقة الشمسية من أهم مصادر الطاقة البديلة في العالم، فهي متوفرة وقليلة التكلفة، خاصة في المناطق التي تكثر فيها الإشعاعات الشمسية مثل بلدنا العراق. كما أنها طاقة نظيفة لا تترك أي أثر بيئي عند استخدامها. وتستخدم في العديد من التطبيقات، مثل الألواح الشمسية المستخدمة لتوليد الطاقة الكهربائية أو من خلال الاستفادة من محتواها الحراري، مثل تلك المستخدمة في تحلية المياه وتسخين المياه والطهي. تعد أجهزة التقطير الشمسية من بين التطبيقات الأكثر انتشارًا لحل مشكلة ندرة المياه العذبة. الهدف الرئيسي من هذه الدراسة هو تحسين أداء أنظمة الطاقة الشمسية الثابتة من خلال استخدام مكثفات الطاقة الشمسية. في هذه الدراسة، تم إنشاء وحدة ثابتة شمسية أحادية الانحدار ووحدة أخرى بنفس الأبعاد والمواصفات متصلة بمجمع حوض مكافئ (بدون عدسات، مع عدسات فوق مجمع حوض مكافئ، ومع عدسات على جانبي مجمع حوض مكافئ) تم اختباره.تم تنفيذ العمل تجريبياً في ظل الظروف المناخية لمدينة الديوانية في العراق (خط عرض ٣١.٩٩ درجة شمالاً، خط طول ٤٤.٩٣ درجة شرقاً) في شهري نيسان وأيار وحزيران من عام ٢٠٢٣.

تم بناء نموذج تجريبي تم على أساسه إجراء التجارب العملية، مع إمكانية تغيير موقع عدسات فريسنل لتركيز الإشعاع الشمسي على الأنبوب داخل أو خارج **PTC**، كما أن هناك إمكانية تدوير النظام باتجاه الإشعاع الشمسي. أجريت التجارب ضمن قيم تصريف الماء (٠.٣٨، ٠.٥، ٠.٧٨) لتر/دقيقة.

وأظهرت النتائج أن درجة الحرارة ترتفع تدريجياً لتصل إلى أعلى قيمة لها عند الظهر، حيث تكون أعلى قيمة للإشعاع الشمسي، ثم تبدأ بالانخفاض تدريجياً. أقصى درجة حرارة لمياه حوض المقطر الشمسي المقترن بمجمع الحوض المكافئ مع عدسات فريسنل خارج الحوض المكافئ كانت ٧٦.٨ درجة مئوية عند الساعة ١:٠٠ ظهراً مع معدل تدفق حجمي ٠.٥ لتر/دقيقة في شهر مايو، في حين أن درجة حرارة حوض الماء القصوى (٧١.٧، ٧٤.٢، و ٧٥.٥) درجة مئوية عند الساعة ١:٠٠ ظهرًا للمقطر الشمسي التقليدي، والمقطر المقترن بحوض القطع المكافئ، و الطاقة الشمسية مقترنة بمجمع الحوض المكافئ مع عدسات فريسنل فوق الحوض المكافئ على التوالي. إن استخدام وحدة التقطير الشمسية مع حوض مكافئ مع عدسات فريسنل على جانبي **PTC** ساهم بشكل كبير في تحسين الإنتاجية. وبلغ إنتاج المياه العذبة في شهر مايو ٧.٧ لتر/م٢ يوم، والكفاءة الحرارية ١٩.٣٢٪، ونسبة التحسن في الإنتاجية ٤٤.١٪ مقارنة بالمقطر التقليدي. في حين أن إنتاجية المقطر الشمسي التقليدي والمقطر الشمسي المرتبط بمجمع حوض مكافئ، والطاقة الشمسية المرتبطة بمجمع حوض مكافئ، وعدسات فريسنل فوق المكثف الشمسي كانت

(٥.٣، ٦.٧، و٧.٥) لتر/م٢ يوم و وكانت الكفاءة الحرارية اليومية (٤٦.٩٪، ١٨.١٪، ٢٠.٣٪) على التوالي. وكان معدل تحسن الإنتاج حوالي (٢٨.٢٪، و٤٣.٣٪) للطاقة الشمسية المرتبطة بمجمع حوضي مكافئ، والطاقة الشمسية المرتبطة بمجمع حوضي مكافئ مع عدسات فريسنل فوق مجمع الحوض المكافئ، على التوالي، مقارنة بالمقطر التقليدي.

دراسة تجريبية لاداء مقطر شمسي احادي الميل باستخدام مركز شمسي مكافئ مع عدسات فريسنل

رسالة مقدمة الى

قسم هندسة تقنيات ميكانيك القوى

كجزء من متطلبات نيل درجة الماجستير في

هندسة تقنيات ميكانيك القوى/ الحراريات

تقدم بها

عقيل سلمان حمود

بكالوريوس في هندسة تقنيات ميكانيك القوى

اشراف

الأستاذ الدكتور

احمد هاشم يوسف

جمهورية العراق

وزارة التعليم العالي والبحث العلمي

جامعة الفرات الاوسط التقنية

الكلية التقنية الهندسية/النجف

دراسة تجريبية لاداء مقطر شمسي احادي الميل باستخدام مركز شمسي مكافئ مع عدسات فريسنل

عقيل سلمان حمود

بكالوريوس في هندسة تقنيات ميكانيك القوى

٢٠٢٣